AN ABSTRACT OF THE THESIS OF

Polly Ann Haessig for the degree of Master of Science in Geology presented on June 1, 1988.

Title: Structure and Petrography of the Schist of Skookum Gulch, Callahan-Yreka Area, Eastern Klamath Mountains, Northern California

Abstract approved: Redacted for Privacy

Arthur J. Boucot

The schist of Skookum Gulch (SSG) is an informal name applied to a fault-bounded melange composed mainly of schistose metamorphic rocks and less abundant sedimentary and igneous rocks located in the eastern Klamath Mountains of northern California. The SSG features outcrops of lawsonite+sodic amphibole blueschist and epidote+sodic amphibole rocks transitional to the greenschist facies. Isotopic dating indicates that the schist was metamorphosed during the Ordovician. The SSG is the oldest known Paleozoic blueschist-bearing melange in California and one of the oldest preserved blueschist terranes in North America. Tonalitic rocks associated with the schist have Early Cambrian ages and are among the oldest rocks yet dated within the Klamath Mountains.

Field relations indicate that the schist of Skookum Gulch is a complex tectonic melange composed of metavolcanic, carbonate, and metasedimentary blocks and lenses of diverse sizes and shapes dispersed without apparent stratigraphic coherency in a sheared matrix of clastic to pelitic schist, metavolcanic schist, and discontinuous thin lenses of marble. Rocks of the matrix have been metamorphosed to chlorite-grade greenschist facies, whereas the blocks have been metamorphosed under a variety of pressure-temperature conditions. Some blocks have been feebly metamorphosed and retain features of the original protolith material; others have been thoroughly recrystallized under blueschist, transitional, and greenschist facies conditions.

Blueschist blocks within the schistose matrix reveal six

deformation events, (D1-D6): four are folding events, and at least two are ductile and brittle shear deformations. One period of metamorphism under blueschist-facies conditions is recorded in the blueschist blocks. The blocks lack evidence of prograde, greenschist-facies overprinting. Schistose rocks of the matrix are less deformed than the blueschist blocks. Matrix schists show at least two phases of folding. The predominant foliation is the result of tranposition of an early foliation or compositional layering. Other deformations include kink folding, ductile shearing, and brittle fracturing. The polydeformed tectonic blocks are hypothesized to have been incorporated into the melange matrix along a system of faults and rotated into a preferred alignment with the pervasive foliation of the matrix during D3. Feebly deformed and metamorphosed blocks such as chert, marble, and tonalite were incorporated prior to the time of brittle shearing.

More is now known about the relative timing of these events. Blueschist-facies and greenschist-facies metamorphism occurred during the Late Ordovician to Early Silurian. Clasts of matrix components and tonalitic plutonic rocks of the SSG melange have been found in exposures of Late Silurian conglomerate beds in nearby units providing evidence that the SSG was uplifted and eroded by the Late Silurian. Minerals within the schist were thermally reset by Devonian metamorphism, possibly related to metamorphism and juxtaposition of the Duzel Phyllite and amphibolite of the Central Metamorphic Belt. However, the SGG does not show direct evidence of Devonian deformation.

Structure and Petrography of the
Schist of Skookum Gulch, Callahan-Yreka Area,
Eastern Klamath Mountains, Northern California

by

Polly Ann Haessig

A THESIS

submitted to

Oregon State University

in partial fulfillment of
the requirements for the
degree of

Master of Science

Completed June 1, 1988

Commencement June 1989

APPROVED:

Redacted for Privacy

Arthur J. Boucot
Professor of Geology in charge of major

Redacted for Privacy

Dr. J. G. Johnson
Head of Department of Geology

Redacted for Privacy

Lyle D. Calvin
Dean of Graduate School

Date thesis is presented June 1, 1988

ACKNOWLEDGEMENTS

The help and advice of many people during the preparation of this thesis is gratefully acknowledged. I would like to thank the members of my committee, Dr. Arthur J. Boucot, Dr. Anita Grunder and Dr. Robert D. Lawrence. Special thanks is given to Arthur J. Boucot for his encouragement and suggestions. Valuable insights into the structure, stratigraphy and lithology of the area were provided by R. D. Lawrence, A. J. Boucot and A. W. Potter during their visits to the field area. Al Potter introduced me to the various metamorphic, igneous, and sedimentary units of the area. His knowledge and our discussions of the complicated geology of the Klamaths were of great help during the course of this study.

Many people living in the Callahan, McConaughy Gulch and Moffett Creek area provided free access to their private lands. Thanks goes to N. Wolford, D. Towne, K. Deppen, Don and Tyler Gresham, and E. Ahmundson.

I am extremely grateful to my friends in Callahan, Rodney Hamilton, Butch Munson, John Thurlby and E. W. Whitman who made field seasons so memorable and enjoyable.

Advice and encouragement in the preparation, editing and organization of this manuscript were given by Al Potter, Gary Davidson, Joe DiPietro, George Moore, and the members of my committee. Financial support for field work and production of this thesis was provided by National Science Foundation grants to A. J. Boucot and the Amoco fund.

Finally I would like to thank my parents for their emotional and financial support especially during this academic endeavor. Special appreciation goes to my mom, who was my field assistant during the summer of 1987. Heidi Hoffmann, Bob Blodgett, Katie Howard, Jim McDougall, S. C. Jones, Kovich and Kalli are thanked for their friendship, entertainment and moral support during my years in Corvallis.

TABLE OF CONTENTS

page

INTRODUCTION 1
Statement of Problem 1
Location and Accessibility 2
Topography, Climate, and Vegetation 4
Exposures 4
Methods of Investigation 5
Previous Work 6

REGIONAL GEOLOGY 9

LOCAL STRATIGRAPHY 11

FIELD RELATIONS 15
Definition of Melange and its Application to the SSG 15
Characterization of the SSG Melange 15
Rock Types and Field Relations of the Matrix 16
Rock Types and Field Relations of Blocks 16
Relative Proportions of Rock Types in the SSG 23

GREENSCHIST-FACIES ROCKS OF THE MATRIX 24
Quartz-Albite Schist 24
Graphitic Schist 27
Quartz-Mica Schist 29
Greenschist. 30
Quartzose Phyllite 31
Comparison of the Phyllitic Quartzite of the SSG to the Sissel Gulch Graywacke 32

WEAKLY METAMORPHOSED SEDIMENTARY TECTONIC BLOCKS 36
Laminated Chert. 36

GREENSCHIST-FACIES TECTONIC BLOCKS 38
Micaceous Quartzite. 38
Micaceous Quartzite of the No Name Gulch Locality . . . 38
Micaceous Quartzite from the Upper McConaughy Gulch Locality 39
Marble 40
Correlation of Marble Lithologies with Limestone Units of of Zdanowicz. 41
Laminated Dolomite Marble 41
Massive Dolomite Marble 46
Foliated Calcite Marble 46
Origin of the Greenschist Facies Metacarbonate Blocks and Lenses. 48
Actinolite Schist. 48

BLUESCHIST AND TRANSITIONAL FACIES TECTONIC BLOCKS 50
Definitions of Blueschist and Transitional Facies. 50
Critical Mineral Assemblages of Blueschist and Transitional Facies in the SSG 50
Blueschist Facies Tectonic Blocks. 51
Metavolcanic Rocks. 51
Assemblages 51
Lawsonite-Sodic Amphibole Schist 53
Chlorite-rich, Sodic Amphibole-Lawsonite Schist. . 54
Actinolite-Lawsonite-Sodic Amphibole Schist. . . . 55
Lawsonite-Actinolite Schist. 58
Metacarbonate Rocks 60
Sodic Amphibole-Lawsonite-Calcite Marble 60
Transitional Facies Blocks 62
Metavolcanic Rocks. 62
Epidote-Sodic Amphibole Schist 62
Volcanic Breccia 64
Metasedimentary Rocks 66
Quartz-Mica Schist 66
Metachert. 67
Mineral Composition. 67
Sodic Amphibole 67
Calcic Amphibole. 68
Coexisting Na-Amphibole and Ca-Amphibole. 68
Trace Element Chemistry. 70

CONDITIONS OF METAMORPHISM 74
Conditions of Metamorphism of Rocks of the Matrix. 74
Metamorphic Conditions of Blueschist and Transitional Facies Rocks 77
Absence of Pumpellyite, Aragonite and Pyroxene in the SSG. . 79

IGNEOUS ROCKS. 82
Plutonic Blocks. 82
Hornblende Tonalite 82
Isotopic Age. 85
Correlation 85
Major-Element and Trace-Element Chemistry 87
Petrogenetic Models 90
Possible Tectonic Setting of Origin 91
Intrusive Gabbro of Unkown Age 96
Clinoyroxene Gabbro 96
Hornblende Gabbro 97
Significance and Possible Age 97
Serpentinite 98

GEOCHRONOLOGY. 99
Isotopic Age of Metamorphic Rocks of the SSG 99
Constraints on the Age of the SSG and Timing of Uplift . . .100

STRUCTURE. 102
Introduction 102
Terminology and Nomenclature. 102
Deformation History of Blocks. 103
Deformations, Fold Styles, and Microscopic Structures of Blocks 103
First Deformation 103
Microscopic Textures of D1 110
Second Deformation. .113
Microscopic Textures of D2 113
Third Deformation 113
Microscopic Textures of D3 114
Fourth Deformation. .114
Microscopic Textures of D4 114
Ductile and Brittle Shear Events, D5 and D6 117
Deformation of Chert, Marble, Plutonic, and Other Blocks . .117
Deformational History of the Matrix Rocks. 118
Deformation Style and Microscopic Structures of Matrix Schist. 119
First Deformation 119
Microscopic Textures of D1 122
Second Deformation. .123
Ductile and Brittle Shear Deformations, D3 and D4 . . .123
Structure Diagrams 124
Planer Elements 124
D1: S_1 of Blocks. 124
D1: S_B of Matrix. 124
D1: S_2 of Blocks. 124
D2: S_3 of Blocks. 127
D3: S_4 of Blocks. 127
D4: Kink Folds of Blocks and Matrix 127
Linear Elements 127
D1: L_M of Blocks and Matrix 129
D2: L_3^2 of Blocks. 129
D3: L_4^2 of Blocks. 129
D4: L_K of Blocks and Matrix 129
Macroscopic Faults and Folds 129
Structural Interpretation. 130

DISCUSSION 133
Deformation and Metamorphism 133
Emplacement of Blocks into the Matrix. 135
Regional Geologic Implications 138

REFERENCES 142

APPENDIX 1 Mineralogy Tables .153
APPENDIX 2 Chemical Analyses: Sample Preparation, Methods and Standards Used. 159
APPENDIX 3 Chemical Data and REE Signature of Quartz Keratophyre of Horseshoe Gulch. 161
APPENDIX 4 Stereonet Plots. .163

LIST OF FIGURES

page

1. Index map of the Callahan-Yreka area, northern California. . 3
2. Subprovinces of the Klamath Mountains province (after Irwin, 1966, and Cashman, 1977) 10
3. Geology of part of the Callahan-Yreka area, modified from Hotz (1978) and Potter and others (1977) 12
4. Thin lens of marble interlayered with quartz-albite schist matrix 17
5. Isolated blueschist block in a poorly exposed greenschist matrix 18
6. Field relations between blueschist and massive marble blocks and graphitic schist and greenschist matrix lithologies. 19
7. Epidote-sodic amphibole schist interlayered with foliated calcite marble. 21
8. Interlayered sequence of sodic amphibole-lawsonite-calcite marble, poorly exposed sodic amphibole-bearing lawsonite-actinolite schist and dark colored actinolite-lawsonite-sodic amphibole schist 22
9. Photomicrograph of a quartz-albite schist, sample HG 15. . . 26
10. A. Photomicrograph of quartzose phyllite (MC96) of the SSG
    B. Photomicrograph of Sissel Gulch Graywacke. 33
11. Laminated dolomite marble block, outcrop HG 24 43
12. A. Photomicrograph of laminated dolomite marble, HG 24
    B. Photomicrograph of a foliated calcite marble, UMG 61 . . 44
13. Photomicrograph of sodic amphibole-lawsonite-calcite marble, NNG 34 61
14. Photomicrograph of a volcanic breccia, UMG 57. 65
15. A. Compositional field of sodic amphibole from the SSG after Cotkin (1987, Figure 2)
    B. Composition of coexisting actinolite (near apex) and sodic amphibole from sample HS-4 after Cotkin (1987, Figure 4) 69
16. A. Chondrite-normalized whole rock REE plot of an epidote-sodic amphibole schist from the Upper McConaughy Gulch Locality (sample UMG 77)
    B. Combined REE patterns of other epidote-sodic amphibole schists reported in the literature. 72
17. P-T grid constructed for the SSG 75
18. A. QAP plot of samples of tonalite of the SSG, subdivisions after Streckeisen (1976)
    B. Modal abundances for selected samples of hornblende tonalite. 83
19. Chondrite normalized REE plot of Early Cambrian tonalite, samples SBQD and TGQD. 89
20. Ocean-ridge granite (ORG) normalized geochemical patterns for: (A) tonalite blocks of the SSG; (B) plagiogranites from ocean-ridge and marginal-basin spreading centers; (C) volcanic arc granites and (D) Balaklala Rhylolite and Mule Mountain Trondhjemite 93
21. Deformational features exhibited by a blueschist block . . .105

22. Tight to close folds of quartz veins in lawsonite Na-amphibole schist, sample HG3. 106
23. Refold pattern in epidote-Na-amphibole-bearing quartz-mica schist, outcrop UMG 69 .107
24. Close-up view of fold style of outcrop UMG 59. 108
25. A. Intrafolial folds with predominant foliation, S_B, parallel to axial surface of fold
B. and C. F_2 folds
D. and E. F_3 folds of quartz vein, and associated axial planer cleavage development, S_4
F. F_4 folds: asymmetric kink folds of S_2 109
26. A. Curved trails of blue amphibole, sphene and lawsonite showing relict S_1 foliation
B. Transposition of S_1 to form S_2 111
27. Lawsonite-Na-amphibole schist displaying predominant foliation, S_2, that anastomoses around colorless lawsonite porphyroblasts 112
28. A. Microfolded quartz vein, representing F_3 fold event
B. Well-developed zonal crenulation cleavage, axial planer to F_3 folds. 115
29. Microscopic view of F_4 kink fold in epidote-Na amphibole schist, UMG 73 116
30. Greenschist matrix rocks showing a predominant foliation, S_B, and asymmetric kink folds of the foliation, F_4, with axial surfaces, S_K 120
31. Isoclinal fold in quartzose phyllite, (matrix rock type), outcrop MC 96. 121
32. A. Stereonet plots showing poles to foliation 125
B. Stereonet plots showing poles to foliation 126
33. Stereonet plots showing trend and plunge of linear elements 128
34. Mineral occurrence in blueschist and transitional schist and relation to deformation stage 134
35. Flow chart recording the deformational history of the schist of Skookum Gulch. 136
A1. A. Chemical analyses of quartz keratophyre samples from Horseshoe Gulch.
B. Chondrite normalized REE pattern of samples of quartz keratophyre of Horseshoe Gulch 162
A2. Structural data for the Horseshoe Gulch Locality 164
A3. Structural data for the No Name Gulch Locality 166
A4. Structural data for the Upper McConaughy Gulch Locality. . .168

LIST OF TABLES

page

1. Age constraints of selected major units in the Callahan-Yreka area. 8
2. Correlation of stratigraphic nomenclature in the Callahan-Yreka area. 13
3. Greenschist-Facies Mineral Assemblages of Selected Samples of the Schist of Skookum Gulch 25
4. Blueschist-Facies Mineral Assemblages of Selected Samples of the Schist of Skookum Gulch 52
5. Transitional Metamorphic Assemblages of the Schist of Skookum Gulch 63
6. Whole-rock trace element data by INAA for an epidote-sodic amphibole schist, sample UMG 77. 71
7. Trace element contents of tonalite samples SBQD and TGQD . . 88
8. Observed structural elements of blueschist blocks, chert, marble, and plutonic blocks, and greenschist-facies matrix rocks of the Schist of Skookum Gulch 104

A1. List of abbreviations used in Tables A2 - A4 154
A2. Mineral Assemblages of the Horseshoe Gulch Locality. 155
A3. Mineral Assemblages of the No Name Gulch Locality. 157
A4. Mineral Assemblages of the Upper McConaughy Gulch Locality .158

LIST OF PLATES

1. Geologic Map of the McConaughy Gulch & Moffett Creek Areas, Etna, China Mountain and Yreka Quadrangles, Northern California. . . . . map pocket
2. Structure Cross Sections, Callahan-Yreka Area, Northern California. . . . . map pocket
3. Geologic Map of the Horseshoe Gulch Locality, T. 42 N., R. 8 W., SE 1/4, Sec. 4, Etna Quadrangle, Northern California. . . . . map pocket
4. Geologic Map of the No Name Gulch Locality, T. 42 N., R. 8 W., SE 1/4, Sec. 33, Etna Quadrangle, Northern California. . . . . map pocket
5. Geologic Map of the Upper McConaughy Gulch Locality, T. 42 N., R. 8 W., NE 1/4, Sec. 27 & NW 1/4 Sec. 26, Etna & China Mountain Quadrangles, Northern California . . . . map pocket
6. Plan map of blueschist and greenschist blocks in a sheared matrix; outcrops HG1 and HG26. . . . . . . map pocket
7. Plan map of blueschist blocks in a sheared matrix; outcrop HG3. . . . . map pocket
8. Plan map of outcrops UMG73 and UMG74 . . . . map pocket

STRUCTURE AND PETROGRAPHY OF THE SCHIST OF SKOOKUM GULCH, CALLAHAN-YREKA AREA, EASTERN KLAMATH MOUNTAINS, NORTHERN CALIFORNIA

INTRODUCTION

The schist of Skookum Gulch (SSG) is an informal name applied to a fault-bounded belt composed mainly of schistose metamorphic rocks and less abundant sedimentary and igneous rocks located in the eastern Klamath Mountains of northern California. The SSG features outcrops of rocks of the lawsonite-glaucophane, blueschist facies and epidote-sodic amphibole transitional, epidote-blueschist facies (Brown, 1987). Radiometric age-dating suggests that the schist was metamorphosed during the Ordovician. The SSG is the oldest known Paleozoic blueschist-bearing terrane in California and one of the oldest preserved blueschist-bearing terranes in North America. Tonalitic rocks associated with the schist have Early Cambrian ages and are among the oldest rocks yet dated within the Klamath Mountains (Wallin, 1986).

This terrane of blueschist blocks, graphitic schist, quartz-albite schist, quartz-mica schist, greenschist, marble, chert, phyllitic quartzite, and micaceous quartzite, serpentinite, and tonalitic rocks has been interpreted as a tectonic melange by Hotz (1977) and Potter and others (1977). Cotkin and Cotkin (written communication, 1985) view the terrane as an intimately interlayered and interstratified sequence of greenschist, blueschist, and marble which reflects the original sedimentary and volcanic depositional features of the protolith.

Statement of Problem

The SSG is a unique melange belt in the Klamath Mountains in that it contains Early Paleozoic lawsonite-glaucophane blueschist and a variety of other rock types, has a complex deformational history, and varies in structural style. Melanges are still controversial geological entities and their origins and tectonic significance are poorly understood. The SSG thus represents an opportunity to study the structure and formation of an Early Paleozoic melange. The SSG is believed to represent part of an subduction complex (Potter, Hotz and Lanphere, 1981; Lindsley-Griffin and Griffin, 1983; Cotkin and Cotkin, 1985; Cotkin 1986). Field relations, structure, and metamorphic history of the SSG have only been briefly described by previous workers. A fine presentation of conditions of metamorphism, mineral chemistry, and petrology of the schist can be found in Cotkin (1987). The primary purpose of this investigation was to examine in detail the field relations, structure, and petrology of the SSG. Detailed mapping, structural study, and petrographic analysis are needed for a more complete understanding of Early Paleozoic history of the Eastern Klamath terranes and for a better knowledge of blueschist-facies metamorphism. Study of the metamorphic and deformational history of the SSG is important to learn how its tectonic history relates to other coeval rocks in the Klamaths. This thesis will: (1) detail the structural and deformational history of the SSG through analysis of mesoscopic and petrofabric elements; and (2) describe the various lithological units associated with the SSG, their areal distribution, gross morphology, petrology and protoliths.

Location and Accessibility

Rocks associated with the SSG are located in the Yreka-Callahan area of the eastern Klamath Mountains of northern California, and encompass parts of the Etna, Yreka, and China Mountain Quadrangles (Figure 1). As a mappable body, the SSG occurs as a northeast-trending, narrow belt, less than one mile (0.62 kilometers) in east-west direction, and approximately 10 miles (16 kilometers) long. The area of investigation includes the east side of McConaughy Gulch to its head, and both sides of the Moffett Creek drainage from its headwaters northward to Sissel Gulch. Three areas were mapped in detail:

1. Horseshoe Gulch Locality, T. 41 N., R. 8 W., SE 1/4, Section 4.

2. No Name Gulch Locality, T. 41 N., R. 8 W., SE 1/4, Section 33.

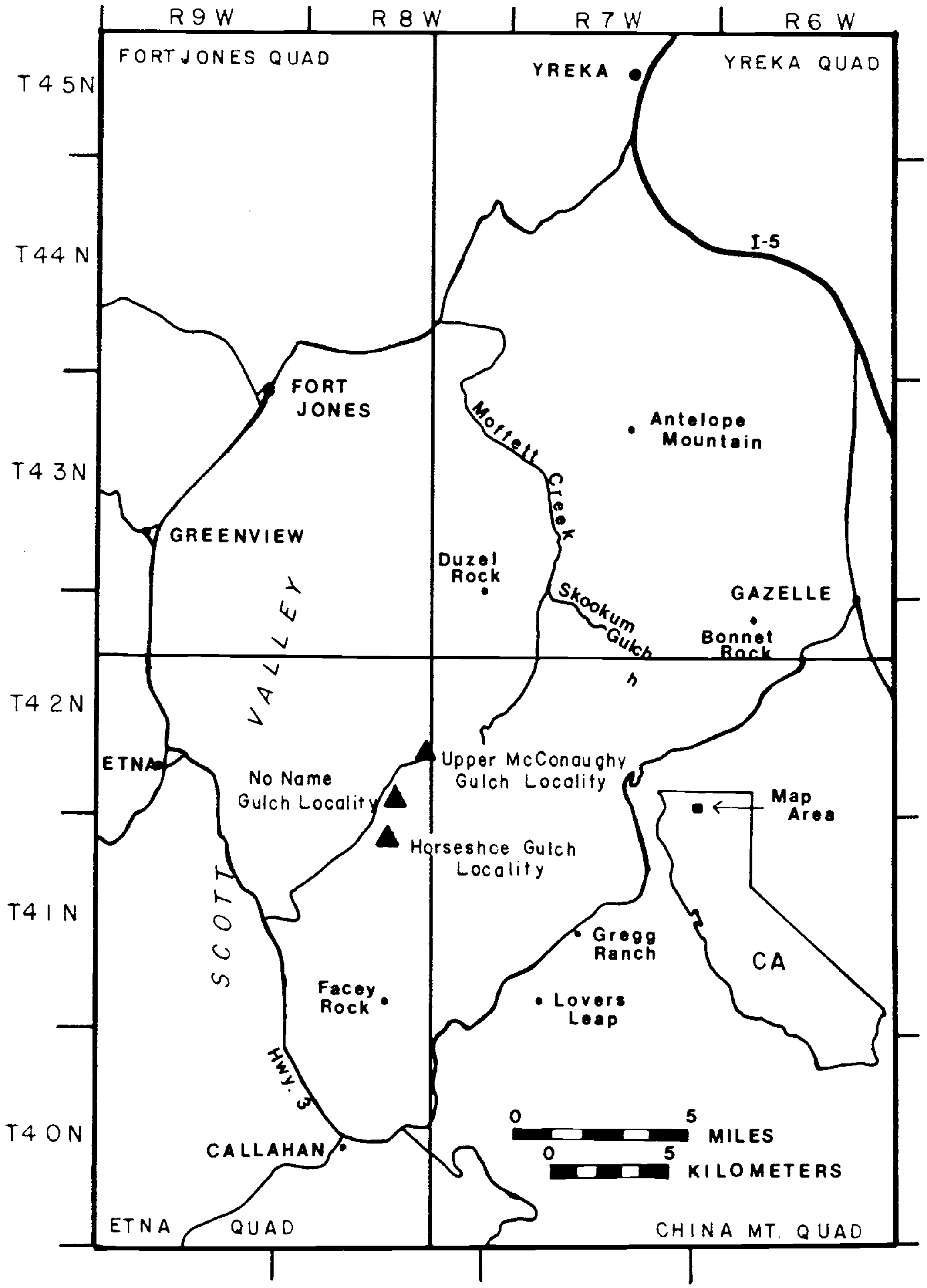

Figure 1. Index map of the Callahan-Yreka area, northern California.

3. Upper McConaughy Gulch Locality, T. 42 N., R. 8 W., NE 1/4, Section 27 and NW 1/4, Section 26.

The majority of the area is privately owned, and the rest is controlled by the Bureau of Land Management. Access to areas in McConaughy Gulch is via California State Highway 3 and local paved and gravel roads through McConaughy Gulch. Access to areas within the upper Moffett Creek drainage is via the Moffett Creek Road, which intersects California Highway 3 approximately 5.7 miles north of the town of Fort Jones. Outcrops are within easy walking distance from the gravel roads.

Topography, Climate, and Vegetation

The lowest elevation in the area of study is 3120 feet (960 m) in McConaughy Gulch and the highest elevation is 5640 feet (1735 m) on Skookum Butte in the upper Moffett Creek drainage, Yreka quadrangle. The maximum topographic relief is 2520 feet (775 m).

The climate of the Scott Valley area is not extreme. Average annual temperature is 50°F (10°C). Temperatures in the summer months are generally in the 80 - 90°F range (26-37°C) and may exceed 100°F (37°C), especially in McConaughy Gulch. Average annual precipitation in the Scott Valley is 52 inches, of which 22 inches (56 cm) are of rain (56 cm) and 30 inches (76 cm) are of snow.

Vegetation over most of the area is characteristic of montane scrub and low chaparral communities. Dominant brush vegetation types include mountain mahogany, *Cercocarpus betuloides*, chamise, deer brush *Ceanothus* species, greenleaf manzanita, and holly bushes *Ilex* species. Western juniper, ponderosa and digger pine, and oak *Quercus* species are the predominant trees noted in the area. Poison oak is common in the dry gulches such as Horseshoe and upper McConaughy Gulch.

Exposures

The rock exposures generally are poor. Outcrops can be found most commonly in creek beds and gullies, along roads, on ridge crests, and on south-facing slopes. North-facing slopes are steep, densely covered with oak and pine trees, and have sparse, widely scattered small outcrops. Ridge tops have better outcrops, but contact relations are obscured by regolith and vegetation. The Moffett Creek road cuts through the SSG in several locations and exposures are good. Otherwise, the Moffett Creek area is characterized by very steep slopes (80-100%), dense tree cover, and timber slash which hides the few outcrops that exist. The best exposures of the SSG are found in south- and southwest-facing slopes in McConaughy Gulch. These slopes are moderately steep, (35-40%), and are less vegetated. Erosion has removed slope deposits so that contact relationships between outcrops can be viewed.

Methods of Investigation

Field work was carried out from July to mid-September 1985 and July to mid-August 1987. Preston Hotz's (1978) geologic map of the Yreka Quadrangle and parts of the Fort Jones, Etna, and China Mountain quadrangles was used as the base map for this study. Preliminary field reconnaissance, mapping, and lithological sampling were conducted at localities where blueschist blocks had been noted by Hotz. Three localities with exceptional exposure and variety of lithologies were selected for intensive study and detailed mapping. These areas were mapped at a scale of 1 inch to 100 feet using measuring tape and an Abney topographic level.

Representative samples of different lithologies were collected for petrographic and geochemical analysis. More than one hundred thin sections were prepared and examined as part of this study. Areal mapping in combination with petrographic studies shows the relationship of blocks of different lithologies and metamorphic grade to the enclosing matrix rocks. Map relations are shown on Plates 3, 4 and 5. Rock samples collected by me and mentioned in the text have the prefixes HG, NNG, UMG and MC which refer to the Horseshoe Gulch, No Name Gulch, and Upper McConaughy Gulch localities, and the Moffett Creek area, respectively.

Thin sections and slabs of igneous lithologies were stained for potassium feldspar to aid in point counting. Ten whole rock and separated mineral powders were analyzed using an X-ray powder diffractometer to verify the presence of key mineral phases. Three samples of limestone weighing a total of 39 pounds (17.7 kg) were dissolved in acid and analyzed for conodonts and insoluble residues. Three samples, two of tonalite and one of epidote-sodic amphibole schist were chemically analyzed for trace and rare-earth elements using instrumental neutron activation analysis at the Radiation Center, Oregon State University.

Previous Work

An Ordovician greenschist unit and an Ordovician trondhjemite unit were first recognized in the Moffett Creek area by Hotz (1974) in his preliminary map of the Yreka Quadrangle (1:62,500 scale). In Hotz's later bulletin (1977) and map (1978) of the Yreka quadrangle and parts of the Fort Jones, Etna and China Mountain quadrangles, (1:62,500 scale) the mappable extent of these units was enlarged. Hotz describes the units as follows:

> A terrane of greenschist, siliceous metamorphic rock, and blueschist, in which discontinuous bodies of limestone and large blocks of altered quartz diorite and trondhjemite of Ordovician(?) age occur, is exposed in a window beneath the Mallethead thrust. The terrane is interpreted as a metamorphosed tectonic melange (Hotz, 1977, p. 2).

These rocks were informally designated as the schist of Skookum Gulch by Potter and others (1977, p. 424).

Ted Zdanowicz (1971) mapped much of the Horseshoe and McConaughy Gulch area. He correlated the finely foliated, dark green, quartz- and chlorite-rich phyllites (SSG) with the Late Triassic Stuart Fork Formation. His "Unnamed Arkose" unit, consisting of quartz- and feldspar-rich unbedded rocks corresponds to the quartz diorite and trondhjemite unit mapped by Hotz. Zdanowicz also noted and described some of the limestone blocks faulted into phyllites (SSG) that are found in Horseshoe Gulch.

Potter and others (1981) reported an Ordovician to Early Silurian metamorphic age for two samples of the SSG. White mica from a semi-schist has a K-Ar date of 439 ± 13 Ma and a crossite-bearing schist has a K-Ar date of 451 ± 14 Ma.

Spencer J. Cotkin, Mary L. Cotkin, and Richard L. Armstrong have conducted petrographic, geochemical, mapping and isotopic-dating studies of the SSG. Mary L. Cotkin mapped and collected rock samples in 1984 from the Horseshoe Gulch area, T. 41 N., R. 8 W., Section 4, and T. 42 N., R. 8 W., Section 33, which corresponds to my No Name Gulch Locality. The abstracts and articles by Cotkin and Cotkin (1985), S. J. Cotkin (1986), S. J. Cotkin and Armstrong (1987) and S. J. Cotkin (1987) report on the results of their investigations.

E. Timothy Wallin (Wallin and others, 1988; Wallin, 1986) has dated two samples of tonalitic rocks within the SSG by U-Pb methods on zircons. The two samples give Early Cambrian crystallization ages for the tonalite. Other dating efforts by Wallin (Wallin and others, 1988; Wallin, 1987; Haessig, and others, 1987) using U-Pb methods on zircon fractions have constrained the ages of other igneous, metamorphic, and sedimentary rocks in the Callahan-Yreka area. The results of these dating efforts are shown in Table 1.

Table 1. Age constraints of selected major units in the Callahan-Yreka area

UNIT	AGE	REFERENCE
Moffett Creek Formation	Silurian or Ordovician	Potter and others (1977); Hotz (1977); Rohr (1977); Irwin and others (1978)
Duzel Formation	Devonian metamorphic age ($^{40}Ar/^{39}Ar$ metamorphic ages 350-392 Ma)	Cashman (1980)
	Late Ordovician to Early Silurian protolith(?) (U/Pb bulk detrital zircon age, 465 Ma)	Wallin, oral communication, 1987
Sissel Gulch Graywacke	Late Ordovician to Early Silurian($^{207}Pb/^{206}Pb$ detrital zircon ages, 432-444 Ma)	Wallin, written communication, 1987
Sedimentary and Volcanic Rocks of Horseshoe Gulch	Ordovician and Silurian	Potter (1982); Potter and others (1977)
Schist of Skookum Gulch	Late Ordovician to Early Silurian metamorphic age (K-Ar date on white-mica schist, 439 $\pm$ 13 Ma; on a crossite-bearing schist, 451 $\pm$ 14 Ma)	Potter and others (1981)
	(Rb-Sr phengite-whole-rock date, on a quartz-albite schist, 447 $\pm$ 9 Ma, metamorphic age; Rb-Sr whole-rock age, 467 $\pm$ 45 Ma, protolith formation)	Cotkin and Armstrong (1987)
Tonalite of Schist of Skookum Gulch	Early Cambrian (U/Pb upper intercept age of 565 $\pm$ 5 Ma.)	Wallin and others (1988)

REGIONAL GEOLOGY

The Klamath Mountains Province of northwestern California and southwestern Oregon is subdivided into four concentric lithologic belts (Irwin, 1960). These belts (also known as subprovinces) are progressively younger to the west; they are: (1) the Eastern Klamath subprovince, (2) the Central Metamorphic subprovince, (3) the Western Paleozoic and Triassic subprovince and (4) the Western Jurassic subprovince (Figure 2).

The study area is in the Callahan-Yreka portion of the Eastern Klamath subprovince. The Callahan-Yreka locale is comprised of Cambrian-Devonian sedimentary, metamorphic, and igneous rocks structurally overlying the Trinity Ultramafic Complex. The Callahan-Yreka area is bordered on the east by Cretaceous and younger sediments and volcanics of the Shasta Valley and on the west by rocks of the Central Metamorphic belt.

Rocks in the northern part of the Eastern Klamath subprovince have been grouped into several tectonostratigraphic terranes by different workers. The "Callahan terrane" is the name given to the Early Paleozoic rocks overlying the Trinity ultramafic mass in the Yreka-Callahan-Gazelle area by Churkin and Eberlein (1977). The "Trinity terrane" of Lindsley-Griffin and Griffin (1983) refers to allochthonous Ordovician-Devonian rock assemblages overlying and including the Trinity ophiolite. The Ordovician to Devonian sedimentary, metamorphic, and volcanic rocks comprising imbricate thrust sheets in the Yreka-Callahan-Gazelle area have been termed the "Yreka terrane" by Silberling and others (1987). The "Eastern Klamath terrane" of Irwin (1985) includes the Trinity ophiolite and the Paleozoic to Jurassic volcanic-arc rocks that overlie it.

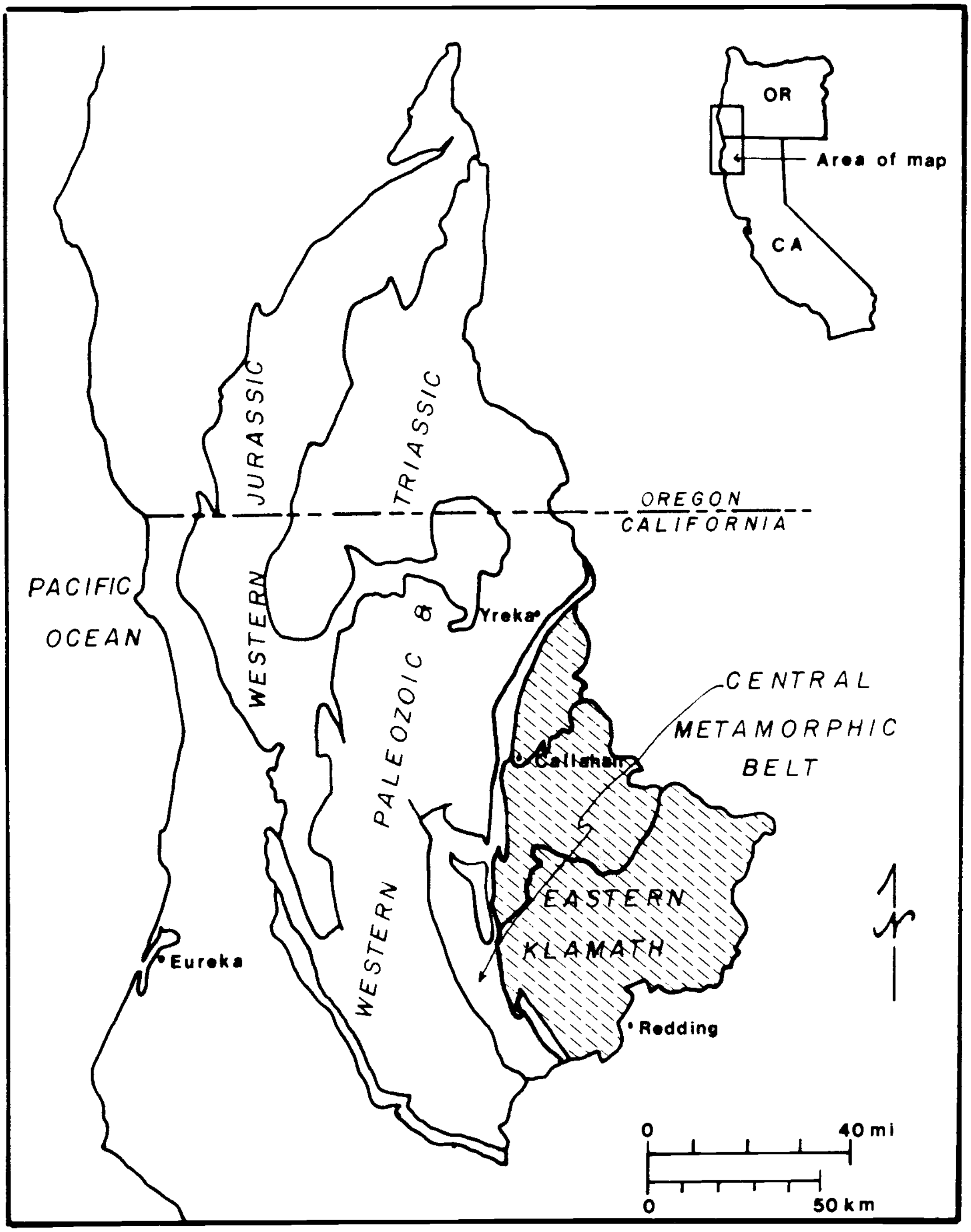

Figure 2. Subprovinces of the Klamath Mountains province (after Irwin, 1966, and Cashman, 1977).

LOCAL STRATIGRAPHY

Paleozoic sedimentary, metamorphic, and igneous rocks in the Callahan-Yreka area of the Eastern Klamath terrane in the vicinity of the SSG are shown in Figure 3. Rocks of this subprovince were assigned by Wells, Walker and Merriam, (1959) to the Upper Ordovician(?) Duzel and Upper Silurian Gazelle Formations. The west-dipping fault contact between the two formations became known as the Mallethead Thrust (Churkin and Langenheim, 1960). Subsequent geologic investigations by other workers have revealed a complex stratigraphy and structural history for the area. New lithologic units and formations have been defined, correlations between units have been expanded and ages of rock units have been further constrained. For further details on the stratigraphic relationships, lithology, and structural characteristics of many units in the Callahan-Yreka-Gazelle area, the reader is directed to Hotz (1977), Potter and others (1977), and Rohr (1977).

Age relationships of selected major lithologic units in the Callahan-Yreka area are shown in Table 1. The SSG is bounded on the west by the Duzel Phyllite and Sissel Gulch Graywacke. The contact has been mapped as the Mallethead Thrust fault which is west-dipping. In the study area, the Mallethead Thrust places the Duzel Phyllite and Sissel Gulch Graywacke structurally over the SSG. The SSG is in fault contact on its eastern boundary with the sedimentary and volcanic rocks of Horseshoe Gulch and the Moffett Creek Formation.

Rock units in the Callahan-Yreka area have been formally named and defined by Hotz (1974, 1977, 1978). In this study, the nomenclature used by Hotz (1978) will be closely followed. However, different stratigraphic nomenclature has been used by various workers (see Table 2), which reflects their tectonic or structural interpretations. The structural and tectonic interpretation of the Duzel Phyllite, offered by S. M. Cashman is most pertinent to this study.

Cashman (1977, 1980) studied the Duzel Phyllite of Hotz (1974, 1977), a narrow band of unnamed amphibolite along the western edge of the Duzel Phyllite, and the Schulmeyer Gulch sequence. Based on similarities in structural style and metamorphic age, she concluded

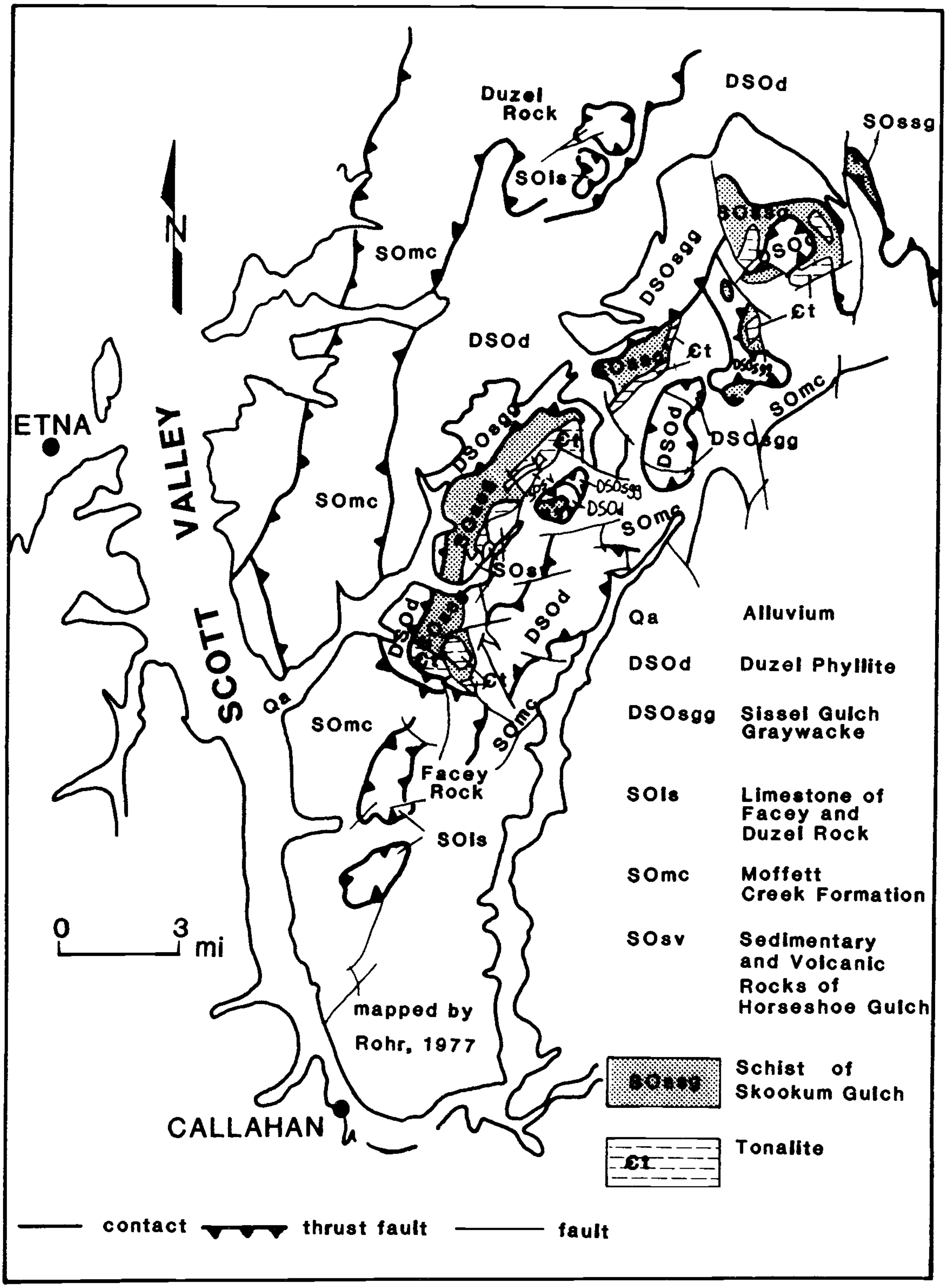

Figure 3. Geology of part of the Callahan-Yreka area, modified from Hotz (1978) and Potter and others (1977).

Table 2. Correlation of stratigraphic nomenclature in the Callahan-Yreka area

UNIT	Hotz (1978)	Potter, Hotz and Rohr (1977)	Cashman, (1977, 1980)	Lindsley-Griffin and Griffin (1983)	This study
			REFERENCE		
Moffett Creek Formation	Smc: Moffett Creek Formation	SOms: Moffett Creek Formation, siliceous siltstone member SOmc: Moffett Creek Formation, disrupted calcareous siltstone member	ms: Moffett Creek Siltstone	Smc: Moffett Creek Formation	SOmc: Moffett Creek Formation
Duzel Formation	Od: Duzel Phyllite	SOd: Duzel Phyllite	(correlates with Grouse Ridge Formation) Ddp: Duzel Phyllite Du: umdifferentizted Duzel Phyllite, marble, and amphibolite Du?: Callahan chert, quartzite, and mudstone	Od: Duzel Phyllite	DSOd: Duzel Phyllite
Sissel Gulch Graywacke	Os: Sissel Gulch Graywacke	SOs: Sissel Gulch Graywacke	——————	Os: Sissel Gulch Graywacke	DSOsgg: Sissel Gulch Graywacke
Sedimentary and Volcanic Rocks of Horseshoe Gulch	SOs: Sedimentary Rocks of Horseshoe Gulch SOv: Volcanic Rocks of Horseshoe Gulch	SOvs: Sedimentary and Volcanic Rocks of Horseshoe Gulch	——————	OSDm: Gregg Ranch Melange	SOs and SOv: Sedimentary Rocks and Volcanic Rocks of Horseshoe Gulch
Schist of Skookum Gulch	Ogs: Greenschist of Skookum Gulch	SOsh: Schist of Skookum Gulch	——————	OSm: Skookum Gulch melange	SOssg: Schist of Skookum Gulch
Tonalite	Oqd: Quartz-diorite, trondjhemite	Oqd: Quartz-diorite, trondjhemite	——————	——————	£t: tonalite

Notes: Stratigraphic units in the vicinity of the SSG are listed. Some units are present in the area studied; where absent, they are represented by dashed lines.

that: (1) all three aforementioned units belong to one Duzel Formation; (2) these greenschist-facies to lower amphibolite-facies rocks were deformed and metamorphosed in Devonian time as part of the Central Metamorphic Belt; and (3) shared lithologies, deformational features, structural trends, grade of metamorphism and metamorphic age suggest correlation of these rocks with those of the Grouse Ridge Formation in the Central Metamorphic Belt. Cashman's conclusions are of significance to this study in two ways. Cotkin and Armstrong (1987) reported a date of 357 $\pm$ 18 Ma from a four-point mineral isochron on a sample of glaucophane schist from the SSG. They interpreted this date as a resetting of the low-Rb/Sr rock due to metamorphism, possibly related to Devonian metamorphism of the Central Metamorphic Belt. If this is true, then the SSG melange must have been emplaced prior to the Devonian metamorphic event and was thermally reset during juxtaposition with the Duzel Phyllite.

FIELD RELATIONS

Definition of Melange and its Application to the SSG

Many definitions of the term melange have been proposed and used by different workers. Various definitions of melange have been offered (for example, Cowan, 1974; Silver and Beutner, 1980, and Raymond, 1975, 1984). The definition of the term melange offerred by Raymond (1984, p. 7) is most apropos for the SSG and is paraphrased below:

> a melange is a mappable body of rock, lacking internal continuity of contacts or strata and containing fragments and blocks of all sizes, both exotic and native, embedded and enclosed in a sheared, fragmented matrix.

As applied to the SSG, exotic blocks include blueschist facies and transitional blueschist to greenschist facies rocks. "Exotic" blocks within the SSG are differentiated from the matrix and other "native" blocks in the matrix by their high pressure - low temperature metamorphic history and deformation style. "Exotic" as used here is not meant to imply an origin far removed from that of the melange matrix, nor does it imply that protoliths and time of metamorphism were necessarily different from those of the melange matrix.

Characterization of the SSG Melange

The SSG is a complex melange composed of metavolcanic, metacarbonate, and metasedimentary blocks and lenses of diverse sizes and shapes dispersed without apparent stratigraphic coherency in a sheared matrix of clastic to pelitic schist, metavolcanic schist, and discontinuous, thin lenses of marble. Rocks of the matrix have been metamorphosed to chlorite-grade greenschist facies, whereas the blocks have been metamorphosed in a variety of pressure-temperature conditions. Some blocks have been feebly metamorphosed and retain features of the orginal protolith material; others have been thoroughly recrystallized under greenschist, blueschist and transitional blueschist facies conditions (Turner, 1981, p. 321).

Rock Types and Field Relations of the Matrix

Rock types comprising the matrix are predominantly medium- to coarse-grained quartzo-feldspathic schist, graphitic schist and minor quartz-mica schist. Laminated marble is commonly interlayered with graphitic and quartzo-feldspathic schist (Figure 4). Greenschist, derived from volcanic flows and volcaniclastic rocks, are volumetrically less abundant as a matrix component. In comparison to the blocks types discussed, matrix lithologies are more coarse-grained and have a rough cleavage. Matrix rocks have a less complicated deformational history. Small-scale, isoclinal, rootless, intrafolial folds of quartz + albite suggest that an original metamorphic layering has been transposed to form the pervasive foliation. Exposures of the matrix show that the steeply dipping to vertical foliation is sheared, contorted, and undulatory; foliations anastomose around or end abruptly against more competent blocks of blueschist and marble. Structural attitudes of the blocks are similar to those of the matrix; the dominant foliation of most, but not all of the blocks is steeply dipping and roughly parallel to the matrix foliation. The parallel alignment of the blocks and matrix may be the result of shear forces during emplacement of the melange.

Rock Types and Field Relations of Blocks

Exposures of blocks range from equant blocks several feet in dimension (Figure 5) to elongate lenses several feet to hundreds of feet in their longest dimension, (UMG 62, UMG 63). Blocks are several feet to several tens of feet in height (MC 98).

Rock types found as blocks in the matrix include: schistose to massive blueschist and transitional blueschist of metavolcanic, metasedimentary and metacarbonate origin, greenschist of metavolcanic protolith, recrystallized chert, marble, micaceous quartzite, and tonalite. Of these types, blueschist, transitional blueschist and marble blocks are most abundant in the melange (Figure 6). Single blocks and large bodies of marble are a conspicuous feature of the melange. Laminated and massive dolomite and laminated calcite marble

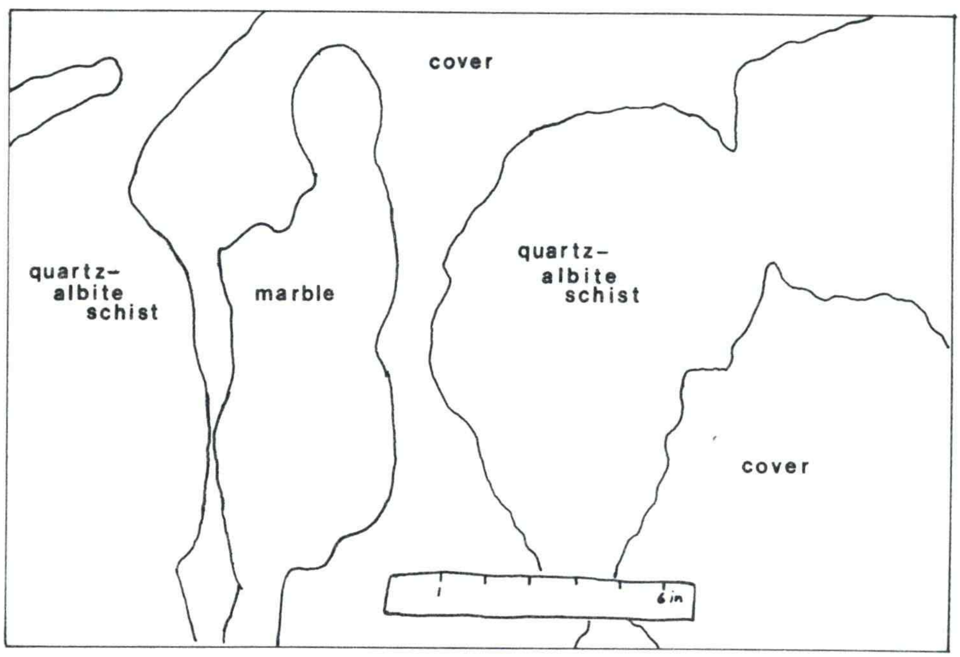

Figure 4. Thin lens of marble interlayered with quartz-albite schist matrix. 16 cm (6.5 inch) ruler for scale. Matrix enclosing outcrop HG 3.

Figure 5. Isolated blueschist block in a poorly exposed greenschist matrix. 16 cm (6.5 inch) ruler for scale. Outcrop HG 5.

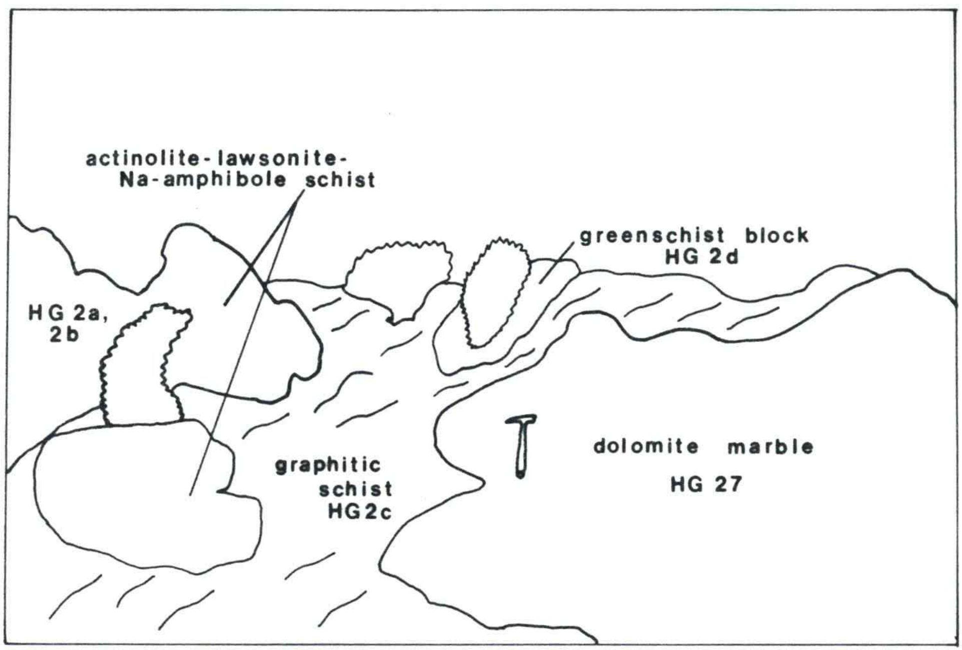

Figure 6. Field relations between blueschist and massive marble blocks and graphitic schist and greenschist matrix lithologies. Hammer for scale. Outcrops HG 2A, 2B, 2C, 2D and 27.

are the most common types. Graphitic schist, quartzo-feldspathic schist and greenschist may be interlayered with the marble exposures. Much of the marble has been metamorphosed to chlorite grade of the greenschist facies. However, sodic amphibole-lawsonite-calcite marble does occur in the SSG in the No Name Gulch locality (NNG 34). Locally, epidote-sodic amphibole schist occurs interlayered with marble (Figure 7). Thus, some of the marble has been metamorphosed in high P/T conditions.

In general, blueschist block types are very fine-grained and dense; schistose lithologies are very finely foliated, complexly folded and have multiple cleavages as well as ductile and brittle shear structures. Greenschist, blueschist, and transitional blueschist facies blocks as well as marble are enclosed by clastic and pelitic schist and metavolcanic schist (greenschist). Mapping and reconnaissance field survey has not revealed any coherent pattern to the distribution of blocks; exposures of metavolcanic and metasedimentary blueschist-facies blocks occur throughout the terrane, although the metasedimentary blocks are more rare. In addition, there are no patterns in the distribution of different types of blueschist-facies blocks. For example, rocks bearing lawsonite-sodic amphibole assemblages are found randomly throughout the SSG, as are rocks of transitional blueschist facies, containing epidote-sodic amphibole $\pm$ calcic amphibole assemblages. Most blocks are discontinuous; their random occurrence throughout the areas studied indicates that relict stratigraphy is not preserved.

One fault-bounded block containing blueschist-facies rocks occurs as a mappable, interlayered unit in the No Name Gulch locality (Figure 8). Three distinct rock types, distinguished by their predominant mineral constituents, occur interlayered with one another in thicknesses ranging from 5 to 100 feet. The three rock types include sodic amphibole-lawsonite-calcite marble, exposures of greenish-gray sodic amphibole-bearing lawsonite-actinolite schist, and blocks of bluish-gray actinolite-lawsonite-sodic amphibole schist. The fault block is interpreted as an interlayered sequence of limestone and volcanic flows or volcaniclastics that were metamorphosed together under blueschist facies conditions and tectonically emplaced as a

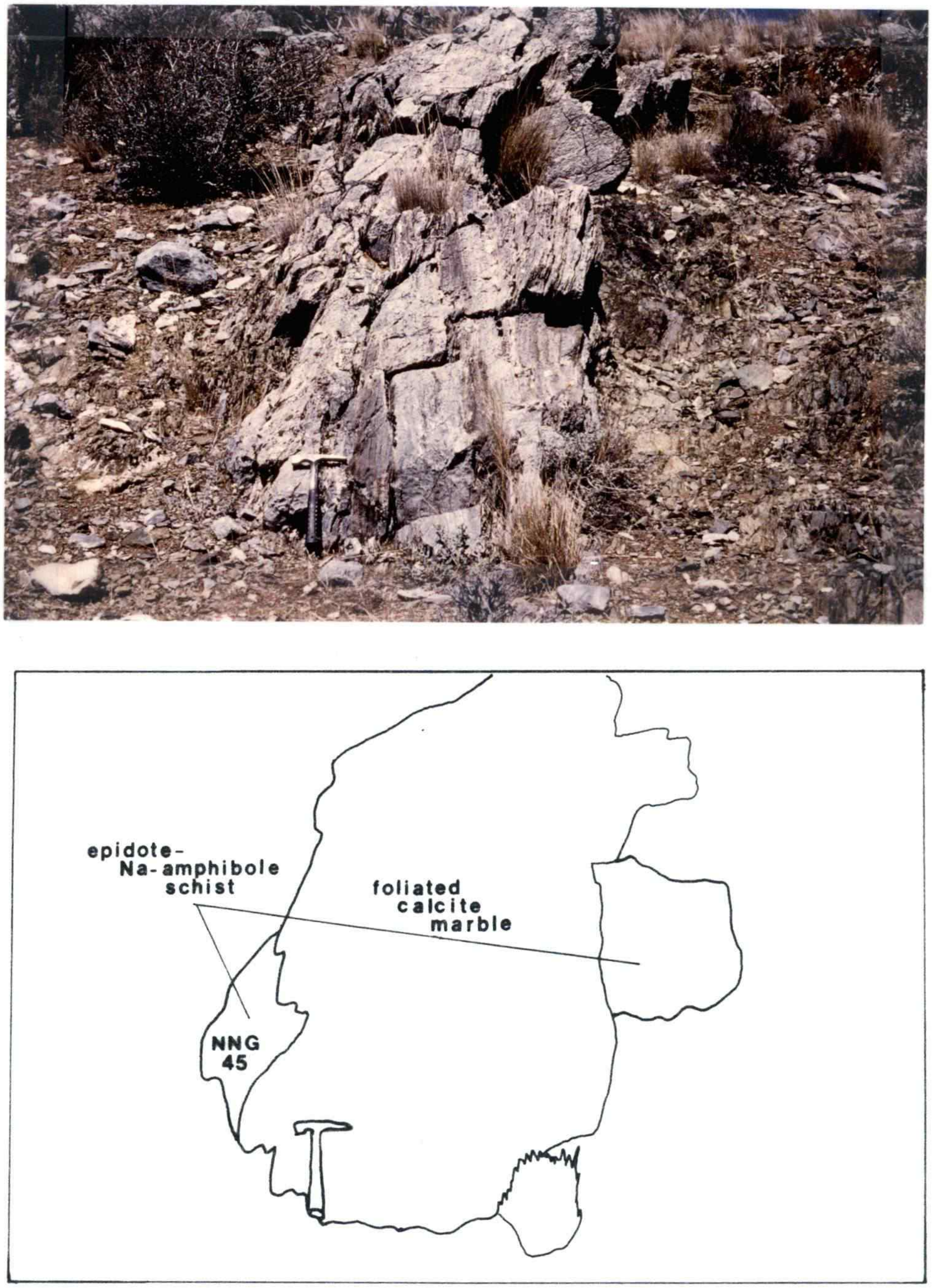

Figure 7. Epidote-sodic amphibole schist interlayered with foliated calcite marble. Hammer for scale. Outcrop NNG 45.

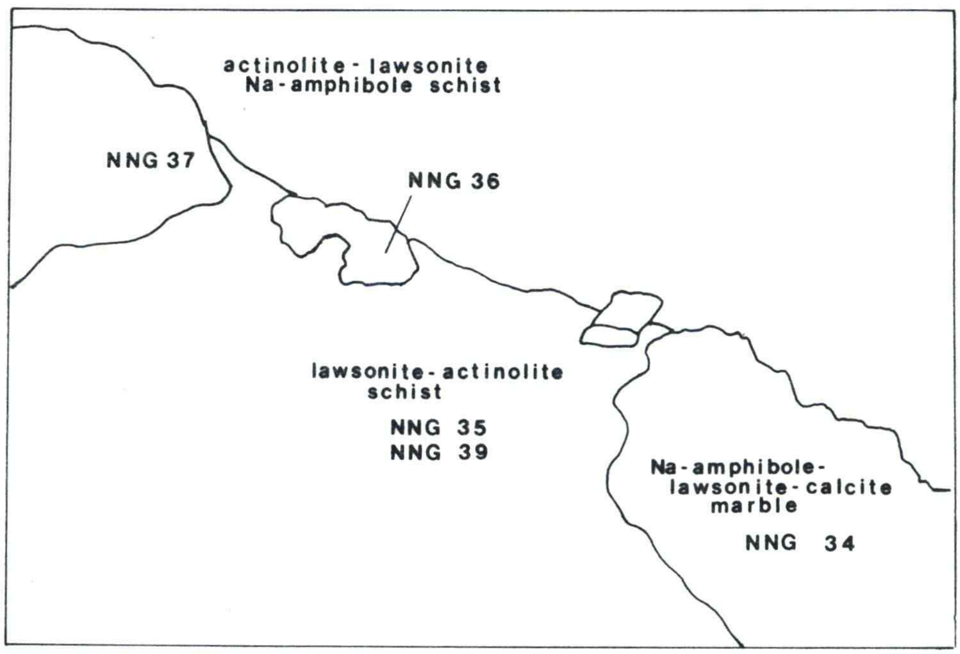

Figure 8. Interlayered sequence of sodic amphibole-lawsonite-calcite marble, poorly exposed sodic amphibole-bearing lawsonite-actinolite schist and dark colored actinolite-lawsonite-sodic amphibole schist. Backpack for scale. Outcrops NNG 34, 35, 36, 37, 39.

coherent fault block in the melange.

Relative Proportions of Rock Types in the SSG

The most common rock types of the melange matrix, in order of decreasing abundance, are quartz-albite schist, graphitic schist, greenschist and marble lenses interlayered with quartz-albite schist and graphitic schist. Together, these rocks comprise roughly 60% of the melange. Minor components of the matrix are quartzose phyllite and quartz-mica schist that make up about 10%. The various blocks found in the melange are enclosed by the matrix and are estimated to comprise 30% of the total estimated volume proportion, with matrix rocks making up the bulk of the rocks present, approximately 70%. Blueschist blocks comprise about 5% of the total proportion of blocks. Marble blocks are most abundant and make up about 12% while the various greenschist blocks, for example, actinolite schist, micaceous quartzite and laminated chert together comprise about 3% of the total estimated volume of block types. Large fault blocks of tonalite comprise roughly 10% of the of the total volume in the melange.

GREENSCHIST-FACIES ROCKS OF THE MATRIX

The following chapter provides detailed descriptions of the lithology and petrology of the various rock types in the SSG melange matrix. Rock types include graphitic schist, quartz-albite schist, quartz-mica schist, quartzose phyllite, phyllite, and greenschist. Typical mineral assemblages of the various lithologic types are in Table 3.

Rock types designated in this thesis are defined by their most abundant or characteristic mineral constituents with the dominant or characteristic mineral species closest to the rock name. Examples are quartz-mica schist and graphitic schist. When a particular mineral assemblage of a rock is presented, the most abundant mineral will be listed first with associated minerals following in order of decreasing abundance. Thin sections of metamorphic rocks were not point counted; modal proportions of particular mineral phases were estimated by visual inspection of thin sections.

Quartz-Albite Schist

Light yellowish-gray to yellowish-brown quartz-albite schist is the dominant constituent of the melange matrix. Exposures are found in all three localities studied. Outcrops stand at most 4 feet high; most exposures are low-lying, standing no more than 1 foot above the ground surface. Foliation surfaces are undulatory, and steeply dipping. Soil associated with the quartz-albite schist is light olive-gray to yellow-brown in color.

Foliation is defined by a segregation banding consisting of alternating layers of quartz + albite and white mica + chlorite. Layer thickness ranges from 0.5 to 2.5 mm. Average grain size of xenoblastic quartz and albite is roughly 0.4 mm. Individual grains are rarely greater than 1 mm in their greatest dimension.

Typical quartz-albite schist (Figure 9) contains the mineral assemblage quartz + albite + white mica + chlorite + hematite $\pm$ calcite, sphene, garnet, apatite, zircon, tourmaline, rutile, graphite, magnetite, and pyrite. Xenoblastic quartz is generally more abundant

Table 3. Greenschist-Facies Mineral Assemblages of Selected Samples of the Schist of Skookum Gulch

	METASEDIMENTARY ROCKS										METAVOLCANIC ROCKS					
	GRAPHITIC SCHIST		QUARTZ-ALBITE SCHIST				QUARTZ-MICA SCHIST	QUARTZOSE PHYLLITE	MICACEOUS QUARTZITE		GREENSCHIST					ACTINOLITE SCHIST
QUARTZ	X	X	X	X	X	X	X	X	X	X	X	X	X	X	X	m
ALBITE	X	X	X	X	X	X	X	plag	tr		X	X	X	X	X	X
CHLORITE	X	X	X	X	X	m	X	X	X	X	X	X	X	X	X	X
WHITE MICA	X	X	X	X	X	X	X	X	X	X	m	X	X	X	m	m
EPIDOTE & CLINOZOISITE		tr						m			X	X	X	m	X	X
CA-AMPHIBOLE																
NA-AMPHIBOLE											ia	ia	ia			
SPHENE		m	m			tr		m			X	X	X	X	X	X
CALCITE	X,sv	X,sv		X,sv	X,sv						tr	tr	X,sv	X,sv		X,sv
HEMATITE	m	m	m	m	m	m	m	m	m	m	m	m	m	m	m	m
GRAPHITE	X	X														
OPAQUE					tr	X		m		tr					m	
CLINOPYROXENE																rlc
GARNET						X			X	tr						
STILPNOMELANE																
APATITE		tr	m	m	m	tr	tr			tr			m	m	m	
ZIRCON	tr	tr	m	tr	tr	tr	tr	tr		tr	tr	tr	tr	m	tr	
TOURMALINE			m	tr	tr	tr	tr		tr	tr	tr		tr			
RUTILE			tr	tr	tr											
PUMPELLYITE									sv							
PYRITE				tr			tr				tr	tr	tr	m		
Sample	UMG 64 mat	HG 2c mat	NNG 43 mat	NNG 47 mat	HG 20 mat	HG 82 blk	UMG 69 mat	MC 96 mat	UMG 56 blk**	NNG 48 blk	UMG 55 blk	UMG 66 mat	UMG 71 mat	NNG 33c mat	HG 2d blk	UMG 70 blk

Notes: Abbreviations are: mat = melange matrix; blk = tectonic block in melange; X = mineral present; m = mineral present in minor amounts, 1-5%; tr = mineral present in trace amounts, < 1%;: ia = inclusions in albite; rlc = relict mineral; sv = secondary mineral present in veins; plag = plagioclase feldspar; ** = metachert

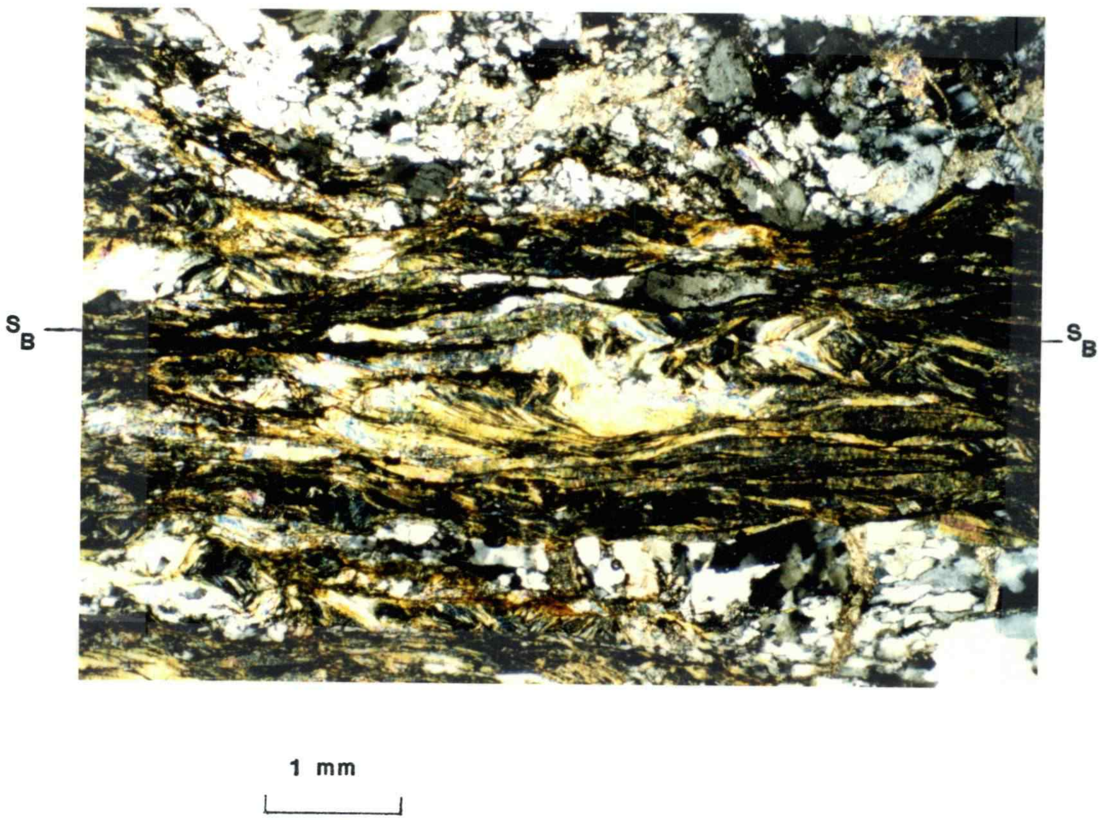

Figure 9. Photomicrograph of a quartz-albite schist, sample HG 15. The foliation, S_B, is defined by white mica. The rock displays a domainal fabric with cleavage domains of white mica and minor chlorite bounded by quartz + albite microlithons, where there is a less continuous cleavage. 20X, XP, FOV = 6.7mm

than albite in the schist; the proportion of quartz and albite together is greater than 50% of the estimated mode in most samples. Mica totals at least 30% of the total abundance. White mica is more abundant than chlorite.

X-ray diffraction studies and electron probe microanalysis by Cotkin (1987) have shown that the white mica is phengitic in composition and contains a significant celadonite component. Some chlorite patches are reddish-brown to yellowish-brown and may be oxychlorite. Patches of calcite occur interstitially with other minerals and as a secondary vein mineral. Tourmaline with brown to green pleochroism is found in most quartz-albite schists. Tiny idioblastic to subidioblastic garnet is present in some schist and is fairly abundant in sample HG 82[1]. Very fine, yellowish-brown to reddish-brown rutile needles also are found distributed throughout most schists, along with apatite and zircon.

Thin sections and cut hand samples show intrafolial folds of quartz + albite + mica. These folds provide evidence of transposition of the original mineralogic layering to form the present folation. A mineral lineation, defined by stretched albite + quartz, occurs oriented roughly parallel to the fold axes of the microfolds. Some samples, (NNG 43, HG 20), show widely spaced asymmetrical, small-amplitude kink folds. The kink folds are probably associated with the latest fold generation; recrystallization did not accompany this fold event.

Abundant quartz associated with albite and micas indicates that the protolith was a quartzo-feldspathic sediment, possibly quartz-rich graywacke or silty arkosic sandstone. The mineral assemblage is characteristic of low-grade greenschist metamorphism of pelitic rocks.

Graphitic Schist

Gray to greenish-gray graphitic schist occurs as a minor constituent of the melange matrix. Exposures of graphitic schist are

[1]A garnet mineral separate from this sample has been sent for isotopic dating by U-Pb methods to E. T. Wallin.

found in all three localities mapped. A typical outcrop (UMG 64) is exposed in a road cut in the Upper McConaughy Gulch Locality. Graphitic schists occur as foliated lenses in gradational contact with the predominant mostly nongraphitic, quartz-albite schist matrix.

The schists are medium-grained with the average grain size of quartz and albite about 0.2 mm. Graphitic schists have a well-developed segregation banding defined by alternating quartzo-feldspathic microlithons 1-4 mm in thickness bounded by chlorite-white mica-graphite cleavage domains about 2 mm or less in thickness. Graphitic films are concentrated in the micaceous zones and give schistosity surfaces a dark gray color. The gray color and presence of graphite (5-10% of the estimated modal proportion) distinguish this rock type from other metasedimentary rocks of the matrix.

These rocks contain the mineral assemblage quartz + albite + white mica + chlorite + graphite + hematite + calcite. Accessory minerals include sphene, clinozoisite, apatite, zircon, tourmaline and pyrite. Xenoblastic quartz is the major phase in all rocks constituting approximatly 30-40% of the modal volume. Quartz exhibits undulatory extinction and sutured grain boundaries. Xenoblastic albite is also found but is somewhat less abundant than quartz. Together, quartz + albite comprise greater than 50% of the estimated modal proportion in thin sections. Inclusion trails of graphite $\pm$ clinozoisite occur in albite porphyroblasts and are generally concordant with foliation. The proportion of white mica and chlorite typically is 15-30% of the estimated mode. Parallel alignment of micas defines the foliation. Calcite occurs as a stable mineral of the assemblage, and in secondary fractures cutting the foliation at a high angle. Xenoblastic sphene occurs in some samples, concentrated in micaceous zones, and locally forms trails of numerous grains aligned parallel to foliation. Brown and green pleochroic tourmaline occurs in places as a trace mineral and is particularly abundant in sample HG 10C.

The assemblage is typical of fully recrystallized low-grade, chlorite-zone greenschist-facies rocks. The protoliths of these graphitic schists are probably quartzo-feldspathic sedimentary rocks with organic and silt-clay constituents.

Intrafolial folds of quartz + albite + mica occur within the prominant foliation. The dominant foliation is interpreted to be a tranposed foliation of an original mineral layering.

Quartz-Mica Schist

Lenses of finely foliated, light yellowish-brown quartz-mica schist are found at the Upper McConaughy Gulch Locality (UMG 69). This lithology contains the same mineral components as the quartz-albite schist but is differentiated by its much finer foliations, discrete compositional banding, and a golden sheen on micaceous cleavage surfaces. Quartz-mica schist is a relatively minor matrix component and has gradational contacts with the more coarse-grained quartz-albite schist lithology.

Quartz-mica schist has a well-defined compositional layering. Mica cleavage domains composed of white mica and minor chlorite may be up to 1 mm in width. Quartz microlithons are generally less than 0.8 mm in thickness and contain minor white mica and chlorite flakes. Micas comprise at least 50% of the estimated mode in thin sections: quartz makes up no more than 40% of the mode. Albite poikiloblasts filled with prismatic inclusions of indeterminate mineralogy are generally confined to mica layers. The inclusion trails vary in aspect and are discordant to the dominant foliation in the rock. Flattened albite poikiloblasts range in size from 0.05 to 0.15 mm. Tails of the albite poikiloblasts contain quartz, which has developed in pressure shadows. Individual quartz grains in the microlithons are 0.01 to 0.25 mm in size; some of the grains are ribbon-like and may be 0.5 mm in length. The quartz is strained and has serrated grain boundaries.

Mineral assemblages typical of quartz-mica schist are white mica + albite + chlorite + hematite $\pm$ accessory minerals zircon, apatite, and tourmaline. A reddish-brown amorphous material (goethite, hematite?) coats the white mica, giving it a yellowish-red color. The mineral assemblage is indicative of chlorite-grade greenschist-facies metamorphism of pelitic sediments.

Quartz-mica schists show several planar and linear elements that are found in other matrix rocks. Because of the abundance of mica and well-developed foliations these elements are much more easily seen than in the quartz-albite schists which are more coarse-grained. Schistosity surfaces show a mineral lineation defined by parallel alignment of white mica. The presence of helicitic inclusions in albite discordant to the dominant foliation indicate that albite grew during or soon after the development of an early foliation. Intrafolial folds of quartz within quartzose microlithons indicate that an early foliation was transposed to form the present foliation. Asymmetric kink folds with prominent kink lineations on schistosity surfaces are related to the latest generation of folding.

Greenschist

Grayish-green chlorite-rich foliated greenschist with albite porphyroblasts are found in all three localities studied. The most extensive exposures are at the Upper McConaughy Gulch locality (UMG 55, UMG 66, UMG 71) and in Horseshoe Gulch locality (HG 2D). These rocks most commonly occur as low-lying exposures enclosing blueschist blocks and marble blocks. More rarely, they are found as large blocks with dimensions up to 20 X 20 X 8 feet (UMG 55). Weathered surfaces of the rocks are reddish-brown in color as are associated soils.

Most of the rocks are schistose and have flattened albite porphyroblasts + quartz in a matrix dominated by chlorite. Some greenschist is strongly banded in appearance and contains mineralogically distinct layers of quartz + albite, and chlorite from 0.2 to 2mm in thickness. Albite poikiloblasts range from to 0.5mm to 2.5 mm in length and appear flattened with pressure shadows in most samples.

Greenschists contain the mineral assemblage chlorite + albite + quartz + white mica + epidote/clinozoisite + sphene + hematite $\pm$ calcite, apatite, zircon, tourmaline, pyrite, and opaques. Inclusion trails of sodic amphibole (+ actinolite?) along with epidote or clinozoisite, and sphene are found in albite. Actinolite is not present in the chloritic matrix of any samples collected. Chlorite is commonly an anomalous brown variety. Both clinozoisite and epidote occur in some samples, as xenoblastic and subidioblastic grains in the matrix and as inclusions in albite. Xenoblastic strained quartz is most commonly found; some samples of banded greenschist contain stretched ribbons of quartz. Calcite occurs in patches in albite and in the matrix and as a secondary vein mineral.

The mineral assemblage of chlorite + albite + quartz + clinozoisite/epidote + white mica is representative of low-grade greenschist facies metamorphism. The protoliths of these rocks are most likely mafic to intermediate volcanic flows, tuffs, and volcaniclastics.

Various structural features are evident in the greenschists. Traces of an earlier foliation are preserved in albite porphyroblasts as small inclusions of sodic amphibole, possible calcic amphibole, sphene, and epidote. The inclusion trails have an internal fabric discordant to the fabric of the chloritic matrix. The inclusion trails are interpreted to be relict hinges of isoclinal folds of an early foliation. Blue sodic amphibole and actinolite do not occur in the matrix of these rocks. The presence of sodic amphibole only within the albite poikiloblasts indicates that high-pressure metamorphic conditions favorable for the formation of these minerals occurred early. P/T conditions changed to low-grade greenschist facies during the formation of the present foliation. Some large blocks of greenschist (UMG 55) show tight, plunging folds of the dominant foliation at outcrop scale. Pressure-solution features are also common and include fibrous quartz fringes on pyrite, and chlorite fringes and quartz pressure shadows associated with flattened albite.

Quartzose Phyllite

Olive-gray to yellowish-brown quartzose phyllite and phyllite occurs as a minor rock type of the melange matrix. Quartzose phyllite (MC 96) is exposed on the eastern cutslope of the Moffett Creek road, SE 1/4, Sec. 6, T. 42 N., R. 7 W, Yreka Quadrangle.

The rock unit varies from thinly layered and fissile phyllite to a compositionally banded rock (quartzose phyllite) featuring thick, light-gray, quartzo-feldspathic layers and thin, grayish-black phyllitic layers (Figure 31). The quartz- and feldspar-rich bands may range in thickness from several millimeters to 20 mm.

Major mineral constituents include quartz, chert, plagioclase, muscovite, and chlorite. The characteristic mineral assemblage of the quartzose phyllite is quartz + plagioclase + muscovite + chlorite + epidote + sphene which is indicative of low-grade greenschist facies metamorphism of a sedimentary rock, possibly a feldspathic to lithic wacke. Minor minerals present include sphene, epidote, hematite, opaques, pyrite, and zircon. Secondary vein minerals include chert, quartz and albite.

In quartz-rich layers, fine to very fine sand-sized subangular plagioclase and quartz grains (0.10-0.25 mm) are enclosed in a matrix composed of microcrystalline quartz and chlorite. Faint outlines of chert and sedimentary lithics are also found. Quartz appears strained and has undulose extinction. Plagioclase grains are generally untwinned; twinned grains may show bent twins. Phyllitic layers contain muscovite, minor chlorite, and traces of sphene and epidote. Mica layers are coated with dark brown organic material or clays, possibly concentrated by pressure solution. Calcite was not found in thin section. In thin section, a weak foliation is defined by preferred orientation of white mica, quartz and plagioclase grains (Figure 10).

Banded rocks have isoclinal to tight folds with fold limbs and axial planes parallel to the pervasive foliation in the phyllites (Figure 34). An incipient axial-planar cleavage is developed in the hinge zones of the folds. The isoclinal to tight folds of the relict bedding are interpreted to be an early stage of layer transposition in the rocks. Two distinct, small-amplitude crenulation lineations are developed in foliation surfaces of typical phyllitic rocks.

Comparison of the Phyllitic Quartzite of the SSG to the Sissel Gulch Graywacke

The phyllitic quartzite of the SSG is lithologically and texturally similar to the Sissel Gulch Graywacke (SGG) (Figure 10). The Sissel Gulch Graywacke structurally overlies the Schist of Skookum

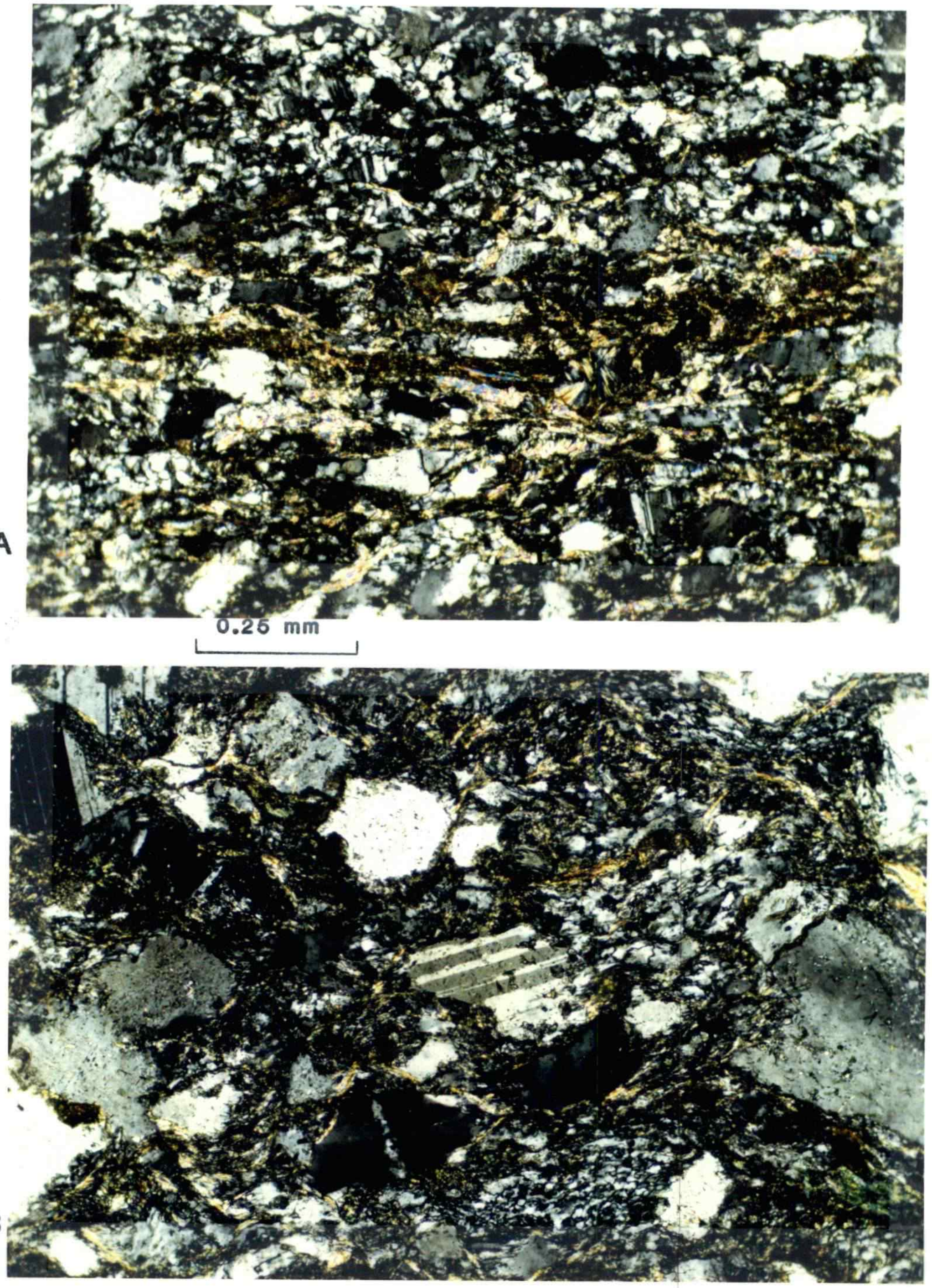

Figure 10. A. Photomicrograph of quartzose phyllite (MC 96) of the SSG. Note the fine-grained quartz matrix and subangular plagioclase grains. A weak foliation is defined by white mica; the long axes of quartz and plagioclase grains are oriented parallel to the foliation. 100X, XP, FOV = 1.31 mm B. Photomicrograph of the Sissel Gulch Graywacke. Grains of quartz and feldspar are larger than in the quartzose phyllite. Note the fine-grained quartz matrix and unoriented white mica. 100X, XP, FOV = 1.31 mm.

Gulch on a thrust fault and is in fault contact with the phyllitic quartzite in the Moffett Creek area. The Sissel Gulch Graywacke unit is composed of thickly bedded feldspathic-lithic arenites and minor interbedded, dark, phyllitic shale. Sedimentary structures include graded beds, partial turbidite sequences and soft sediment folds. The graywacke is generally medium- to coarse-grained and poorly sorted. Grain sizes range up to 3 mm. Mineral constituents and lithic types found in the SGG include angular quartz, plagioclase, felsic, microlithic and lathwork volcanics, and microcrystalline quartz. Accessory minerals include sphene, epidote, apatite, and chlorite. The matrix is extremely fine-grained and comprised of chlorite and minor sericite in addition to the very fine-grained mineral and lithic components listed above. Carbonate is absent. Mineral grains in thin section have a preferred mineral orientation.

Recent U-Pb isotopic dating on detrital zircon and garnet fractions from the Sissel Gulch Graywacke (Wallin, written communication, 1987) have provided new information on the source and depositional history of the graywacke. Homogeneous detrital zircon fractions yield $^{207}Pb/^{206}Pb$ ages from 432-444 Ma and an upper intercept age of 441 $\pm$ 11 Ma. A single fraction of detrital garnet yields a $^{207}Pb/^{206}Pb$ age of 1180 $\pm$ 34 Ma. The new age data constrains the maximum age of the Sissel Gulch Graywacke to be Late Ordovician to Early Silurian. The graywacke appears to have been derived from erosion of both a volcanic source terrane and Precambrian crystalline basement.

The deformation style of the quartzose phyllite of the SSG is different from what is known of the Sissel Gulch Graywacke. Relict bedding has been tightly folded and an axial-planar cleavage has developed in the hinge regions of the folds. The dominant foliation in the quartzose phyllites is an incipiently developed transposition foliation. I have not observed similar structures in the Sissel Gulch Graywacke. Wallin and others, (1988) has noted that the textural and lithological similarities between the phyllitic quartzite of the SGG and the Sissel Gulch Graywacke may mean that the SSG represents a lower level of the graywacke unit. My mapping indicates that the phyllitic quartzite is but a minor constituent of the melange matrix of the SSG; the rest of the matrix and block components of the SSG are quite dissimilar to the Sissel Gulch Graywacke and thus are considered not to be part of that sedimentary unit. However, it is likely that the quartzose phyllites may have been derived from similar sources as the Sissel Gulch Gaywacke but underwent a greater degree of textural reconstitution and deformation. Another possibility may be that the quartzose phyllites is a fault slice of the SGG which became incorporated into the melange. Similarities in age between the Sissel Gulch Graywacke and isotopically dated quartz-albite schists of the SSG melange matrix, both Late Ordovician to Early Silurian in age, indicate close ties.

WEAKLY METAMORPHOSED SEDIMENTARY TECTONIC BLOCKS

Laminated Chert

A very large block of laminated chert (MC 97) is found on the northern slope of Skookum Butte, in the SW 1/4 of the NW 1/4 of Section 8 T. 42 N., R. 7 W., Yreka Quadrangle. The matrix enclosing the chert block is not exposed. The color of the chert is variable and may be creamy white, gray, blue-gray, and green. Weathered surfaces are reddish-brown to yellow-brown. Parallel dark-colored laminae and subtle variations in grain size of the quartz define bedding in the rock. Width between laminae is variable and may range from <5 mm to 15 mm. The bedded to laminated chert is cut by many microfaults; displacements range from millimeters to several centimeters. No traces of fossils were observed in outcrop or thin section.

In thin section, the chert is remarkably pure, and consists of a mosaic of recrystallized quartz. The chert is very fine grained; flattened quartz grains are approximately 0.02 - 0. 04 mm in width and length. The laminae are composed of silt and clay, and carbonaceous material ± traces of muscovite and chlorite. Mica is more prevalent in the thicker laminae (up to 0.2 mm in width) and are in places coated with iron oxide. Laminae are wavy and undulatory and are interpreted to be seams where insoluble residue has collected after the dissolution of quartz. The solution seams are parallel to bedding in the rock, which indicates that flattening and burial stresses perpendicular to bedding resulted in pressure solution and seam formation.

The solution seams are cut by vertical fractures. Minerals within the veins are predominately quartz and microcrystalline silica. Quartz veins also run parallel to bedding and are terminated by vertical quartz veins. The brittle deformation represented by the vertical fracturing postdates the deformation associated with flattening and burial that presumably caused solution seams to form. The traces of chlorite and muscovite found in solution seams attest to low-grade greenschist metamorphism.

The bedded to laminated chert is interpreted as a fragment of a primary siliceous deposit that was faulted or tectonically emplaced into the melange. The purity of the chert and absence of detrital clastic and carbonate material is indicative of a well-circulated deep-water ocean-basin environment of deposition that was free of or blocked off from influxes of detrital materials.

Possible correlations of the chert block in the SSG with other known chert deposits in the sedimentary units in the area are uncertain. Other chert localities include: varicolored bedded to laminated cherts in the White's Gulch limestone and chert sequence in the vicinity of Duzel Rock; laminated to thin-bedded blue chert underlying the massive limestone of the Duzel Rock Group; the Callahan Chert; member 1 of the Gazelle Formation, and large blocks of chert in the Moffett Creek Formation.

GREENSCHIST-FACIES TECTONIC BLOCKS

This chapter describes the lithology and petrology of various metasedimentary, metachert, metacarbonate, and metavolcanic blocks in the SSG melange that have been metamorphosed to greenschist facies. Rock types include micaceous quartzite, dolomite and calcite marble, and actinolite schist.

Micaceous Quartzite

Blocks and discontinous lenses and bands of micaceous quartzite are found in the No Name Gulch and Upper McConaughy Gulch localities. The quartzites in the two localities are different in general appearance and mineralogy and will be discussed separately.

Micaceous Quartzite of the No Name Gulch Locality

Typical blocks of micaceous quartzite in the No Name Gulch locality (NNG 48) are light-colored, pale gray to pale pink with reddish-orange-colored weathered surfaces. The blocks stand out from the quartz-albite schist matrix and are clearly differentiated from the matrix by their quartz-rich mineralogy. Rocks readily fracture along white mica-rich schistosity surfaces.

Microscopically, the rocks contain the mineral assemblage quartz + white mica + chlorite + magnetite with trace amounts of hematite, garnet, apatite, zircon, and tourmaline.

Xenoblastic quartz grains average roughly 0.2 mm in size and may be up to 0.5 mm in their greatest dimension. Quartz has undulatory extinction, and grain boundaries are serrated. Some individual quartz grains have undergone cataclasis and have been broken down into very fine subgrains, resembling microcrystalline quartz.

The quartzite exhibits a domainal cleavage. Thin fibers of white mica and patches of blocky chlorite form trails that define the dominant foliation. Green pleochroic chlorite is conspicuous in the rock, and some of the plates are kinked. The mica trails are bounded by quartzose microlithons up to 1 mm in thickness.

Oxide minerals include magnetite and hematite. Idioblastic to subidioblastic magnetite is commonly associated with chlorite and also occurs interstitial to quartz. Edges of magnetite are altered to hematite. Small patches of hematite also occur disseminated throughout thin sections.

A few (< 5 grains) of subidioblastic to idioblastic colorless garnet occur in one thin section of this rock type.

Microscopically, the rock exhibits a weakly developed S-C fabric. S-C refers to a shear band structure, where shear bands (cisaillement in French) correspond to c-surfaces, and s-surfaces correspond to schistosity surfaces oblique to the shear surface. Discussions of S-C fabrics, their terminology and usage can be found in Berthe and others (1979), Simpson and Schmid (1983), Lister and Snoke (1984), and Passchier and Simpson (1986). C-surfaces are defined by trails of mica, including white mica and chlorite. Elongated quartz grains and single fibers of white mica interstitial to quartz are oriented obliquely to the foliation and define the S-surface. The sense of shear is sinistral. Nearly vertical fine fractures cut the S-C fabric and are evidence of brittle-shear deformation. The fractures are very fine and are not filled in with secondary minerals.

The mineral assemblage quartz + white mica + chlorite + iron oxides + garnet is characteristic of low-grade greenschist-facies metamorphism. The possible protolith of these rocks is most likely sedimentary in origin and may be a quartz arenite sandstone, or less likely, chert.

Micaceous Quartzite from the Upper McConaughy Gulch Locality

Thin lenses and bands of micaceous quartzite occur within the greenschist and quartz-albite schist matrix of the Upper McConaughy Gulch locality. The quartzites are gray and are characterised by blueish-gray bands of quartz, 1 - 4 mm thick, bounded by thin, (1 mm or less), brown cleavage traces of white mica.

The mineral assemblage is quartz + white mica, with minor amounts of garnet, magnetite, and trace amounts of tourmaline, albite, and chlorite.

Xenoblastic quartz is the dominant mineral phase. Quartz grains are flattened, have undulose extinction and sutured grain boundaries. Individual grains range in size from 0.1 to 0.2 mm. Some quartz occurs as long, narrow ribbons.

Tiny, subidioblastic to idioblastic, colorless garnet crystals occur in mica and quartz domains.

Texturally, the rock has a domainal cleavage with quartz microlithons bounded by cleavage traces of mica. Mica trails range from smooth to stylolitic. The mica cleavage traces may be recrystallized remnants of pressure-solution seams. In thin section, the rock shows a weakly developed S-C fabric. Elongated quartz grains and single fibers of mica along the edges of quartz grains are oriented at a low angle to the foliation direction (C-surface) and define a S-surface. Sense of shear is sinstral in the one sample examined. Fractures crosscut the fabric. Spherulitic pumpellyite and microcrystalline quartz occur together in 1 mm wide fractures cutting across the foliation in one rock sample. Their occurrence is associated with secondary low-grade mineralization or alteration during late-stage brittle deformation.

The mineral paragenesis of quartz + white mica + iron oxides + garnet + chlorite is characteristic of low-grade greenschist-facies metamorphism. The protolith of this rock type is probably a fairly pure chert.

Marble

Laminated and massive marble occurs as large blocks in the matrix, lenticular bodies or thin discontinuous lenses, interlayered with the matrix. In outward appearance, this marble appears to be massive or laminated limestone. On close examination, they are thoroughly recrystallized, and hence termed, marble. Various types of marble are found in all three localities mapped. Three varieties are differentiated and include: gray to blue-gray laminated dolomite marble; massive light gray to white dolomite marble; and gray foliated calcite marble.

Relatively few samples of these metacarbonate lithologies were obtained for this study as compared to metasedimentary and metavolcanic rock types.

Correlation of Marble Lithologies with Limestone Units of Zdanowicz(1971)

Zdanowicz (1971) differentiated and described two limestone units within what is now known as the SSG. The first unit is his "unnamed Silurian? limestones faulted into phyllites". The phyllites consist of various matrix lithologies of the SSG. He noted both massive, coarsely crystalline, sparry-calcite limestones and well-laminated limestones. No fossils or conodonts were found. The characteristic feature of these limestones was their fractured, sheared, and crushed texture in outcrop and in thin section. The laminated and massive dolomite marble, and the foliated calcite marble of the SSG are correlative with this unit.

The second limestone unit described by Zdanowicz (1971) is his "unnamed limestone" unit consisting of blocks of massive limestone faulted into "arkosic wacke and feldspathic wacke sandstones". The sandstones are actually tonalite blocks of the SSG. A fault breccia is commonly found along the contact between the limestone blocks and the tonalite. The blocks can be found in the N1/2 of the NE1/4 of Section 34, T. 42 N., R. 8 W., (east of the No Name Gulch locality), and in Upper McConaughy Gulch, W1/2 of Section 26, T. 42 N., R. 8 W., Etna Quadrangle. No thin sections were made of these massive carbonate blocks for this study. The limestone is characterized by the absence of megafossils and chert nodules. In addition, the rocks display marked brittle-deformation features and strained calcite. In thin section the limestone is made up of sparry calcite with minor unrecrystallized micrite (Zdanowicz 1971).

Laminated Dolomite Marble

Large blocks and scattered thin lenses of finely laminated dolomite marble are common the the SSG. Type examples are located in the Horseshoe Gulch locality and include samples HG 22, HG 23 and HG 24

(Figure 11). Typical block dimensions may be as small as 3 X 5 feet or as large as 30 X 100 feet. Individual blocks may stand 10 feet or more in height above ground. Large lenticular exposures of laminated to massive marble occur throughout the SSG. These exposures are interlayered with greenschist, graphitic schist, and quartz-albite schist. The surface texture of the laminated marble is finely etched and pitted and is extremely rough. Preferential dissolution is apparent along laminae. The very fine, dark gray laminae mark solution seams where insoluble residues have collected. Thin white quartz and calcite veins run subparallel to the laminae. Larger calcite-filled extension veins and faults with variable offset cut the solution seams and subparallel veinlets. In thin section, these larger fractures seem to have been first infilled by quartz, which has been partially replaced by calcite. Traces of chlorite are observed along the margins of the larger vein fractures filled in by calcite.

X-ray diffraction studies of several bulk-rock powders, and stained thin sections confirm that the rocks are composed of dolomite (Figure 12a). The dolomite is interpreted to be of secondary replacement origin. The dolomite is very finely crystalline. Individual grains range in size from 0.03 to 0.08 mm. The dolomite exhibits a xenotopic-A (anhedral) texture (Gregg and Sibley, 1984). Boundaries between dolomite grains are undulatory and rarely straight. Pore space is minimal. Xenotopic dolomite textures can result from: (a) replacement of limestone by dolomite or (b) neomorphic recrystalization of preexisting dolomite with both processes occurring at elevated temperatures in excess of 50°C (Gregg and Sibley, 1984). Possibility "a" is favored for these rocks, that is, dolomitization of limestone occurred during migration of hot fluids along solution seams and fractures.

Wavy to serrated, anastomosing solution seams define the laminae observable in hand sample. Some of the laminae are composed of multiple seams that can only be differentiated microscopically. Seams are very thin, approximately 0.02 mm. In some samples, laminae are spaced exceedingly close with one or two dolomite grains beween the seams. The solution seams are composed of dark carbonaceous material, silt and clay.

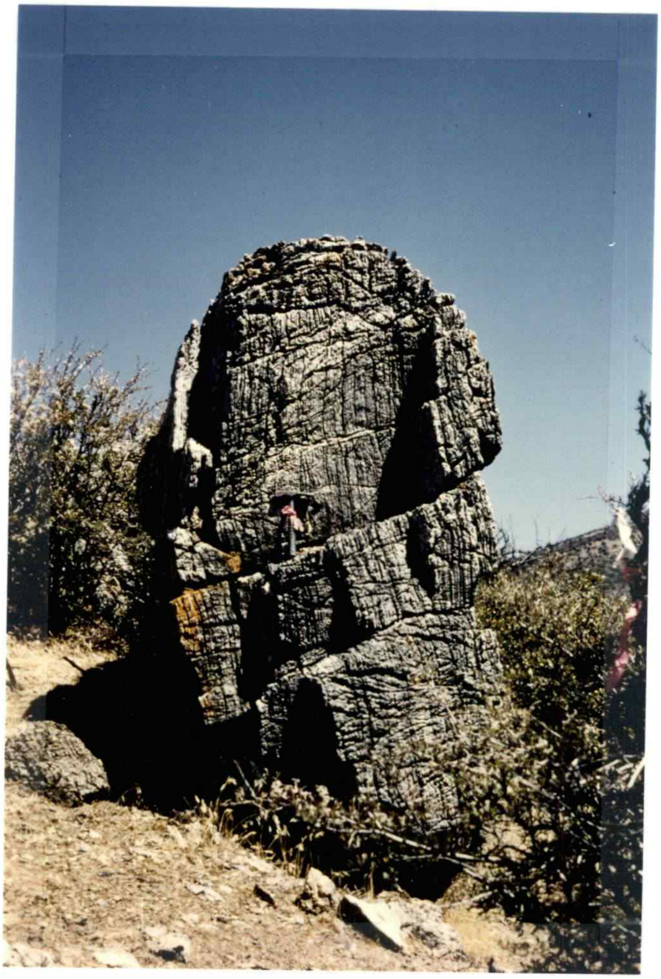

Figure 11. Laminated dolomite marble block, outcrop HG 24. Note the solution cleavage, (vertical) which defines the foliation, S_1.

A

0.25 mm

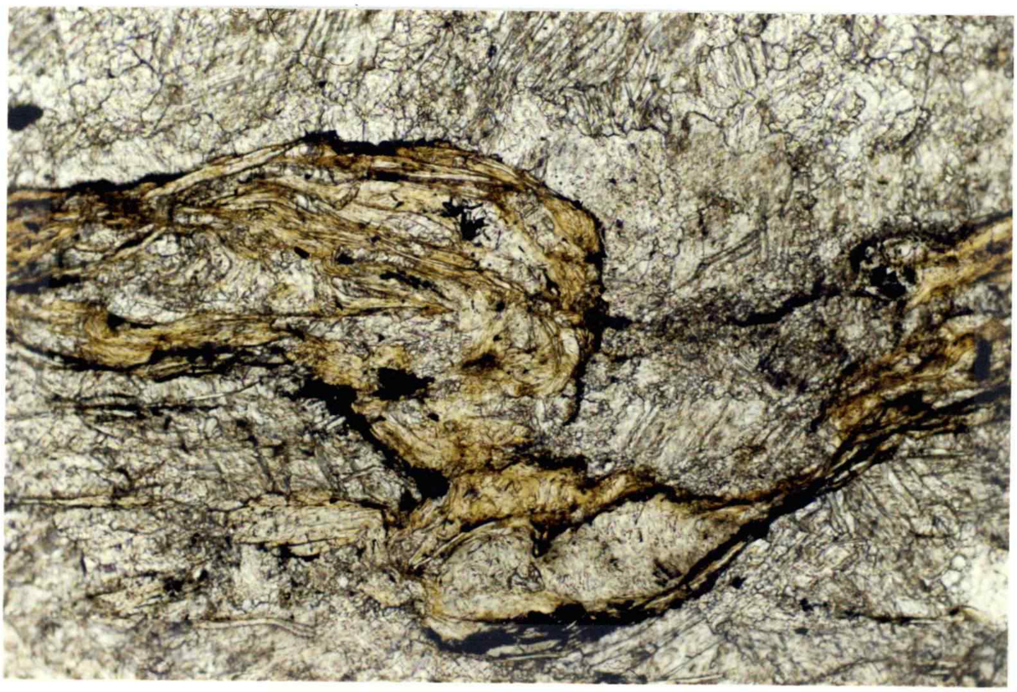

B

0.25 mm

Figure 12. A. Photomicrograph of laminated dolomite marble, HG 24. Solution seams define the cleavage. This is an example of a microstylolite swarm. 40X, PL, FOV = 3.3 mm. B. Photomicrograph of a foliated calcite marble, UMG 61. The minerals white mica + chlorite + opaques (graphite, hematite?) have crystallized in the stylolite. Note anhedral grain boundaries of individual calcite grains. 100X, PL, FOV = 1.31 mm.

Dolomitization has occurred through processes of massive recrystallization and the formation of solution seams which have destroyed orginal carbonate textures. The solution seams are similar to nonsutured solution seams described in a model proposed by Wanless (1979). Nonsutured solution seams or microstylolites, and microstylolite swarms form as a response to pressure solution in clayey or silty limestones. Formation of microstylolites occurs as a response to stress conditions such as load stress from burial. At points of high stress, carbonate solution begins, concentrating insoluble materials, such as silt and clay, along a small solution seam. The seam acts as a path for the removal of dissolved carbonate and as a site where insoluble material concentrates. Dolomite may also form along the seams. As dissolution of carbonate continues, initially formed seams become choked with insolubles and cannot serve as a pathway for fluids. Developed silt and clay seams relieve built-up stresses by lateral shearing. The whole process can then begin again as high stresses gradually increase in new zones, creating microstylolite swarms (Wanless, 1979).

Three samples of laminated dolomite marble, each weighing from 11 to 14.5 pounds, were dissolved in acid. During the acid bath, organic material, released from microstylolites in the rock, formed a black film on the surface of the acid and water. Total insoluble residue ranged from 6 to 10% for the samples. Insoluble materials of sand size include quartz, plagioclase and magnetite.

Temperature and pressure conditions of recrystallization are difficult to assess. Fairly pure marbles with the assemblage calcite/dolomite + quartz + white mica + chlorite are stable through the biotite zone of the greenschist facies (Turner, 1981). Metamorphic minerals such as tremolite, diopside, and epidote are not observed in the SSG metacarbonate rocks. Furthermore, in most samples, mica such as muscovite or chlorite has not developed in solution seams. The dark carbonaceous material in the solution seams has not been fully ordered to form graphite. It is likely, based on the minerals and textures described, that these laminated dolomite marbles have experienced from very low to low-grade greenschist facies metamorphism, at temperatures in excess of 50^{o}C and less than 400^{o}C.

Massive Dolomite Marble

Light gray to white, massive dolomite marble occurs as blocks of diverse sizes and thin lenses interlayered with matrix lithologies, particularly, quartz-albite schist and graphitic schist. Massive dolomite marble rocks occur at all three localities. Type examples include HG 27 (see Figure 6) and HG 7.

Examination of two thin sections reveals that the rocks are almost entirely a coarse-grained mosaic of anhedral dolomite crystals, ranging in size from 0.05 to 0.5 mm. Grain-to-grain contacts are typically curved and undulatory. Dolomite shows sweeping extinction. The texture is typical of xenotopic-anhedral dolomite (Gregg and Sibley, 1984).

Trace minerals (less than 1% estimated mode) consist of chlorite and quartz. The rocks are cut by veins filled by strained calcite and minor chlorite. The mineral assemblage is typical of a pure dolomite limestone metamorphosed under low-grade greenschist-facies conditions.

Foliated Calcite Marble

One exposure of foliated calcite marble was sampled for petrographic study and occurs in the Upper McConaughy Gulch locality (UMG 61). This type of marble is fairly common and widespread in the SSG and is second in abundace to laminated dolomite marble.

Typically, the marbles are light gray. These rocks are foliated with cleavage defined by concentrations of aligned micas. The foliation is stylolitic to undulatory, and parallel to bedding.

Texturally, the rock is composed of calcite domains with minor quartz and feldspar impurities, bounded by stylolites or pressure-solution seams (Figure 12b). The stylolites are generally very thin but may be up to 1 mm in thickness. Platy minerals, such as chlorite and white mica, define the stylolitic cleavage in the rock. The mica recrystallized from clay and silt concentrated along the stylolite by pressure solution. In addition, large grains of plagioclase and quartz are found associated with the stylolites, possibly concentrated there as a result of carbonate dissolution. Traces of original bedding are defined by subtle differences in grain size of calcite and by thin sandy to silty layers discernible in thin section. The majority of stylolites are parallel to bedding and may be offset by secondary calcite veins. A few stylolites crosscut bedding and seem to be related to the calcite veins in the rock.

In thin section the rock is composed of recrystallized calcite + quartz + plagioclase + chlorite + white mica + magnetite. A dark, opaque-looking mineral (graphite?) coats micas.

Calcite ranges in size from 0.05 to 0.8 mm. Grain boundaries are finely serrated and curved. Straight crystal terminations are rare. The texture is similar to xenotopic-anhedral textures observed in the previously described dolomite marbles.

Plagioclase is abundant. Single grains may be up to 1 mm in their longest dimension. Though small, subangular to subrounded grains are disseminated along with quartz in the calcite domains, there seems to be a concentration of larger, broken and fragmented plagioclase along stylolites. The fragmentation of the plagioclase grains may be the result of shear stresses acting along the stylolite.

Subangular quartz grains are disseminated through calcite domains and are concentrated along stylolites, similarly to plagioclase. Quartz grains may be up to 0.5 mm in their greatest dimension. Both quartz and plagioclase appear to be detrital, based on their grain shape and abundance.

Veins of coarsely crystalline calcite crosscut the fabric. Calcite crystals are strained and have mostly straight boundaries. Some of the stylolites continue uninterrupted through the veins, while others are offset or end abruptly against the vein. Evidently, more than one brittle fracturing event is recorded in these rocks. Further, pressure solution processes were aided by the brittle fracturing and fluid flow accompanying fracturing.

The mineral assemblage calcite + quartz + plagioclase + chlorite + white mica + magnetite is characteristic of low-grade greenschist facies metamorphism of an impure carbonate rock.

Origin of the Greenschist-Facies Metacarbonate Blocks and Lenses

The origin and depositional texture of the carbonate lithologies that occur as blocks and thin lenses interlayered with matrix lithologies is obscured by recrystallization and pressure solution. Mesoscopic and microscopic fossils are not associated with the carbonate rocks, including the least metamorphosed blocks that lack chlorite or mica. Cotkin (written communication) suggests that carbonate blocks represent fragments of a reef deposit. Absence (lack of preservation) of fossils and bioturbation may be due to recrystallization; thus, there is a lack of evidence to substantiate the hypothesis of reef origin or other possible environments of origin, i.e. deep water.

Actinolite Schist

A moderately extensive exposure of actinolite schist blocks occurs in a northeast trending gully at the Upper McConaughy Gulch locality (UMG 70). These rocks are gray-green in color, fine-grained, and foliated. Actinolite needles define a conspicuous mineral lineation in these rocks.

The characteristic mineral assemblage is actinolite + epidote + albite + quartz + chlorite + sphene + white mica + calcite + hematite. This assemblage is typical of greenschist facies metamorphism of a metavolcanic rock. Actinolite occurs as fine, pale yellow-green to colorless needles ($\leq$ 0.5 mm in width) which define the foliation. Albite and quartz occur in the groundmass and have been largely replaced by actinolite. Patches of anomalous-brown to blue chlorite are found. Some of the chlorite patches enclose remnants of colorless clinopyroxene (augite), which is considered to be a relict igneous phase. Patches of calcite are replacing plagioclase (albite). Pale yellow-green xenoblastic epidote (0.04 mm) occurs aligned parallel to the prominent foliation. Trails of finely crystalline sphene run parallel to the foliation. Vein minerals consist of calcite and albite.

At least two sets of small-scale kink folds disrupt the foliation and define a hinge lineation on schistosity surfaces. The kink bands intersect to form conjugate kink bands. Bent actinolite needles are found in the kink hinges.

BLUESCHIST AND TRANSITIONAL FACIES TECTONIC BLOCKS

Definitions of Blueschist and Transitional Facies

Blueschist facies and transitional or (epidote)-blueschist (Brown, 1987) facies assemblages are occur in tectonic blocks in the SSG. The recent literature on blueschist-bearing metamorphic terranes shows a variety of parageneses designated as belonging to the blueschist facies. The definitions of Turner (1981) and Brown (1974; 1987) will be used here. Blueschist parageneses (Turner, 1981, p. 208) are confined to those containing glaucophane + lawsonite, glaucophane + omphacite or glaucophane + jadeite + quartz. Parageneses containing glaucophane, or crossite but lacking in other high pressure phases such as aragonite, lawsonite, or jadeitic pyroxene are treated as transitional toward the greenschist facies (Turner, 1981, p. 231).

Rocks bearing glaucophane without other critical high pressure minerals have been termed glaucophanitic greenschists (Sorensen, 1986) and more recently (epidote)-blueschists (Brown, 1987). The (epidote)-blueschist facies is transitional to the greenschist facies and is defined by the reaction:

sodic amphibole + epidote
= actinolite + albite + chlorite + iron oxide
(Brown, 1974).

Pressures inferred for terranes with transitional epidote-glaucophane assemblages are as high as those bearing lawsonite-glaucophane blueschist assemblages.

Critical Mineral Assemblages of Blueschist and Transitional Facies in the SSG

Many tectonic blocks of the SSG contain the critical mineral assemblage lawsonite + sodic amphibole (glaucophane) ± actinolite; these are regarded as blueschists (Table 4). In addition, some tectonic blocks in the SSG contain transitional assemblages. Critical minerals observed are epidote + sodic amphibole + iron oxide ± actinolite.

Blueschist Facies Tectonic Blocks

Metavolcanic Rocks

Blueschist-facies metavolcanic rocks are found at all three localities and are conspicuous block types in the melange, probably second in abundance to marble blocks. The rocks are blue-black to dark grayish-blue and have dark reddish-brown weathered surfaces. The rocks are finely foliated and very dense. Relict igneous features such as pillows or amygdules have not been found. The rocks have been thoroughly recrystallized in high P/T conditions and are penetratively deformed. Mineral lineation is difficult to see in outcrop; only the very coarse-grained rocks have a lineation defined by blue amphibole prisms. Lawsonite is rarely discernible in hand samples. Extension fractures and veins are common. Vein minerals include calcite, albite, chlorite, and stilpnomelane.

Blueschists are distinguished mineralogically from other tectonic blocks bearing transitional assemblages by the presence of lawsonite + sodic amphibole in association with quartz, albite, chlorite, sphene, hematite, or magnetite (Table 4). Additional minerals that may occur include epidote/clinozoisite, white mica, actinolite, calcite, garnet, and stilpnomelane. Trace amounts of apatite and zircon occur in a few samples. Jadeite does not occur.

Texturally, blueschists are very finely crystalline. Mineral dimensions range from about 0.02 to 0.10 mm. Rare coarse-grained blueschist contains lawsonite and sodic amphibole minerals up to 1.0 mm in size.

Assemblages

Up to four varieties of lawsonite-bearing blueschists have been differentiated based on their predominant mineral phases. The types are:

lawsonite-sodic amphibole schist;
chlorite-rich, sodic amphibole-lawsonite schist;
actinolite-lawsonite-sodic amphibole schist;
lawsonite-actinolite schist.

Table 4. Blueschist-Facies Mineral Assemblages of Selected Samples of the Schist of Skookum Gulch

	METAVOLCANIC ROCKS														METACARBONATE
QUARTZ	X	X	X	X	X	X	X	X	X	X	X	X	X	X	m
ALBITE	m	X	X	X	X,sv	X	X,sv	X	X,sv	X	X	X	m	X,sv	X
CHLORITE	X	X	X	X	X	X	X	X	X	X	X	X	X	m	X
WHITE MICA	m	X		X		m		X	X	m	m	X	m		X
EPIDOTE & CLINOZOISITE			m		m	m	X	m	m	X	m	m	tr	X	m
LAWSONITE	X	X	X	X	X	X	X	X	X	X	X	X	X	X	X
CA-AMPHIBOLE							X	X	X	X	X	X	X	X	
NA-AMPHIBOLE	X	X	X	X	X	X	X	X	X	X	X	m	m		X
SPHENE	X	X	X	X	X	X	X	X	X	X	X	X	X	X	
CALCITE	X,sv	X,sv	X,sv	X,sv	X,sv	X,sv	X,sv	X,sv	X,sv	X,sv	X	X	X,sv		X
HEMATITE	tr		m	tr	m	m	m	m	m	m	tr	m	m		m
GRAPHITE													m		
OPAQUE		mag		mag			mag				mag				
CLINOPYROXENE															
GARNET				X					X						
STILPNOMELANE							sv				X				
APATITE								tr	m			tr			
ZIRCON	tr		tr	tr			tr					tr			tr
TOURMALINE															
PYRITE															
Sample	NNG 31a blk	NNG 42 blk	HG 1 blk	HG 8a blk	HG 4c blk	HG 3b blk*	UMG 62 blk	NNG 37 ils	NNG 44 ils	HG 5 blk	HG 2a blk	NNG 35 ils	NNG 39 ils	HG 9c blk	NNG 34 ils
	Lawsonite- Na-Amphibole Schist						Actinolite-Lawsonite-Na-Amphibole Schist					Lawsonite-Actinolite Schist			Na-Amphibole-Lawsonite-Calcite Marble

Notes: Abbreviations are: blk = tectonic block in melange; ils = interlayered sequence within a coherent fault block in the melange; X = mineral present; m = mineral present in minor amounts, 1-5%; tr = mineral present in trace amounts, 1% or less; sv = secondary mineral present in veins; mag = magnetite.
* = Chlorite-rich Na-amphibole-Lawsonite Schist

—Lawsonite-Sodic Amphibole Schist

Lawsonite-sodic amphibole schist is common at the Horseshoe Gulch and No Name Gulch localities. It probably occurs at the Upper McConaughy Gulch locality although none of the rocks sampled there contain this particular assemblage.

Sodic amphibole is the predominant mineral in these rocks and comprises at least 30% of the estimated mode in most thin sections. Sodic amphibole is commonly zoned from core to rim. Pleochroism may be patchy throughout an individual grain or, more commonly, the amphibole grades to colorless rims and ends. I infer that the rims and ends are calcic in composition. Chlorite is intimately intergrown with sodic amphibole, and the two minerals form the predominant foliation in the rocks.

Idioblastic lawsonite porphyroblasts are enclosed in the schistose ground mass composed of sodic amphibole, chlorite, and quartz.

Flattened albite poikiloblasts, filled with inclusions of clinozoisite, epidote, sodic amphibole, and lawsonite occur in the groundmass. Inclusion trails are generally concordant with the predominant foliation. Albite porphyroblasts, along with thin bands of polygonized quartz, occur in thin discontinuous bands that seem to be what is left of an early metamorphic compositional layering. In more fully reconstituted rocks, (NNG 31a, HG 8a), albite along with chlorite are minor phases; quartz is the predominant constituent of the groundmass and sodic amphibole and lawsonite are the principle minerals.

Calcite occurs interstitially within the groundmass and associated with albite. Small tablets of lawsonite seem to have crystallized after calcite.

Sphene is ubiquitous in these rocks and occurs as light brown xenoblastic grains, enclosed by sodic amphibole or chlorite, and aligned parallel to foliation.

Very fine-grained, pale yellow-green to colorless xenoblastic epidote is present in small amounts (<10%) in most of the lawsonite-glaucophane schist. Clinozoisite also occurs in places as tiny grains in the groundmass, associated with quartz and albite, or commonly as inclusions in albite.

White mica occurs in small amounts associated with chlorite, sodic amphibole and lawsonite. In some samples, pressure fringes composed of white mica have developed on the ends of flattened lawsonite porphyroblasts.

Oxide minerals found in the schist includes hematite and magnetite. Hematite is most common and may also appear as an alteration product of magnetite and pyrite.

Garnet is abundant in one sample, HG 4c, and occurs as colorless idioblastic to subidioblastic porphyroblasts in contact with sodic amphibole, lawsonite, quartz, sphene, and chlorite. Garnet and lawsonite porphyroblasts are enclosed by prisms of sodic amphibole and chlorite and are interpreted to have formed syn- to post- development of the cleavage.

Stilpnomelane is found in one sample, HG 4c, in association with quartz and albite in a secondary vein. The vein minerals are considered to be retrograde minerals developed under greenschist-facies conditions.

--Chlorite-rich Sodic Amphibole-Lawsonite Schist

Chlorite-rich blueschist blocks are common at the Horseshoe Gulch locality. These rocks are gray-green on fresh surfaces and weather to reddish-brown. The mineralogy and characteristics of this schist are similar to that of the lawsonite-sodic amphibole schist. However, chlorite and lawsonite are the predominant phases. Blue amphibole is less abundant than chlorite and usually comprises less than 15% of the estimated mode. At least 20% of the estimated mode is made up of chlorite.

The mineral assemblage of these rocks consists of lawsonite + chlorite + sodic amphibole + quartz + albite + sphene and minor amounts of epidote and hematite. Accessory minerals may include calcite, white mica, and stilpnomelane. The chlorite-rich sodic amphibole-lawsonite schist is probably similar in mineralogy to the chlorite schist from Horseshoe Gulch described by Cotkin (1987).

The rocks are well foliated with stretched and flattened lawsonite porphyroblasts and small grains of sphene and epidote set in a matrix of chlorite and sodic amphibole. In some rocks, stretched albite poikiloblasts and fine-grained quartz define thin discontinuous bands within the rock.

Minor sodic amphibole and abundant chlorite indicate that formation of glaucophane has not gone to completion or even as far as in the lawsonite-sodic amphibole schist, where chlorite and albite are much less abundant. Presence of abundant chlorite and minor sodic amphibole relates directly to various proposed reactions for the formation of sodic amphibole. Possible reactions include:

(1) albite + chlorite + carbonate ($CaCO_3$) + iron ores
= epidote + crossite + CO_2 (Vance, 1957)

(2) albite + quartz + chlorite + calcite
= glaucophane + lawsonite + CO_2 + H_2O (Ernst, 1963)

(3) chlorite + albite $\pm$ actinolite
= glaucophane/crossite + H_2O (Winkler, 1979)

Actinolite may or may not be a reactant in the formation of sodic amphibole. As actinolite is uncommon in many of the greenschist rocks in the SSG, it seems unlikely that it is a reactant. Therefore, reaction 3 is not applicable. The chlorite-rich sodic amphibole-lawsonite schists indicate that the sodic amphibole-forming reaction is only incipiently developed.

—Actinolite-Lawsonite-Sodic Amphibole Schist

Tectonic blocks bearing lawsonite and two amphiboles are fairly common in the SSG. Examples of rocks containing these three critical minerals are found at all three localities (Table 4). Most commonly, actinolite-lawsonite-sodic amphibole schist is bluish-gray and is very finely foliated. Schistosity surfaces have a blue sheen to them and when struck with a hammer break easily into plates along foliation planes. Mineral lineations are not apparent in hand samples. A very fine crenulation lineation (intersection of the strain-slip and crenulation cleavage with the foliation) is found on foliation planes. The rocks are cut by white mineral veins composed of calcite, albite, quartz, and microcrystalline quartz.

The characteristic mineral assemblage of these rocks is sodic amphibole + lawsonite + actinolite + chlorite + hematite + albite + quartz + sphene + calcite ± epidote/clinozoisite, white mica, stilpnomelane, apatite, garnet, opaques, and zircon.

Microscopically, these rocks are extremely fine-grained and are texturally complex. In thin section, statically grown porphyroblasts of lawsonite and grains of sphene are set in a matrix of fine-grained blue amphibole, actinolite, chlorite, and quartz. Some of the rocks are mineralogically segregated, with cleavage domains composed of blue amphibole + chlorite enclosing domains of lawsonite + actinolite and minor blue amphibole, ± sphene and apatite.

Tight to isoclinal microfolds of lawsonite + actinolite with minor sodic amphibole and chlorite are observable in thin section. The dominant foliation cuts through these microfolds. This primary foliation has been microfolded and a strain-slip cleavage has developed at a high angle to the schistosity.

Small, (≤0.05-0.1 mm) microboudinaged lawsonite tablets, aligned parallel to foliation, occur enclosed in a finely crystalline matrix of sodic amphibole, chlorite, and actinolite. These small lawsonite tablets without inclusions probably grew after development of the foliation. Much larger lawsonite porphyroblasts (0.5-1 mm) occur and contain inclusions of matrix minerals. The foliation, defined by blue amphibole, sphene and chlorite, wraps around the blocky lawsonite tablets. Pressure shadows occur where the foliation is deflected around porphyroblasts. Lawsonite probably grew synchronously with to after formation of the foliation and was rotated with respect to the foliation during microfolding.

In general, albite porphyroblasts are rarely in evidence, having been reduced during the formation of sodic amphibole and actinolite. Ragged outlines of remaining poikiloblastic albite are filled with inclusions of clinozoisite, lawsonite, sphene, and sodic and calcic amphibole. A few samples do have significant amounts of twinned and untwinned albite in the groundmass. One sample, HG 5, shows albite overprinted by clinozoisite, lawsonite, blue amphibole, actinolite, chlorite, and patchy calcite.

Epidote and clinozoisite are absent altogether or occur in minor to trace amounts. Clinozoisite is commonly associated with albite and also as small grains in the ground mass. Granular sphene is ubiquitous in most samples. Oxide minerals consist of hematite or opaque minerals altered to hematite. Calcite occurs as a vein mineral and as small granoblastic patches interstitial to other phases or replacing albite.

Pale-yellow to colorless garnet porphyroblasts are found in some samples (NNG 40, NNG 44). The small fractured garnets are associated with lawsonite, blue amphibole and actinolite, and occur in microfolds in thin sections studied. The pervasive foliation cuts through the garnet and indicates that the garnet was an early crystallizing phase, similar to the albite.

Stilpnomelane occurs oriented parallel to the foliation in several samples (HG 2a, HG 2b) and thus is considered part of the equilibrium assemblage. Blades of stilpnomelane also occur as a secondary vein mineral (UMG 62). Actinolite fibers grow preferentially along ductile shear surfaces at a high angle to the foliation in one sample (NNG 40). Pumpellyite was not detected in thin section or during routine X-ray powder diffraction.

Sodic amphibole and chlorite have a lepidoblastic texture and are finely intergrown. Actinolite occurs as fine needle-like prisms intergrown with chlorite and sodic amphiblole. Fine prisms of actinolite also occur as inclusions in albite. In some cases, the pale blue sodic amphibole and pale green actinolite are difficult to distinguish in the matrix. Actinolite coexisting with sodic amphibole and lawsonite was not recognized by Cotkin (1987) in samples from the Horseshoe Gulch area. The presence of actinolite was verified by me optically and by X-ray diffraction of a whole-rock powder (NNG 37).

In all of these rocks, sodic amphibole is zoned or shows patchy intergrowths of calcic or sodic-calcic amphibole. Rims and ends are colorless to pale green and are inferred to be calcic amphibole (actinolite). These types of grains are similar in appearance to the composite sodic amphibole-actinolite needles described by Liou and Maruyama (1987). Most of the larger sodic amphibole prisms have blue cores and colorless to pale green actinolitic rims. Green amphibole (actinolite) enclosed by blue amphibole is a rare occurrence in these rocks.

The occurrence of pale-green calcic amphibole and blue sodic amphibole as distinct separate grains or fibrous intergrowths in association with lawsonite is regarded as a stable assemblage. Other evidence supporting this interpretation is, (1) actinolite is only found in association with other-high pressure phases, namely lawsonite and sodic amphibole, and (2) textural evidence of grain-to-grain contact between the three phases. The apparent zoning in the sodic amphibole may indicate disequilibrium with calcic amphibole, but an approximate domain equilibrium among the minerals may exist over the space of a few mineral grains (Brown and Ghent, 1983).

Calcic amphibole- and sodic amphibole-bearing assemblages have been noted in other high P/T terranes in Sanbagawa, New Caledonia and the Franciscan (Ernst and others, 1970; Black, 1973; Coleman and Papike, 1968; Liou and Maruyama, 1987).

--Lawsonite-Actinolite Schist

Rocks containing lawsonite porphyroblasts set in a groundmass consisting largely of actinolite and minor sodic amphibole are restricted in their occurrence in the SSG. Two samples are known (NNG 35, NNG 39) and occur interlayered with actinolite-lawsonite-sodic amphibole schists and sodic amphibole-lawsonite-calcite marble. The lawsonite-actinolite schists are gray-green and finely foliated. Foliation is defined by parallel alignment of actinolite needles and lawsonite porphyroblasts. The schistosity has been microfolded and a strain-slip cleavage has developed.

The mineral assemblage consists of actinolite + lawsonite + calcite and minor amounts of sodic amphibole, clinozoisite, sphene, chlorite, white mica, hematite, and quartz. Trace amounts of apatite and zircon occur. Actinolite comprises roughly 50% of the total estimated mode in thin sections. Actinolite needles are very fine-grained, usually <0.02 mm in width. Small lawsonite tablets (<0.04 mm) lie parallel to the foliation. Pale-blue sodic amphibole comprises less than 10% of the estimated mode and where found is concentrated in thin bands, interlayered with actinolite. Grain size of the two fibrous amphiboles makes it difficult to determine zoning patterns or the existence of composite grains. Thin-section relations between grains strongly indicate that the two amphiboles and lawsonite are in chemical equilibrium. Calcite occurs interstitially in the groundmass and as crosscutting veins. Albite veins also are common.

An unusual rock type with the mineral assemblage lawsonite + actinolite + clinozoisite + graphite and minor quartz, albite, chlorite, and calcite is found at the Horseshoe Gulch locality (HG 9C). The rock is schistose and light gray with graphitic laminae. The rock occurs as a small block associated with lawsonite + sodic amphibole ± actinolite schist.

In thin section, large lawsonite porphyroblasts, replacing twinned plagioclase, occur in a matrix of actinolite prisms and quartz. Clinozoisite porphyroblasts (0.1-0.25mm) also are found and are differentiated from lawsonite by their pale-yellow color, higher relief, anomalous blue interference colors and more fractured appearance. Ragged lawsonite porphyroblasts (0.5 x 0.25 mm) are fractured and broken; some show partial replacement by clinozoisite. Less deformed lawsonite tablets are also found and others have pressure shadows filled by quartz and chlorite. The replacement of lawsonite by clinozoisite in this rock is evidence of greenschist-facies retrograde metamorphism. The block is very small in size (approximately 4 feet X 2 feet); the retrograde metamorphism is probably the result of reaction with the surrounding matrix of graphitic and quartz-ablite schist.

Actinolite is colorless to very pale yellow-green. Prisms are generally 0.05 mm in width and define a lineation.

The protolith of this rock is uncertain, but it is probably not a mafic volcanic rock. One possibility may be a calcic volcaniclastic rock (graywacke?) that contained organic material.

Metacarbonate Rocks

—Sodic Amphibole-Lawsonite-Calcite Marble

Calcite marbles bearing lawsonite and sodic amphibole occur at the No Name Gulch locality (NNG 34). These rocks are gray and display an undulatory foliation defined by chlorite and minor white mica. Although marble is a common block type in the SSG, the presence of the minerals lawsonite and blue amphibole is unusual. These two minerals indicate high P/T conditions of metamorphism. This rock type is interlayered with metavolcanic blueschist-facies lithologies at the No Name Gulch locality.

Lawsonite-bearing marble is rarely reported in the literature on blueschist. Lawsonite marble lenses interbedded with lawsonite metagraywacke and slate are found in the Permian Maitia Group, Nelson District, southern New Zealand (Coombs, 1960, p. 343).

The marble rock type in the SSG contains the mineral assemblage calcite + chlorite + quartz + albite + lawsonite + sodic amphibole + white mica + sphene + epidote + hematite (Figure 13). Traces of zircon and tourmaline also may occur. The presence of lawsonite was verified by X-ray diffraction. Carbonate domains range up to 2 mm in thickness and contain individual grains of quartz, patches of broken quartz, and albite grains, single tablets of lawsonite and prisms of sodic amphibole. Granoblastic calcite is very finely crystalline. Individual grains are roughly 0.1-0.25 mm in dimension.

Mica-rich cleavage domains, though variable in thickness, are generally less than 0.5 mm thick. Sphene and epidote are the most common minerals associated with the chlorite-rich cleavage domains.

Fairly abundant quartz and albite indicate that the protolith was an impure silty limestone.

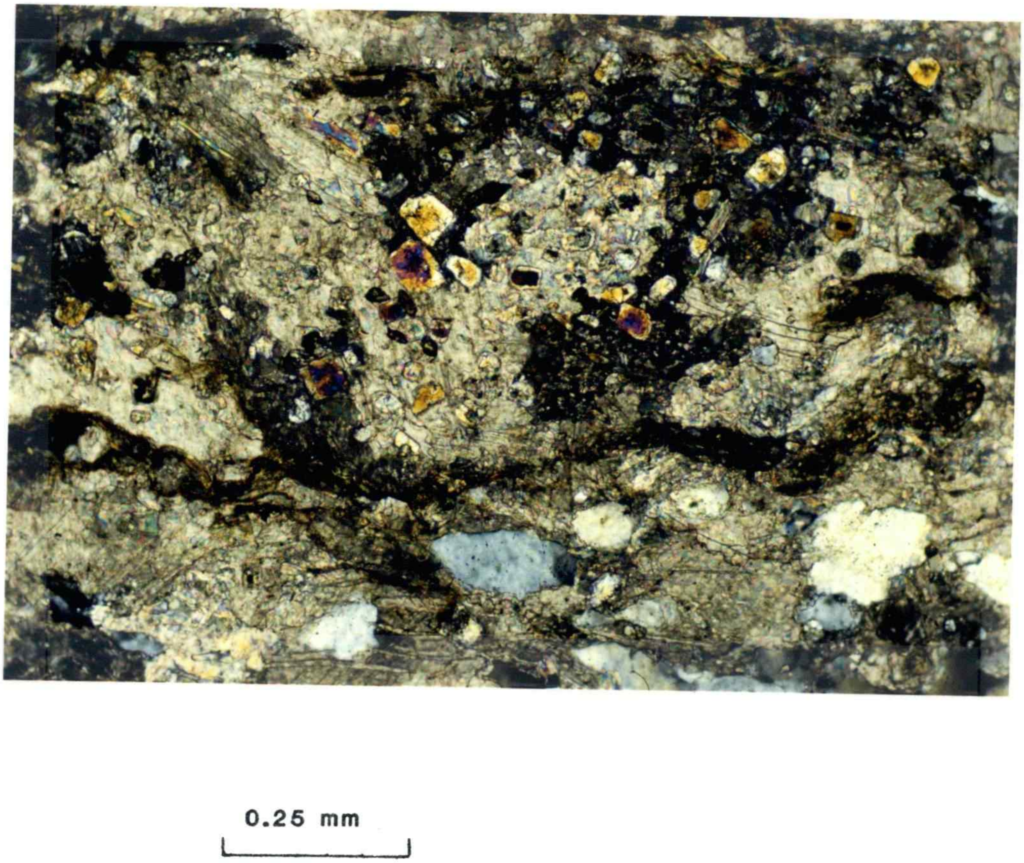

Figure 13. Photomicrograph of sodic amphibole-lawsonite-calcite marble, NNG 34. Note static growth of lawsonite tablets in calcite matrix and stylolite which defines cleavage in the rock. 100X, XP, FOV = 1.31 mm.

Transitional Facies Blocks

Metavolcanic Rocks

—Epidote-Sodic Amphibole Schist

Blocks containing sodic amphibole and epidote are found at the No Name Gulch and Upper McConaughy Gulch localities; this rock type probably exists at Horseshoe Gulch, but was not sampled. The rocks are dark green to blue-green and weather to reddish-brown. Table 5 shows typical mineral assemblages of transitional facies rocks. Porphyroblasts of epidote and albite and thin bands of quartz are visible in hand samples. Some rocks are finely layered, with chlorite + white mica + blue amphibole-rich layers alternating with quartz-rich layers. Foliation is defined by mica and sodic amphibole; prisms of sodic amphibole define a prominent lineation in thin section. Mineral lineations of blue amphibole on schistosity surfaces are not evident. Schistosity surfaces on outer surfaces of blocks and lenses are shiny and striated, and some appear have slickensides.

The mineral assemblage of typical samples (NNG 45, UMG 67, UMG 77) is sodic amphibole + epidote + chlorite + albite + quartz + white mica + sphene $\pm$ hematite, ilmenite, calcite. Traces of apatite, zircon and tourmaline are found in some samples.

Both epidote and albite poikiloblasts contain curved inclusion trails generally discordant to the dominant foliation. Minerals observed as inclusions include sodic amphibole, clinozoisite, epidote and sphene in albite, and sodic amphibole in epidote. Textural evidence observed in thin section (see UMG 67) indicate that an early foliation defined by blue amphibole was transposed to form the prominent foliation. Most samples show a compositional banding. Quartz and albite microlithons $\leq$ 1.5 mm in width are bounded by cleavage domains of chlorite + sodic amphibole + white mica. Sphene and pale yellow epidote porphyroblasts (up to 1 mm x 0.5 mm) are generally confined to the cleavage domains. Albite shows evidence of flattening, and pressure shadows of chlorite form adjacent to albite grains.

Table 5. Transitional Metamorphic Assemblages of the Schist of Skookum Gulch

	METAVOLCANIC ROCKS					METACHERT	METASEDIMENTARY ROCKS
QUARTZ	X	X	X	X	X	X	X
ALBITE	X	X	X	X	X	m	X
CHLORITE	X	X	X	X	X	m	X
WHITE MICA		m	X	m	X	X	X
EPIDOTE & CLINOZOISITE	X	X	X	X	X	X	X
CA-AMPHIBOLE	X				X		
NA-AMPHIBOLE	X	X	X	X	X	X	X
SPHENE	X	X	X	X	X	X	X
CALCITE	X,sv	sv	X	X	X	m	
HEMATITE	m	m	m		m	m	m
OPAQUE			ilm				
CLINOPYROXENE					rlc		
STILPNOMELANE							
APATITE		tr	m		tr		tr
ZIRCON		tr	tr			tr	tr
TOURMALINE		tr	tr				tr
PYRITE	tr	tr					
Sample	UMG 73 blk	UMG 77 blk	UMG 67 blk	UMG 45 blk	UMG 57 blk*	UMG 72 blk	UMG 59 blk

Notes: Abbreviations are: blk = tectonic block in melange; * = Volcanic Breccia; X = mineral present; m = mineral present in minor amounts, 1-5%; tr = mineral present in trace amounts, 1% or less; sv = secondary mineral present in veins; mag = magnetite; ilm = ilmenite.

Blades of an opaque mineral, identified as ilmenite, are abundant in one sample, UMG 67. The ilmenite crystals are tabular and are associated with blue amphibole.

The mineral assemblages of these rocks indicates a mafic to intermediate volcanic protolith. The presence of abundant quartz and white mica in some rocks suggests that the protolith was quartz-rich, and volcaniclastic.

--Volcanic Breccia

One block is notable in that it retains relict volcanic texture. The block is found at the Upper McConaughy Gulch locality (UMG 57). In outcrop the rock is massive, very fine grained, and pale-green to grayish-green. Cut surfaces reveal green angular to subrounded clasts up to 1 cm x 1 cm in dimension in a fine-grained chlorite-rich matrix.

In thin section the clasts are composed of cryptocrystalline greenish brown amorphous clay and sericite. Small euhedral clinopyroxene phenocrysts and granular plagioclase are enclosed by the clasts. Glomerocrysts of plagioclase + clinopyroxene are found in the matrix (Figure 14). The matrix surrounding the clasts and glomerocrysts is composed of equigranular twinned and untwinned plagioclase ($\leq$ 0.5 mm), relict clinopyroxene (augite), chlorite, sericite and clay. Accessory minerals found in the matrix include clinozoisite and epidote, sphene, calcite, sodic amphibole, actinolite, and white mica. Both chlorite and pale-blue sodic amphibole replace clinopyroxene within the clasts and in the matrix, leaving the clinopyroxene ragged-looking. Patches of calcite replace plagioclase. The plagioclase seems to have been altered to an albitic composition, based on comparison of its refractive index with the thin section epoxy. Prisms of sodic amphibole and actinolite along with clinozoisite, epidote, and sphene are found as inclusions in albite.

The mineral assemblage of the block is albite + epidote/clinozoisite + chlorite + sodic amphibole + actinolite + calcite + sphene + white mica. This assemblage is characteristic of high P/T transitional facies.

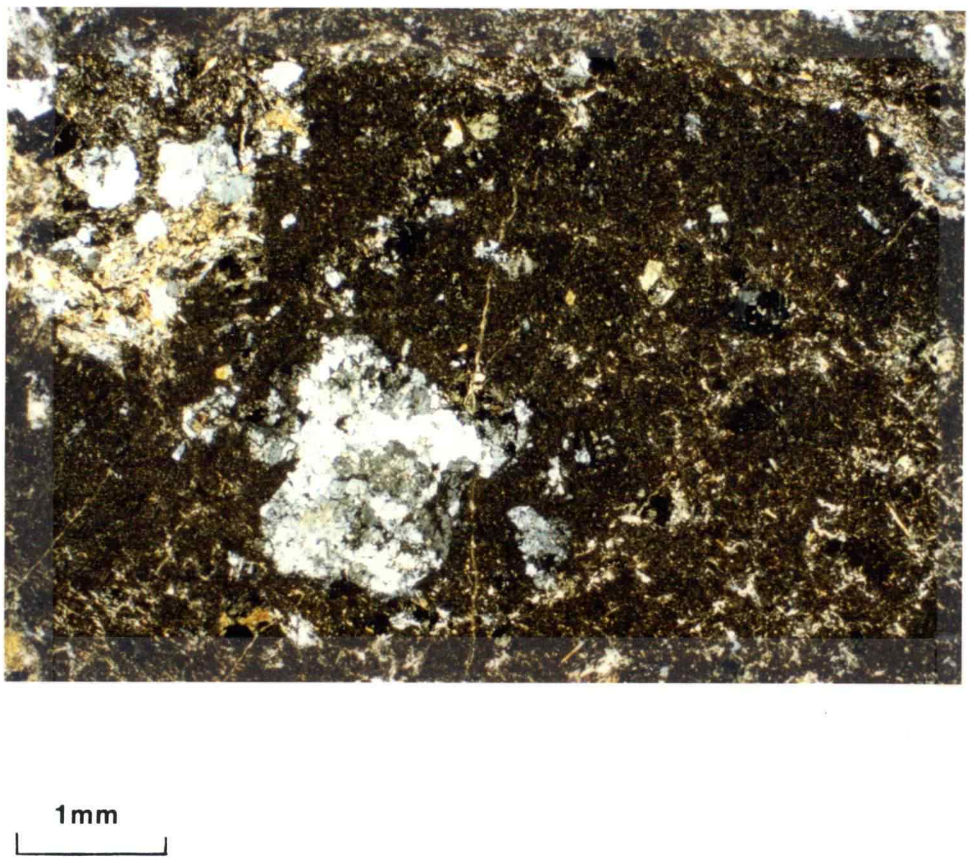

Figure 14. Photomicrograph of a volcanic breccia, UMG 57. Note glomerocryst of plagioclase in lower left. Dark matrix is composed of clay + sericite. Small, bright yellow clinopyroxene grains are enclosed by clay material which is a clast in the breccia. Clinopyroxene is replaced by chlorite. 20X, XP, FOV = 6.7 mm.

The texture of the rock indicates that it is a mafic volcanic breccia. The clasts were perhaps orginally ash or tuff fragments with inclusions of plagioclase and clinopyroxene. The clasts were incorporated into a crystalline volcanic matrix of fine ash. Subsequent alteration and metamorphism has formed new minerals, but recrystallization has not totally obliterated the orginal texture and mineral constituents.

Metasedimentary Rocks

--Quartz-Mica Schist

Metasedimentary tectonic blocks containing sodic amphibole and epidote are rare in the SSG. A group of polydeformed quartz-mica schist blocks that contain sodic amphibole and epidote are found at the Upper McConaughy Gulch locality (UMG 59). The blocks are reddish-brown on weathered surfaces, foliated, and compositionally banded.

Quartz microlithons are generally $<$ 2 mm in thickness. Cleavage domains consist of white mica + sodic amphibole + chlorite and range in size from <0.5 to 2.5 mm in thickness. Pale-blue sodic amphibole prisms and fibers of white mica and chlorite define a lineation in thin section. Blue amphibole is not observable in outcrop or hand specimen. Yellow epidote porphyroblasts and helicitic albite occur in the micaceous domains. Quartz has grown in the pressure shadows of strained albite. Quartz grains have sutured grain boundaries and show uneven extinction. Blue amphibole prisms occur interstitial to quartz.

The mineral assemblage found in these blocks consists of white mica + quartz albite + chlorite + epidote + sodic amphibole + sphene + hematite. Traces of apatite, zircon, and tourmaline are also found. The assemblage is typical of a pelitic rock which has undergone high P/T metamorphism. The critical minerals sodic amphibole and epidote are characteristic of rocks transitional to the greenschist facies.

These rocks are strongly foliated and display a complex deformational history that includes transposition of a preexisting foliation, folding, and refolding of the foliation, and outcrop-scale kink and chevron folds. The fold history is well expressed in these pelitic sedimentary rocks due to their compositional contrasts.

--Metachert

One small lens (<10 X 50 cm) of micaceous quartzite or metachert was found enclosed in greenschists in a road cut in the Upper McConaughy Gulch locality (UMG 77). Distinguishing features of this lithology are quartz-rich microlithons of blue quartz alternating with white mica-rich cleavage zones.

The mineral assemblage of this rock consists of quartz + sodic amphibole + white mica + epidote + albite + chlorite + sphene. Trace amounts of calcite, apatite, hematite, zircon, and pyrite occur.

In thin section, quartz domains 0.5 to 2.0 mm in thickness are bounded by cleavage domains containing the minerals sodic amphibole + white mica + chlorite. Sodic amphibole is dark blue in color and prisms are broken and fractured. Blue amphbibole is grown interstitially with quartz. Curved inclusion trails in albite and intrafolial fold hinges of quartz and albite suggest that an earlier foliation was transposed to form the present foliation. Albite porphyroblasts occur sporadically and are found in cleavage domains and intergrown with quartz.

Mineral Composition

Cotkin (1987) has published results of mineralogical studies of rocks of the SSG collected in the Horseshoe Gulch Locality. Unfortunately, it is impossible to correlate any of his samples with mine. No attempt will be made here to detail all of the results of his mineralogical studies. Only data on sodic and calcic amphibole composition, which are most pertinent to this study, will be presented here.

Sodic Amphibole

Analyses of blue sodic amphibole from nine samples, plot in a band ranging from ferro-glaucophane and glaucophane to magnesioriebeckite (Figure 15a). Figure 15a follows the classification scheme of Miyashiro (1958). Cotkin (1987) notes a correlation between phase assemblage and sodic amphibole composition. Rock samples that contain magnetite or no iron oxide phase (i.e. hematite) have sodic amphibole compositions with an $Fe^{3+}/Fe^{3+} + Al$ ratio > 0.4. One sample, (HS-4) with the critical mineral assemblage actinolite + epidote + sodic amphibole, characteristic of transitional blueschists, contains blue amphibole that plots in the crossite to glaucophane field. A rock sample containing trace amounts of stilpnomelane as part of the stable assemblage contains the most Fe^{2+}-rich ferro-glaucophane (Cotkin 1987). A similar situation is found in the Shuksan schist where Na-amphibole occurring with stilpnomelane or magnetite has a high Fe^{2+}/Mg ratio (Brown 1974).

Zoning in blue amphiboles is conspicuous in most samples. Due to the fine-grained nature of the sodic amphiboles, patterns in zoning were difficult to obtain during microprobe analysis (Cotkin, 1987). Where sodic amphibole grains were large enough to probe, Cotkin (1987) observed that Ca and Mn increased from core to rim.

Calcic Amphibole

Colorless to pale yellow-green calcic amphibole (actinolite) occurs in actinolite schist and in some blueschist and transitional schists along with sodic amphibole and/or lawsonite. Calcic amphibole from an epidote- and sodic amphibole-bearing schist are close to the actinolite-tremolite join and contain small amounts of Na and Al (Cotkin 1987).

Coexisting Na-amphibole and Ca-amphibole

Two amphiboles, blue sodic amphibole and pale yellow-green to colorless calcic amphibole are found in blueschists and transitional schists. In thin section, sodic and calcic amphibole occur as single separate grains, as patchy intergrowths of blue and pale green to colorless amphibole, and as composite grains where blue amphibole cores are rimmed by colorless amphibole.

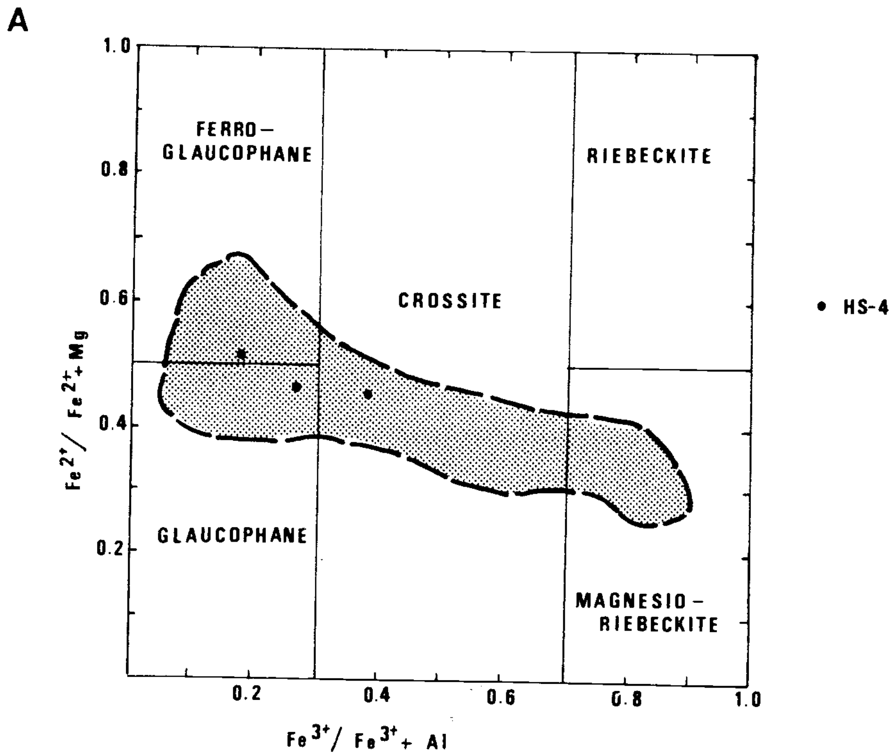

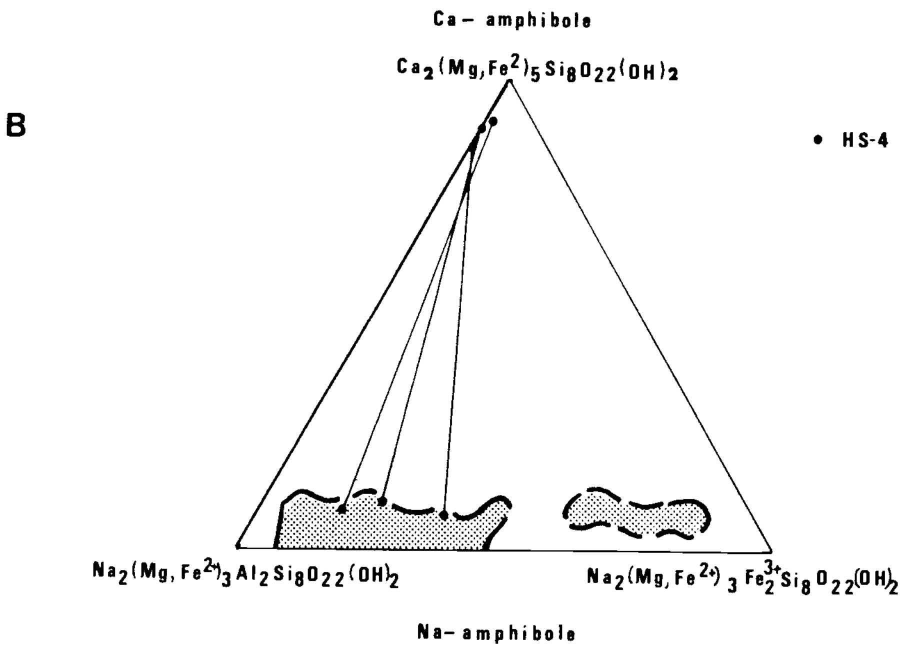

Figure 15. A. Compositional field of sodic amphibole from the SSG after Cotkin (1987, Figure 2). Sample HS-4 is an actinolite-bearing epidote-sodic amphibole schist. B. Composition of coexisting actinolite (near apex) and sodic amphibole from sample HS-4 after Cotkin (1987, Figure 4). Patterned area shows field of analyzed sodic amphiboles from the SSG.

There is really no data on the compositional variation of the zoned, intergrown, and composite amphibole grains. On the basis of these textural relationships coupled with the observation that the two amphibole assemblages occur with another high-pressure phase, namely lawsonite, sodic and calcic amphibole are considered to be phases coexisting at equilibrium. Similar textural relationships and interpretations have been reported for high P/T assemblages in the Franciscan terrane (Lee and others, 1966; Coleman and Papike, 1968; Klein, 1968; Liou and Maruyama, 1987) the New Caledonia metamorphic belt (Black, 1973), the Sanbagawa belt of Japan (Ernst and others, 1970; Toriumi, 1974; Nakajima and others, 1977; Maruyama and Liou, 1985) and the Nome Group blueschist terrane (Thurston, 1985) among others. Although the present data are very limited (Cotkin, 1987), a compositional gap between the coexisting Ca- and Na-amphiboles is indicated (Figure 15b). The single analyzed pair of coexisting amphiboles for the SSG come from an epidote-sodic amphibole schist. Coexistence of two amphiboles with limited miscibility is consistent with pressure and temperature estimates for high P/T blueschist and transitonal facies rocks (Ernst, 1979; Cotkin, 1987; Maruyama and Liou, 1987). Lower P/T assemblages, for example the Shuksan schist, display complete miscibility between coexisting actinolite and crossite (Brown, 1974).

Now that more samples are known from the SSG that bear two amphiboles, plus lawsonite or epidote, the compositional gap between amphiboles can be further defined.

Trace Element Chemistry

Whole-rock trace element concentrations for one sample of epidote-sodic amphibole schist (UMG 77) are listed in Table 6 and a chondrite-normalized plot of rare-earth element (REE) abundances is shown in Figure 16a. Analytical procedures and sample preparation methods used for INAA are discussed in Appendix 2.

Trace-element and REE contents of the rock suggest that protolith material was probably a volcanic rock of basaltic composition. Similar results were obtained from twelve whole-rock X-ray fluorescence

Table 6. Whole-rock trace element data by INAA for an epidote-sodic amphibole schist, sample UMG 77.

Sample:	UMG 77
element	ppm
Sc	21.1
V	176
Cr	214
Co	50.4
Ni	168
Zn	57
Rb	-----
Sr	276
Zr	-----
Cs	-----
Ba	-----
La	6.18
Ce	12.54
Nd	16
Sm	4.15
Eu	1.76
Tb	0.54
Dy	4.2
Yb	1.58
Lu	0.22
Hf	2.99
Ta	0.56
Th	0.67
(La/Lu)c	2.91

Notes: estimated analytical errors at one standard deviation are: ± 1% for Sc, V, Co, Sm; ± 2-5% for La, Ce, Eu, Yb, Lu, Hf; ± 5-10% for Cr, Dy, Ta; ± 10-15% for Zn, Tb, Th; ± 15 - 25% for Ni, Nd, Sr. Rb, Cs, Zr and Ba were analyzed, however analytical error exceeds 25%.

A

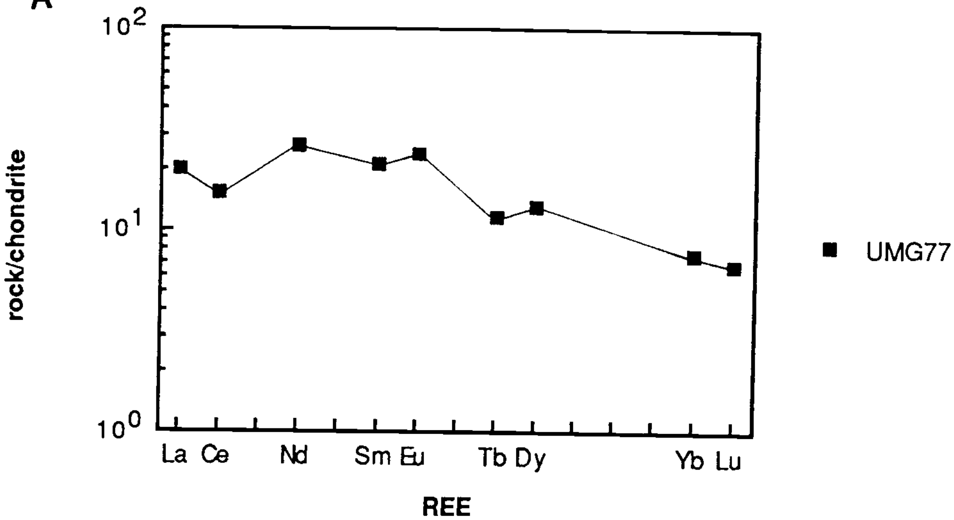

B

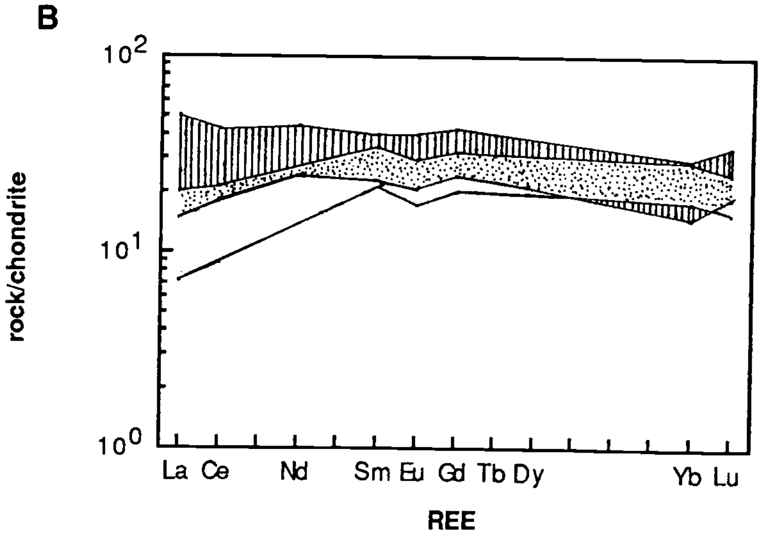

Figure 16. A. Chondrite-normalized whole rock REE plot of an epidote-sodic amphibole schist from the Upper McConaughy Gulch locality (sample UMG 77). B. Combined REE patterns of other epidote-sodic amphibole schists reported in the literature. Vertical ruled lines = field for blueschists of the Catalina Schist terrane of Early to Late Cretaceous age. Data are from Sorensen (1986). Unpatterned area = field from blueschists of the Shuksan Schist of Early Cretaceous age. Data are from Dungan and others, (1984). Dot pattern is area of overlap between the two groups of analyses.

analyses of blueschist-facies rocks from the SSG (Cotkin and Armstrong, 1987). Their data indicate that protoliths were basaltic and may have been formed in an oceanic island environment.

Light rare-earth elements (LREE) are enriched with respect to the heavy rare-earth elements (HREE) and are 15-27X chondrite. Chondrite values to which all REE values are normalized to are those of Anders and Ebihara (1982). HREE are 6.5-15X chondrite. The sample analyzed exhibits a moderately enriched LREE pattern, with a (La/Lu)c ratio of 2.9. The sample has a small positive Eu anomaly. The enriched LREE character and La/Ta ratio of 11.0 are similar to transitional or "T" type mid-ocean ridge basalts (MORB) (Saunders, 1984; Wood and others, 1979). The overall rare-earth pattern is rather erratic, and may reflect alteration and REE mobility accompanying metasomatic and metamorphic processes.

Figure 16b shows the combined REE patterns of other epidote-sodic amphibole blueschist rocks from the Catalina Schist terrane (Sorensen, 1986) and the Shuksan Schist (Dungan and others, 1984). The REE patterns are flat to LREE depleted, and on the basis of their trace element characteristics, both are interpreted as indicative of an ocean-floor tholeitic basalt protolith. In contrast, the REE pattern of UMG 77 is enriched in LREE, and depleted in HREE relative to the other examples shown.

CONDITIONS OF METAMORPHISM

The data presented in previous chapters and sections and summarized in Tables 4 and 5 indicate that metamorphism of tectonic blocks of the SSG took place under greenschist, blueschist and transitional blueschist-greenschist facies conditions (Figure 17). Metamorphism of sedimentary and volcanic rocks of the matrix took place under greenschist facies conditions.

Conditions of Metamorphism of Rocks of the Matrix

Metasedimentary and metavolcanic rocks of the matrix contain a principal mineral assemblage of albite + quartz + chlorite $\pm$ epidote/clinozoisite, sphene, calcite, hematite, magnetite, garnet, rutile and graphite. These minerals are characteristic of low-grade, greenschist facies metamorphism (Winkler, 1979, p.74). Absence of high P/T minerals such as lawsonite and sodic amphibole indicate that pressures attained were low, probably less than 3 kbar (lawsonite stability, Liou, 1971; glaucophane stability, Maresch, 1977). Petrographic evidence indicates that some rocks of the matrix and blocks have a more complex P-T history. These rocks (greenschist) crystallized sodic amphibole under high P/T conditions early in their history. Pressure conditions were reduced and prograde greenschist-facies minerals crystallized to form the equilbrium assemblage. Some clues to the temperature of metamorphism of the melange matrix can be found in the texture and mineralogy of the matrix schist. Thermal modeling of the subduction-zone environment and analyses of textures and mineral assemblages of melange matrix rocks by Cloos (1983, 1985) has shown that temperatures greater than 200°C are necessary to coarsen pelitic sediments and obtain phyllitic and schistose rocks. Temperatures above 200°C are indicated by the fine- to medium- grain size (0.1-1 mm) of quartz, albite, and mica of schistose rocks of the SSG. The presence of graphite in graphitic schist also constrains temperature estimates. Studies of graphite from metapelites indicate that organic matter becomes ordered at high temperature, 250 to 350°C (Landis, 1971; Frey, 1978; Diessel and others, 1978) in Cloos (1983).

Figure 17. A. P-T grid constructed for the SSG. (1) Lawsonite + Albite = Zoisite + Paragonite, (Holland, 1979); (2) Heulandite = Lawsonite + Quartz, (Nitsch, 1968); (3) Pumpellyite + Chlorite + Quartz = Epidote + Actinolite + H_2O, (Nakajima and others, 1977); (4) Lawsonite + Na-amphibole = Epidote + Quartz + Albite + Chlorite + H_2O $\pm$ Pumpellyite, (Brown and Ghent, 1983); (5) Jadeite(100) + Quartz = Albite, (Newton and Smith, 1967); (6) Clinozoisite + Glaucophane + Quartz + H_2O = Tremolite + Chlorite + Albite, (Maruyama and others, 1986); (7) Epidote + Mg-riebeckite + Chlorite + Quartz = Tremolite + Albite + Hematite + H_2O, (Maruyama and others, 1986); (A) glaucophane stability field of Maresch, (1977); (B) Calcite/Aragonite transition, (Johannes and Puhan, 1971); (C) Pumpellyite + Na-amphibole + Quartz = Epidote + Ca-amphibole + Albite + Chlorite + H_2O, (Brown and Ghent, 1983); (D) Pumpellyite + Chlorite + Quartz = Epidote + Actinolite + H_2O, (Brown, 1977); (E) stability range of barroisitic amphibole and actinolite (High T), (Ernst, 1979). Solid lines: experimentally determined equilibria. Dashed lines: equilibria approximated by experiments or extrapolated from experiments. Dot-dash: empirically calibrated. Patterned area corresponds to estimated P-T conditions for the SSG, from Cotkin, (1987). B. Estimated P/T paths during uplift for blueschists and greenschists of the SSG.

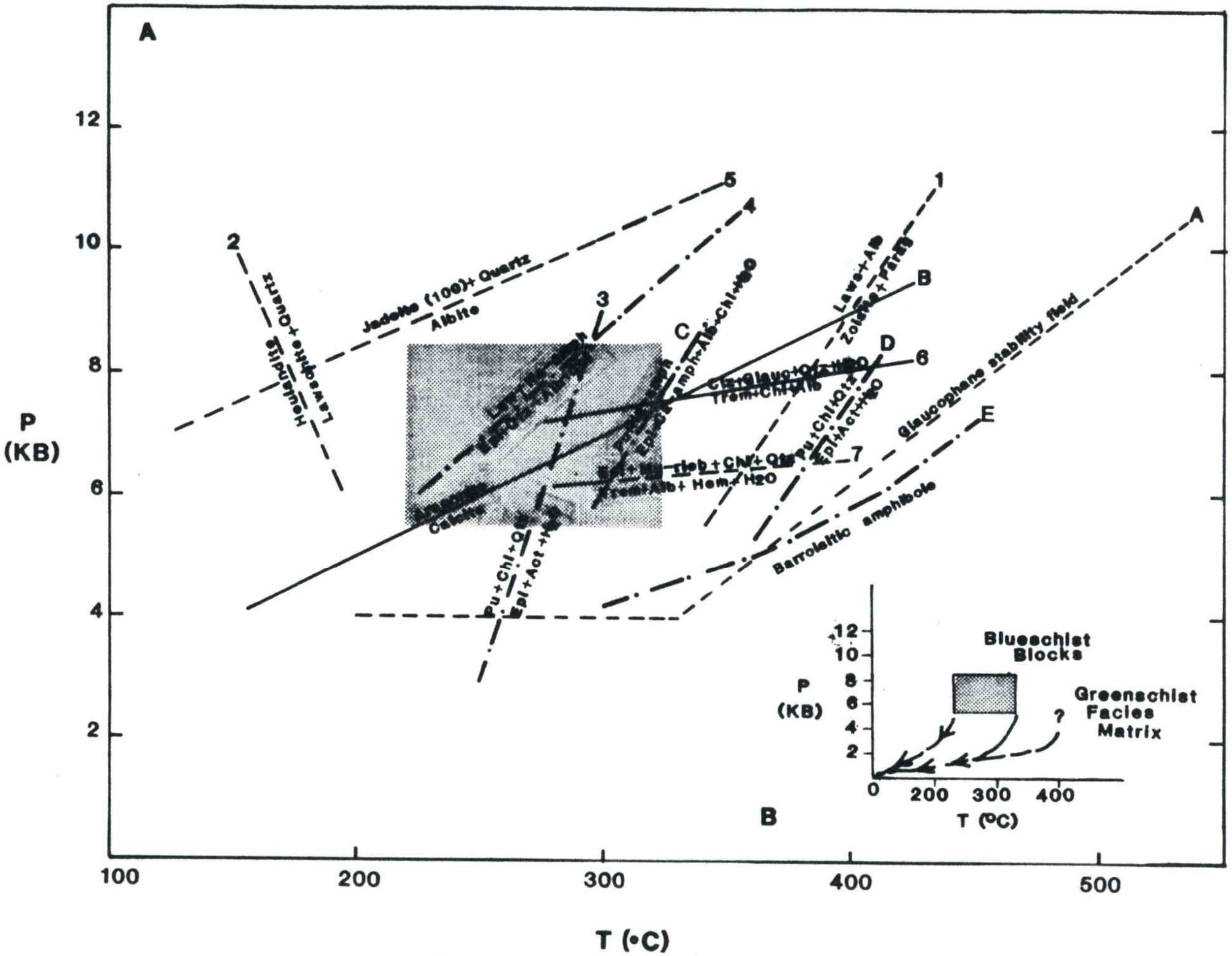

Figure 17. A. P-T grid constructed for the SSG. B. Estimated P/T paths during uplift for blueschists and greenschists of the SSG.

Temperature of metamorphism was probably not in excess of 400°C, as biotite and actinolite are not found (Turner, 1981).

Metamorphic Conditions of Blueschist and Transitional Facies Rocks

Metamorphic temperature and pressure conditions of blueschist and transitional facies rocks of the SSG have been estimated at 275 $\pm$ 50°C and 7 $\pm$ 1.5 kbar by Cotkin (1987) (Figure 17). Mineral equilibria and reactions which provide the basis for estimates of pressure and termperature of metamorphism are discussed below.

Temperature of recrystallization for these high P/T assembages is limited by the reaction,

lawsonite + albite
= zoisite + paragonite (1)

which constrains temperatures to 350°C at 6 kbar and 400°C at 9 kbar (Holland, 1979). The reaction,

heulandite = lawsonite + quartz (2)

defines the lower temperature limit of lawsonite formation (Nitsch, 1968) and occurs at 185 $\pm$ 25°C at 7 kbar.

Epidote + actinolite + Na-amphibole assemblages in the SSG indicate conditions on the high temperature side of the reaction,

pumpellyite + chlorite + quartz
= epidote + actinolite + H_2O (3)

calibrated by Nakajima and others (1977). The X_{Fe} of epidote can be used to determine the location of the reaction (Nakajima and others, 1977 and Maruyama and others, 1986). An epidote composition of Ps_{29} was used by Cotkin (1987) to determine the location of this pumpellyite-actinolite facies to greenschist facies transition reaction, and shows that temperatures for this assemblage are in excess of 250°C. Microprobe analyses of sodic amphibole and epidote in additional samples are recommended (for example, on samples UMG 73 and UMG 67) to verify temperature estimates of Cotkin.

Many blocks in the SSG contain lawsonite + sodic amphibole (+ quartz, chlorite, albite). Similar assemblages are common in the Ball Rock area of Franciscan terrane in northern California (see Brown and Ghent, 1983). The position of the reaction:

lawsonite + Na-amphibole
= epidote + quartz + albite + chlorite + H_2O
± pumpellyite (4)

was estimated by Brown and Ghent (1983) using available oxygen isotope data from their rocks to constrain temperature and the

jadeite + quartz = albite (5)

reaction curve of Newton and Smith (1967) to constrain pressure. Assemblages of the SSG fall on the high pressure side of reaction 4.

Two key mineral assemblages found in blocks indicate temperatures and pressures that are transitional from blueschist to greenschist facies. These mineral parageneses include:

Na-amphibole + epidote + Ca-amphibole (actinolite) + quartz
+ albite + chlorite ± iron oxide
(Cotkin's HS-4; UMG 73, this study)

and

Na-amphibole + epidote + quartz + albite + chlorite + iron oxide
(UMG 67, UMG 77).

Various workers have defined boundary reactions between the blueschist and greenschist facies. Miyashiro and Banno (1958) used the reaction

epidote + glaucophane + quartz + H_2O
= albite + chlorite + actinolite

to define the boundary. Brown (1974) used a similar reaction,

Na-amphibole (crossite) + epidote
= albite + actinolite + chlorite + iron oxide

to define the blueschist-greenschist transition. For most natural metabasites, this reaction is trivariant, that is, if iron oxide is eliminated from the reaction and Fe and Mg are considered as separate components. The Fe^{3+}/Al and Fe^{2+}/Mg ratios are the critical element ratios affecting the boundary of this reaction. Thus, depending on the bulk-rock composition, blueschist and greenschist lithologies can occur together at the same pressure and temperature.

In order to better understand the stability range of sodic amphibole and the blueschist-greenschist facies transition, Maruyama and others (1986) have experimentally investigated two key reactions. The two reactions:

clinozoisite + glaucophane + quartz + H_2O
= tremolite + chlorite + albite (6)

and

epidote + Mg-riebeckite + chlorite + quartz
= tremolite + albite + hematite + H_2O
(Maruyama and others, 1986; Brown, 1977) (7)

are useful as geobarometers. In the P-T zone between the two reactions, both blueschist and greenschist facies assemblages occur, along with the transitional assemblage consisting of sodic amphibole (glaucophane - Mg-riebeckite) + epidote $\pm$ actinolite. Reaction 6 delimits the maximum stability of glaucophane in the model Fe-free basaltic system investigated by Maruyama and others (1986). The reaction occurs well above the glaucophane stability field of Maresch (1977), (line A, Figure 17). Maruyama and others (1986) show that introduction of Fe^{3+} into the system lowers the maximum pressure limit of glaucophane and causes the reaction to be multivariant.

Cotkin (1987, p. 197) obtained a pressure estimate of 6.6 to 6.9 kbar by evaluating the activities of the phases in a blueschist containing the minerals sodic amphibole, epidote, and actinolite (Cotkin's sample HS-4) and the starting materials used in the experiments of Maruyama and others (1986). The Al_2O_3 content of sodic amphibole in stable equilibrium with actinolite, epidote, chlorite, albite, and quartz can also be used as a geobarometer. A pressure estimate of 7.1-7.2 kbar was obtained for sample HS-4 by using the Newton and Smith (1967) curves for low albite = jadeite + quartz to recalibrate the Al_2O_3 geobarometer. Using the Na(M4) Ca-amphibole geobarometer of Brown (1977), Cotkin obtained a pressure estimate of 6.8-7.1 kbar. These pressure estimates center around 7.0 kbar; uncertanties are difficult to determine but probably are less than $\pm$ 3 kbar.

Absence of Pumpellyite, Aragonite and Pyroxene in the SSG

Calcite is the carbonate phase observed in apparent equilibrium with other minerals in blueschist and transitional schists of the SSG. Aragonite does not occur in Paleozoic blueschists (Ernst, 1972), being strictly confined to Mesozoic and younger blueschist-bearing terranes. Estimated pressures and temperature ranges of blueschist metamorphism of the SSG is within the calcite-aragonite transformation; this reaction curve goes through 250°C at 6 kbar and 300°C at 7 kbar (Johannes and Puhan, 1971; see reaction B, Figure 17). Possibly, the original metamorphic carbonate phase was aragonite. However, Paleozoic aragonite is not likely to be preserved during uplift and decompression of the terrane (Carlson and Rosenfield, 1981).

Pumpellyite is a common mineral phase occurring in high P/T metamorphic terranes, for example, Ward Creek of the Franciscan Complex, (Liou and Maruyama, 1987); the Ouegoa District, New Caledonia, (Black, 1973; Yokoyama and others, 1986); Sanbagawa, Japan, (Nakajima and others, 1977). Pumpellyite has not been identified in thin section or in whole-rock X-ray studies conducted by Cotkin (1987) and by me. The upper temperature stability limit of pumpellyite at pressures of 5-7 kbar is roughly 300 to 350°C, using reaction curves of Maruyama and Liou (Journal of Petrology, in press) and the petrogenetic grid of Brown (1977). The estimated temperature and pressure of metamorphism of the SSG seems to be at the upper temperature limit of pumpellyite stability. In fact, the absence of pumpellyite makes a good case for temperatures in the range of 300 to 350°C. Cotkin (1987) uses the argument that the bulk compositions of SSG protolith material was not rich enough enough in calcium to favor pumpellyite and coexisting calcic and sodic amphiboles. My petrographic studies of rocks not sampled by Cotkin indicate that assemblages bearing lawsonite, sodic amphibole and calcic amphibole in the SSG are more common than previously thought. Evidently, lawsonite formation is favored over pumpellyite in these rocks. Similar assemblages occur in the Ouegoa District of New Caledonia, in the lawsonite-epidote transitional zone. The temperature of formation of even these lawsonite + two-amphibole assemblages may be too high for pumpellyite to be stable.

Minor to trace amounts of relict clinopyroxene are found in a volcanic breccia containing epidote + sodic and calcic amphibole and in an epidote-actinolite schist (UMG 73 and UMG 70). Metamorphic pyroxene has not been observed in any high P/T blueschist rocks in the SSG. Metamorphic pyroxene is observed in rock units metamorphosed under similar high P/T conditions such as the Black Butte and Ball Rock units of the Franciscan (Brown and Ghent, 1983), Ward Creek rocks of the

Franciscan (Maruyama and Liou, 1987), and blueschist of New Caledonia (Black, 1973). Ca-Na pyroxene occurring with sodic amphibole is not common in intermediate pressure higher temperature metamorphic terranes such as Sanbagawa, Japan, and New Zealand (Marayuama and Liou, 1987). Considering the temperature and presure estimates of the SSG and common mineral parageneses, it is rather anomalous that pyroxene is not observed in the higher P/T assemblages containing sodic amphibole and lawsonite. On the basis of experimental data, Na-pyroxene with about 30 mole% jadeite could be expected in the SSG, coexisting with quartz and albite (Holland, 1983). The presence of impure jadeite would lower pressure estimates for the SSG considerably. On the other hand, jadeitic pyroxene would not be expected in the higher temperature, transitional schists, that is those bearing epidote-sodic amphibole ± actinolite assemblages.

IGNEOUS ROCKS

Igneous rocks found in the SSG include large tonalitic plutonic blocks, small bodies of gabbro intrusive into or faulted into the melange, and small exposures of serpentinite. Classification of igneous and volcanic rocks follows the I.U.G.S. nomenclature (Steckeisen, 1976; 1979). Minerals preceding the rock name are listed in order of increasing abundance.

Plutonic Blocks

Large exposures of plutonic rocks occur in a thin irregular belt along the eastern edge of the SSG (see Figure 3 and Plate 1). Contacts with surrounding sedimentary and volcanic units and schistose metamorphic rocks are poorly exposed, but generally the transition from plutonic rocks to the other units is fairly sharp. The contacts between the tonalite and other units are mapped as faults with unknown displacement. Areas near the boundary of plutonic bodies are commonly brecciated. Lack of evidence of contact metamorphism and the brecciated nature of plutonic rocks near contacts suggests that contacts are tectonic in nature.

Hornblende Tonalite

Conspicuous outcrops of hornblende tonalite occur on upper slopes and hilltops. Skookum Butte, a prominent peak, 5382 feet in elevation, located in the southern part of Yreka Quadrangle is composed of the plutonic rock. The rocks are light colored on fresh surfaces and are composed of dull white plagioclase and gray quartz with dark colored clots of mafic minerals, hornblende and biotite. The rocks weather to pinkish-brown.

The plutonic rocks are classified as tonalite based on modal composition. Representative samples plot in the tonalite field of the quartz-alkali feldspar-plagioclase feldspar diagram (Figure 18a,b). Some rocks observed in the field are estimated to be quartz-diorite to trondhjemitic in composition. Mafic minerals consist

A

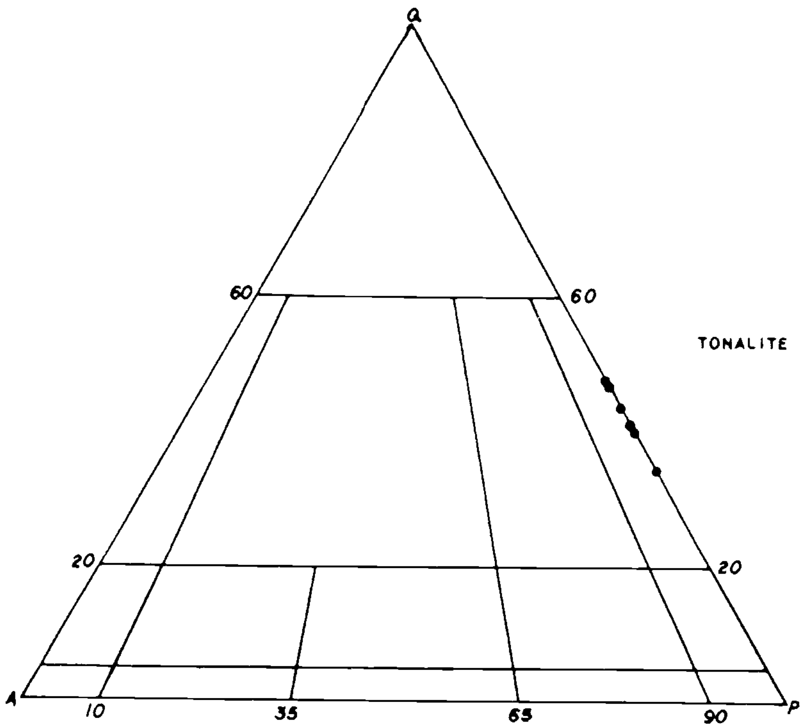

B

Rock Sample	SBQD	TGQD	86H-4 (103)	86H-8 (107)	86H-10 (109)	86H-14 (113)
QUARTZ	38	31	27	36	32	33
PLAGIOCLASE	44	46	52	43	48	45
MAFICS	18	23	21	21	20	22
K-SPAR	—	tr	tr	—	tr	tr
HORNBLENDE	6	14	14	9	12	14
BIOTITE	12	9	7	12	8	8

Notes: Accessories and secondary alteration minerals: zircon, apatite, magnetite, hematite, muscovite, sphene, epidote/clinozoisite, chlorite, sericite, calcite, prehnite. tr = mineral present in trace amounts, less than 1%.

Figure 18. A. QAP plot of samples of hornblende tonalite of the SSG, subdivisions after Streckeisen (1976). B. Modal abundances for selected samples of hornblende tonalite.

of hornblende and biotite that together comprise up to 23% of the mode. Plagioclase comprises from 43 to 54% and quartz from 27 to 38% of the mode. Hotz (1977) first described the silicic plutonic rocks and called them altered quartz diorite. Those that contain less than 10% mafics were called trondhjemite.

Microscopically, the rocks are fine- to medium-grained, with a hypdiomorphic texture. Plagioclase is altered and is partially saussuritized. Sericite, calcite, and epidote/clinozoisite are the alteration minerals. Most of the plagioclase is twinned; twins are bent and strained. Some plagioclase crystals have altered cores and clear albitic rims. Hotz (1977) noted that some rocks have myrmekitic intergrowths of sodic plagioclase, quartz, and traces of potassium feldspar. None of the 15 thin sections examined as part of this study showed myrmekitic or micrographic intergrowths. Potassium feldspar was not observed in thin section. Only traces of potassium feldspar, interstitial to quartz and plagioclase were observed on stained slabs.

Quartz is anhedral, strained and has curved to serrated edges. Hornblende is bluish-green and commonly occurs as anhedral plates altered to chlorite. Brown biotite occurs as large plates and is partially replaced by chlorite. Some biotite flakes are bent and kinked. Small grains of clinozoisite, with anomalous blue birefringence, and yellow-green epidote occur associated with altered plagioclase, chlorite and in places, with quartz. Other trace minerals found in these rocks include zircon, apatite, magnetite, hematite, and sphene.

Thin microbreccia zones filled with brecciated plagioclase, quartz, and epidote grains in a very fine-grained chlorite-rich matrix cut through the rocks. Larger mesoscopic breccia zones are observable in outcrop. Other thin fractures are filled with secondary minerals, calcite, or prehnite + chlorite + epidote + sericite.

The cataclastic and brecciated texture of these rocks and evidence of secondary low-grade alteration minerals, suggests that these rocks have undergone some degree of brittle deformation and hydrothermal alteration. But, none of the rocks are foliated. The very low-grade metamorphism exhibited by the tonalite suggests that the blocks were faulted into the melange matrix sometime after greenschist metamorphism of the matrix had occurred.

Isotopic Age

Two samples of tonalite from plutonic blocks within the SSG melange have been dated by Wallin and others (1988), using U-Pb methods on zircons. The two samples, TGQD and SBQD, come from the south side of Trail Gulch, a tributary gully into McConaughy Gulch, and Skookum Butte in the upper Moffett Creek drainage in the southern part of Yreka Quadrangle (see Plate 1 for location).

The tonalite is Early Cambrian in age. Concordia upper intercept ages of 564 + 7 and 565 $\pm$ 4 Ma were obtained from seven zircon fractions out of sample SBQD (Wallin and others, 1988). The sample from Trail Gulch, TGQD, gives somewhat similar results. Two zircon fractions from TGQD give $^{207}Pb/^{206}Pb$ ages of 566 $\pm$ 4 and 572 $\pm$ 7 Ma but have an older upper-intercept age of 640 Ma. The older upper-intercept age may be due to the following factors: (a) high degrees of discordance between zircon fractions, (b) presence of inherited zircons within the populations analyzed, or (c) the age may be the true crystallization age (Wallin and others, 1988). Wallin and others (1988) discount the upper-intercept age and believe that TGQD is Early Cambrian in age.

Correlation

The hornblende tonalite blocks of the SSG can be correlated with the plagiogranite of Gregg Ranch (PGR), an informally designated unit in the Lovers Leap and Gregg Ranch area of the China Mountain Quadrangle (Wallin and others, 1988; Potter, 1987; Haessig and others, 1987). Correlation between the plutonic rocks is based on similarities in lithology and age, both having Early Cambrian crystallization ages. Plagiogranite, as used here, refers to leucocratic tonalite-trondhjemite which is commonly associated with ultramafic, mafic, and intermediate rocks of oceanic or volcanic arc origin. The PGR, as described by Potter (personal communication), crops out in a discontinuous northeast-trending belt approximately 10 km long and less than 1.8 km wide. Exposures extend from southwest of Lovers Leap to northeast of Crater Creek in the China Mountain Quadrangle. The PGR occurs within map units of the Trinity ultramafic complex (Lindsley-Griffin, 1982). The PGR structurally overlies the intrusive rocks of the Trinity ultramafic complex and structurally underlies Middle Ordovician or older keratophyre of Lovers Leap and Middle Ordovician to Devonian sedimentary and volcanic rocks. Contacts between the PGR and other units are usually concealed and are inferred to be faults. A contact between the PGR and Middle Ordovician to Devonian sedimentary rocks is interpreted by Potter (1977; 1982) as depositional in places near Gregg Ranch. Dikes $\pm$ volcanics cut the PGR and overlying sedimentary rocks (Potter, 1977; 1982).

Mineral assemblages are essentially similar between the PGR and SSG tonalite. Hornblende, biotite and plagioclase are more thoroughly altered than in the SSG. Mafic minerals are commonly altered to chlorite; other alteration products include Fe-Ti oxides, sphene/leucoxene, sericite and epidote. The PGR, however, is less deformed and less brecciated on the whole. Calcite is the common vein mineral in small microfractures.

Four samples from the PGR have been dated by Mattinson (see Wallin and others, 1988). Data from these four samples yield $^{207}Pb/^{206}Pb$ ages from 572 to 550 Ma and concordia upper-intercept ages from 571 to 565 Ma.

Early Cambrian ages from the SSG tonalite and the PGR plagiogranite suggest that they may have once belonged to the same plutonic body or group of related bodies, which were later separated by faulting (Haessig and others, 1987; Wallin and others, 1988).

More recent U-Pb isotopic dating efforts by Wallin (personal communication) show that one zircon fraction from a sample of amphibolitic gabbro is Eocambrian to Early Cambrian in age (570 Ma). The amphibolitic gabbro was mapped as part of the Trinity complex by Lindsley-Griffin (1982). She found that the amphibolitic gabbro is in fault contact with the layered gabbro unit and is intruded by the pegamatitic gabbro unit. Locally, the amphibolitic gabbro grades down into clinopyroxenite. The presence of these Eocambrian to Early Cambrian ultramafic to mafic gabbro and plagiogranite is important new information. These bodies may be part of an igneous intrusive complex (ophiolite?) developed in the Early Cambrian, distinct from the later and more well known Ordovician Trinity ultramafic-mafic complex. Magmatism associated with the Trinity complex has occurred over a long period of geologic history, from 470 Ma (layered gabbro unit) to 412 Ma (pegmatitic gabbro unit) (Wallin and others, 1988).

Plagiogranite bodies of Early Cambrian age have been found in other Lower Paleozoic melanges and dismembered terranes in western North America and may be correlative. Early Cambrian or Eocambrian plagiogranite have been reported from the Sierra City melange of the Shoo Fly complex in the northern Sierra (personal communication from J. Saleeby to Wallin, 1987). A K-Ar age of 554 $\pm$ 16 Ma from a hornblende-bearing pegmatite was obtained from a sample of the Turtleback Complex on Orcas Island (Whetten and others, 1978).

Major-Element and Trace-Element Chemistry

Information on major-element composition of tonalite from Skookum Butte comes from two analyses published by Hotz (1977, p. 37). The tonalite is characterized by less than 1.5 weight percent K_2O, 3.5% Na_2O, and 14.5-16.2% Al_2O_3. SiO_2 content is approximately 63%.

Two sampls of tonalite were analyzed for trace and rare-earth elements by INAA (Table 7). The samples come from Skookum Butte (SBQD) and the Trail Gulch area (TGQD) and are Early Cambrian in age.

The distinctive features of the REE patterns of the tonalites are their flat unfractionated patterns, and their low REE abundances (Figure 19). The patterns show a small, negative europium anomaly. Low total REE (La = 5 to 8 X chondrite), and low Ta and Th abundances suggest a depleted source of magma for these rocks. Interestingly, heavy rare earths Tb to Lu are depleted relative to N-type MORB (see Saunders and Tarney, 1979; Frey and others, 1974; and Schilling, 1975 for REE field of MORB).

Insufficient data are available to definitively characterize the range in abundance of major, trace, and rare-earth element for the tonalite of the SSG. Replicate chemical analyses should be run as well as additional samples from other tonalite blocks in the melange.

Table 7. Trace-element content of hornblende tonalite samples SBQD and TGQD

Element	SBQD	TGQD
K_2O	590 ppm	1080 ppm
Sc	25.5	26.0
V	143	109
Cr	5	5
Co	14.4	11.9
Rb	10	21
Zr	------	------
Cs	0.37	0.58
Ba	92	284
La	1.7	2.5
Ce	4.0	4.7
Nd	------	------
Sm	0.76	1.06
Eu	0.28	0.33
Tb	0.22	0.18
Dy	1.3	2.0
Yb	0.95	1.30
Lu	0.14	0.23
Hf	0.55	1.20
Ta	0.12	0.08
Th	0.57	0.36
Sum REE*	12.3	16.0
$(La/Lu)_c$	1.27	1.13

Notes: *Sum REE is the sum of all REE (ppm) including estimates from chondrite normalized plots for elements not determined. Analytical errors at one standard deviation are: $\pm$ 1-3% for Sc, Co, Sm; $\pm$ 3-7% for V, La, Eu, Yb, Lu, Hf; $\pm$ 12-16% for K_2O, Rb, Cs, Ce, Dy; $\pm$ 18-19% for Th; $\pm$ 25-35 % for Cr, Ba, Tb, Ta. Concentration of Zr and Nd are below the limit of detection.

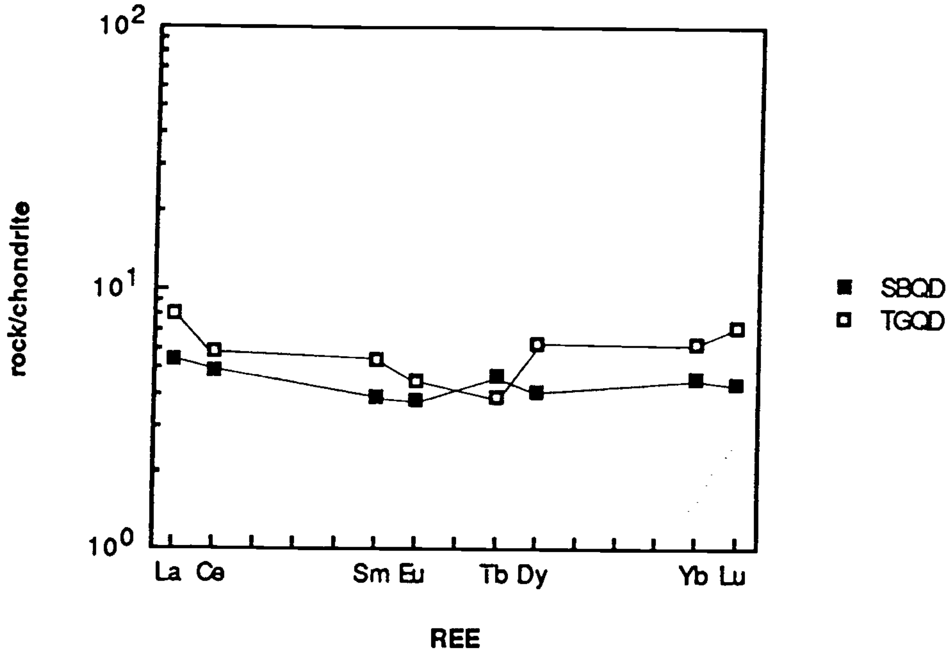

Figure 19. Chondrite normalized REE plot of Early Cambrian tonalite, samples SBQD and TGQD.

Rare-earth elements should also be studied from correlative Early Cambrian plagiogranite and amphibolitic gabbro of the Gregg Ranch area.

Petrogenetic Models

The major models for generation of plagiogranite, tonalite and trondhjemite include: (1) hydrous partial melting of a mafic source, typically oceanic basalt of a subducting slab or depleted upper mantle of a wedge above a zone of subduction (Defant and others, 1988; Johnston, 1986; Gromet and Silver, 1987; Pederson and Malpas, 1984; Gerlach and others, 1981; Malpas; 1979, Barker, 1979; Arth and Barker, 1976; (2) extensive levels (greater than 80%) of fractional crystallization of a tholeiitic magma (Spilber and Rutherford, 1983; Pallister and Knight, 1981; Stern, 1979; Coleman and Peterman, 1975); and (3) immiscibility of a highly differentiated silicate magma (Wildberg, 1987; Dixon and Rutherford, 1979). Of these three models, formation of the tonalite by partial melting seems most appropriate for the tonalites of the SSG. The low REE abundance and the flat unfractionated pattern of the analyzed samples make it unlikely that the tonalite was derived from high of fractional crystallization. Furthermore, a full suite of differentiates from mafic to silicic composition is unkown related to the Early Cambrian tonalites. The amphibolitic gabbro may be the mafic end member of a differentiation suite, but partial melting of this gabbro could also have formed the magma source for the tonalite-plagiogranite. The amphibolitic gabbro is an important key to determination of an appropriate model for the genesis of the plagiogranite. The liquid immiscibility model works well when there are no rocks of intermediate composition. The model implies that a differentiated basaltic melt separates into two immiscible melts: one of iron-rich basaltic composition and one of plagiogranitic composition. A possible Fe-rich basaltic member may be the Bonnet Rock volcanics which are high Fe-Ti submarine basalt, Silurian or older in age (Potter and others, 1976). But a genetic tie between the two is speculative.

Models using partial melting to explain the genesis of plagiogranite vary in terms of whether the slab or overlying mantle wedge undergo small degrees (15-30%) of partial melting at various pressures, to produce a silicate melt. In addition, models differ in whether the basalt precursor was in the amphibolite, garnet-granulite, or eclogite facies and what phases are in the residue after melt extraction (for example, clinopyroxene, plagioclase, amphibole, garnet). A possible model to explain the origin of the tonalite would be low levels of partial melting of a depleted upper-mantle source, or a basaltic source with LREE more depleted than N-MORB. Similar, flat REE patterns (Ce = 10-22 X chondrite) of the San Telmo tonalite of the the western region of the Peninsular Ranges Batholith (Gromet and Silver, 1987) indicate a probable source dominated by a LREE-depleted basaltic source.

Possible Tectonic Setting of Origin

Signatures of trace and rare-earth element and the local geologic setting of the tonalite of the SSG and correlative plagiogranite of Gregg Ranch can provide evidence as to the original tectonic setting of these Early Cambrian plutonic bodies. Plagiogranite is thought to originate in settings that produce ophiolites, such as, mid-ocean spreading axes, marginal-basin or back-arc-spreading axes and within volcanic arcs. Commonly, geochemical data on plagiogranite are compared with data on similar rocks from present-day tectonic environments. Although the total number of chemical analyses of plagiogranite from known settings is rather small, some progress has been made in using trace and rare-earth elements to differentiate oceanic plagiogranites from those formed within island arcs (Pearce and others, 1984a; Jahn, 1986). As used here, oceanic plagiogranites include those formed at mid-ocean ridges, as well as back-arc, marginal-basin and supra-subduction-zone trench-forearc environments.

The limited data on the chemistry of the tonalites of the SSG has some similarities to plagiogranite formed in island-arc settings and may be evidence for formation in an island-arc influenced environment rather than in an ocean ridge, marginal-basin or back-arc-spreading axis. Plagiogranite associated with island arcs is more enriched in K, Ba, Rb, and Sr and is more depleted in Th to Yb than similar rocks formed in ocean-ridge settings. REE signatures are flat and may or may not have negative europium anomalies (Cullers and Graf, 1984). High Th to Ta ratios are also indicative of volcanic arc plagiogranite (Pearce and others, 1984a). Plagiogranite from mid-ocean ridges or marginal-basin spreading ridges are depleted in K, Rb, and Ba and show LREE depleted to flat patterns (Jahn, 1986).

The elements K, Rb, Sr, and Ba are considered to be mobile under conditions of hydrothermal alteration and, low-grade metamorphism, and therefore, concentrations should be viewed with caution. The precise effect alteration has on mobile elements of mafic volcanics and plagiogranite are not fully predictable. However, interaction of seawater with basalt is thought to cause enrichment in K, Rb, and Sr, and that low-grade hydrothermal alteration or metamorphism causes leaching of these elements (Saunders and Tarney, 1984; Humphris and Thompson, 1978). The incompatible elements Th to Yb (in Figure 20) are thought to be essentially immobile.

SSG tonalite is compared to plagiogranite from well-known tectonic settings in Figure 20. The ocean-ridge granite, (ORG), values used as normalizing factors were calculated as the product of fractional crystalization of average N-type MORB and thus represent a hypothetical ocean-ridge granite composition (see Pearce and others, 1984a, p. 963-964 for discussion). The important characteristics of the hypothetical ORG composition are: (a) it reflects a granite composition derived from an unenriched upper-mantle source, and (b) its composition is unaffected by assimilation or melting of crustal components and is unaffected by volatile-influenced processes. Thus, plagiogranite which varies from an idealized flat pattern reveals a different genetic history which should vary in a systematic way with tectonic setting.

"Normal" ocean-ridge plagiogranite (OM3071 and Smartville) has a flat pattern with values close to unity (Figure 20b). Depleted values of K_2O and Rb may be due to alteration. The "anomalous" ocean ridge (MAR45N) has a relatively high abundance of Th, Ta, Nb, and Ce, typical of an enriched mantle source. Troodos departs from the normal pattern and shows high ratios of Th to Ta and is depleted in Nb, Ce, Hf, Zr, and Sm, which is more typical of basaltic rocks of tholeitic island

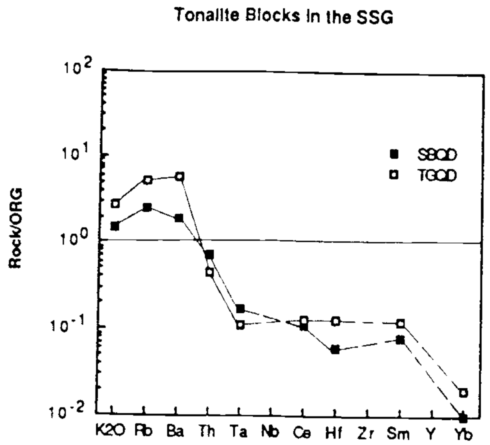

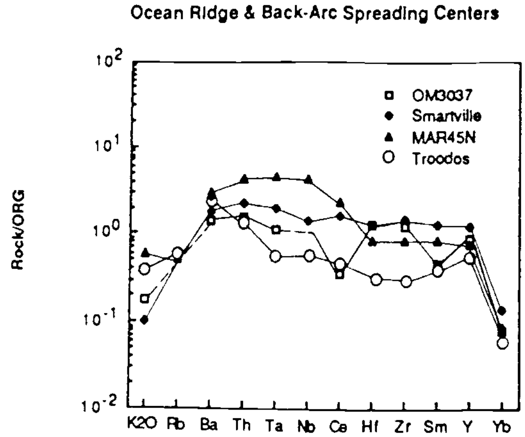

OM3037:	Oman ophiolite, "Spreading Axis Event, Alabaster and others, 1982
Smartville:	Smartville Complex, Sierra Nevada, Back-arc basin spreading ridge, Aldiss, 1982
Troodos:	Supra-subduction ridge, Aldiss, 1978
MAR45N:	E-type mid-cean ridge, Aldiss, 1978

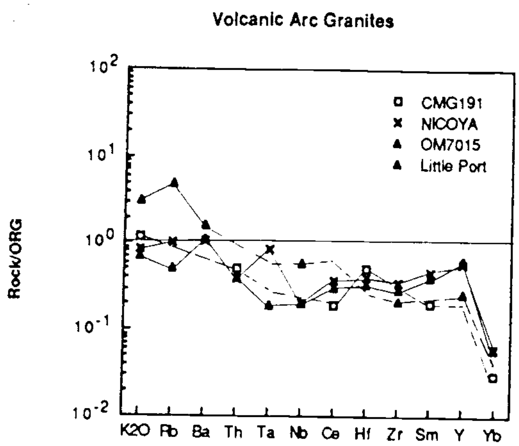

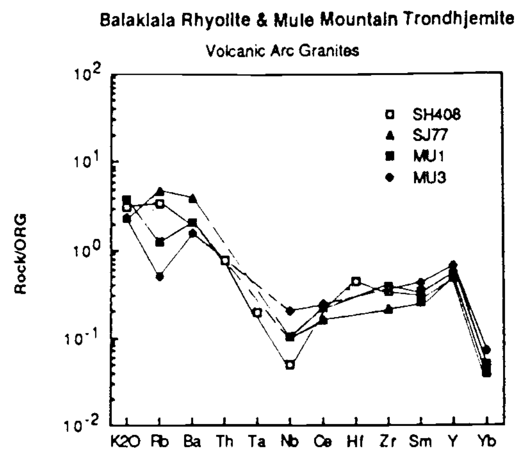

CMG191:	Canyon Mountain Oregon, Gerlach and others, 1981
NICOYA:	Nicoya ophiolite complex, Costa Rica, Wildberg, 1987
OM7015:	Oman, "Seamount event" or Late Intrusive Complex, Alabaster and others, 1982
Little Port:	Little Port Complex, Newfoundland, Malpas, 1979

SH408:	most depleted representative sample of Balaklala Rhyolite, Brouxel and others, 1987
SJ77, MU1, MU3:	Mule Mountain Trondhjemite, Brouxel and others, 1987

Figure 20. Ocean-ridge granite (ORG) normalized geochemical patterns for: (A) tonalite blocks of the SSG; (B) plagiogranites from ocean-ridge and marginal-basin spreading centers; (C) volcanic arc granites and (D) Balaklala Rhyolite and Mule Mountain Trondhjemite.

arcs. The plagiogranite from Troodos is considered to be representative of a supra-subduction zone setting where sea floor spreading occurs above a subduction zone at the very earliest stages of volcanic arc magmatism (Pearce and others, 1984a;1984b). The geochemical signature reflects a mantle source, modified by a subduction-zone component.

Volcanic arc granite shows patterns typified by Canyon Mountain, Little Port, Oman, and Nicoya (Figure 20c), and Balaklala Rhyolite and Mule Mountain trondhjemite (Figure 20d). The sample from Oman represents a primitive plagiogranite of the tholeitic island-arc series; its pattern is unusual and has a positive slope from Ta to Yb. Characteristic features of these patterns are the strong negative slope from Ba to Ta and overall low abundances of Ta to Yb.

Tonalite of the SSG shows similar patterns to the volcanic-arc granite, the Balaklala Rhyolite and Mule Mountain trondhjemite, and the subduction-influenced oceanic granite from Troodos. Note, however, that the Early Cambrian tonalite is more depleted in Ce, Hf, Sm, and Yb, which may reflect the magma source. The patterns of SBQD and TGQD seem to show show a mantle-dominated source; no evidence exists for crustal contamination.

Other discrimination diagrams using the elements Rb, Ta, and Yb can be used to distinguish the tectonic origin of granite. Both samples SBQD and TGQD plot in the volcanic-arc field on the Ta vs Yb and Rb vs Yb + Ta discrimination diagrams (see Pearce and others, 1984a, figures 3b and 4b).

Consideration of the local geology is also relevant to a discussion of the tectonic origin of the tonalite. Two different, as yet undated, keratophyre units are found locally related to the PGR of the Lovers Leap-Gregg Ranch area and the tonalite blocks of the SSG. These are the Middle Ordovician or older keratophyre of Lovers Leap and the quartz keratophyre of Horseshoe Gulch. REE patterns of three samples of the quartz keratophyre of Horseshoe Gulch are flat, (La/Lu_C = 0.88), and have low REE abundances, La = 11 X chondrite (Appendix 3, Figure 1). The REE patterns are more like low potassium tholeiitic (LKT) arc type volcanics than N-MORB mid ocean-ridge volcanics. Although the orgin of these keratophyres and locally associated volcaniclastic sediments is obscure, they record evidence of possible arc or marginal basin volcanism and sedimentation in the Middle Ordovician or earlier (Potter and others, 1975; Potter and others, 1977).

Finally, the crystallization age of the tonalites of the SSG and plagiogranite of the PGR correlates with a postulated rifting event of the western North American margin in the Eocambrian to Early Cambrian (625-555 Ma) (Bond and Kominz, 1984; Bond and others, 1984). These Early Cambrian plagiogranites may have been intruded during magmatic events associated with continental rifting (Wallin and others, 1988). If associated with the rifting event, and in consideration of the geochemical evidence presented, continental crust did not influence the magma source for the plagiogranite. Further, if the plagiogranite formed during a period of ocean-crust formation connected to continental rifting, the evidence seems to indicate that subduction was occurring nearby.

Intrusive Gabbro of Unknown Age

Two distinct gabbro bodies with sheared contacts were found in the SSG. A body of clinopyroxene gabbro with accessory hornblende (MC 95) is associated with serpentinite in the upper Moffett Creek drainage along a skid road east of the intersection of Sections 5, 6, 7, and 8, T. 42 N., R. 7 W., Yreka Quadrangle. The clinopyroxene gabbro crops out near bodies of marble, greenschist and phyllitic quartzite. A hornblende gabbro body (UMG 68) occurs in the Upper McConaughy Gulch locality where it ia exposed along the road and in a gully north of the road.

Clinopyroxene Gabbro

These rocks are brown on weathered surfaces and dark gray on fresh surfaces. Microscopically, the rock is fine-grained with a hypidiomorphic granular texture. The rock is composed of 42% plagioclase, 44% mafics, and 8% quartz, based on point-count data from one thin section. Accessory minerals include opaques, (magnetite-ilmenite), zircon, and sphene. Alteration minerals present include calcite and chlorite.

In thin section, plagioclase appears hazy and shows evidence of saussuritization. Cores of prismatic plagiocalse are sericitized and may have inclusions of clinozoisite. Patches of calcite seem to be replacing plagioclase as well. Rims of plagioclase are clear (albitic?). Granophyric to micrographic intergrowths of plagioclase and quartz are common. Augite is the predominant mafic mineral, comprising 23% of the mode, and occurs as colorless to pale brown euhedral grains and aggregates of grains. Amphibole in these rocks is pale to dark olive-green, ($Z \wedge C = 15\text{-}20^{\circ}$) and is slightly less abundant (21% of the mode) than clinopyroxene. Amphibole shows two types of alteration: (a) alteration to a Fe-Ti oxide phase + sphene (leucoxene) and (b) alteration to chlorite. Amphibole also occurs as overgrowths on augite.

Hornblende Gabbro

Hornblende gabbro crops out in the Upper McConaughy Gulch locality and is recognized by its fine-grained igneous texture, brown weatherd surfaces, and speckled, gray-brown fresh surfaces. Contact relations of this gabbro body are obscure. The body seems to be dike-like, but evidence of contact metamorphism of the surrounding metamorphic rocks is not apparent. Furthermore, the gabbro is associated with local small northeast-trending faults. The gabbro may have been intruded along faults, and subsequent deformation may have obliterated intrusive contacts and evidence of contact metamorphism, or the entire gabbro body may be a fault slice in the melange.

Microscopically, these rocks have a hypidiomorphic texture. Altered saussuritized plagioclase is abundant and comprises 61% of the mode. Plagioclase prisms have sericitized cores and clear rims. Small grains of clinozoisite appear in plagioclase; patches of calcite also are replacing plagioclase. Hornblende is the primary mafic mineral and appears altered. Fe-Ti oxides occur as skeletal replacements of hornblende. The oxides have altered to sphene + leucoxene. Some of the amphibole has altered to chlorite. Quartz is present in minor amounts (5% or less). Micrographic intergrowths of quartz and plagioclase were noted, but are not nearly as pervasive as in the clinopyroxene gabbro.

Significance and Possible Age

Gabbro bodies, similar to the one from in the upper Moffett Creek area, are commonly associated with serpentinite along faults in the Callahan-Yreka-Gazelle area (Hotz, 1977). Other dikelike bodies of mafic rocks simlar to the hornblende gabbro in Upper McConaughy Gulch are known to intrude the Moffett Creek, Duzel Phyllite, Sissel Gulch Graywacke, and Gazelle Formations (Hotz, 1977; Rohr, 1977).

The ages of these gabbros are not known. They are probably younger than the SSG, based on contact and map relations. The low-grade alteration they show may be related to Devonian metamorphism.

Serpentinite

Serpentinite bodies or lenses are rare in the SSG. The only serpentinite found during the course of mapping and reconnaissance is that noted by Hotz (1977) in the southern part of the Yreka Quadrangle. The serpentinite crops out on a logging skid road along the north side of a gully that enters into Moffett Creek near the corner of Sections 5, 6, 7, and 8, T. 42 N., R. 7 W., Yreka Quadrangle. The serpentinite body occurs in quartz-albite schist and greenschist matrix. It is approximately 120 feet long and 30 feet wide. Marble lenses, greenschist, and quartzose phyllite exposures also occur locally. The serpentinite body encloses a weathered pyroxene gabbro intrusive body (MC 95).

The serpentinite may be related to an undated belt of ultramfic rocks and gabbro found in the northwest part of the Yreka Quadrangle. The ultramafic belt and various isolated serpentinite bodies such as that found in the SSG may be a continuation or part of the Ordovician Trinity ultramafic complex (Hotz, 1877, p. 35). Or, the ultramafics and gabbro may be part of a distinct, separate ultramafic body as postulated by D'Allura and others (1974) and Cashman (1980). Serpentinite is locally and rarely found along faults in other formations in the Callahan-Yreka-Gazelle area, such as in the Duzel Formation, Moffett Creek, and Gazelle Formations and along their contacts (Hotz, 1977; Rohr, 1977).

GEOCHRONOLOGY

Isotopic Age of Metamorphic Rocks of the SSG

K-Ar and Rb-Sr isotopic techniques have been used to date the age of metamorphism of metamorphic rocks in the SSG. The two K-Ar dates are on phengitic white mica and give dates of 439 $\pm$ 13 Ma from a siliceous semi-schist and 451 $\pm$ 14 from a crossite-bearing schist (Potter and others, 1981). The Late Ordovican to Early Silurian dates obtained should be viewed with caution as ages of metamorphism of the schists, because the presence of detrital white mica cannot be ruled out. More recently, Rb and Sr data on whole-rock and mineral separates have been used to date schists from the SSG by Cotkin and Armstrong (1987). They report a date of 447 $\pm$ 9 Ma on a phengite whole rock pair from a quartz-albite schist. This date is interpreted as the time of blueschist-facies metamorphism (Late Ordovician). A whole-rock isochron age of 467 $\pm$ 45 Ma on four glaucophane schists is interpreted by them as the time of protolith formation in the Middle Ordovician. A four-point mineral isochron on a lawsonite-glaucophane schist gives a date of 357 $\pm$ 18 Ma. This date is interpreted to indicate resetting of the Rb-Sr system in the rock during a later metamorphic event in the Devonian.

Attempts to date sphene from a blueschist block using U-Pb methods were unsuccessful due to low uranium contents (J. M. Mattinson, written communication). Conodonts or other fossils have not been found in any of the carbonate or chert lithologies.

The new Rb-Sr ages are concordant within analytical uncertainty with previously reported K-Ar ages on the SSG and show that a metamorphic event occurred in the Late Ordovician to Early Silurian. Note that the Rb-Sr age on the quartz-albite schist is greater than or equal to the K-Ar date on siliceous schist. In many high-pressure metamorphic terranes, the problem of inherited radiogenic ^{40}Ar is common (Armstrong and others, 1986). K-Ar ages on phengite are generally older than Rb-Sr ages of the same white micas, indicating the presence of inherited argon in the white mica. The few dates on quartzo-feldspathic schist (greenschist facies matrix rocks) of the

SSG appear not to have the problem of inherited argon. In the Franciscan Complex of California, inherited argon is not a problem because the protolith age and time of metamorphism are similar (Armstrong and others, 1986; Coleman and Lanphere, 1971; Suppe amd Armstrong, 1972).

In addition, the K-Ar ages on phengite from these matrix-rock lithologies of the SSG do not seem to be reset by Devonian metamorphism. The Devonian age obtained from the lawsonite-glaucophane schist fits in the range of ages determined for the time of metamorphism of the Central Metamorphic Belt, about 350-400 Ma (Cashman, 1980). The minimum age of metamorphism of matrix rocks and blueschist facies blocks appears to be constrained to the Early Silurian; the age of blueschist facies metamorphism is not well defined and may be older than the K-Ar age of 451 $\pm$ 14 Ma, that is, if one assumes that the K-Ar age is the cooling age. I believe that the metamorphic age of blueschist-facies blocks may be slightly older than that of matrix lithologies. A similar situation is found in the Franciscan Complex, where-high grade blueschist and eclogitic blocks yield older dates than the high-pressure mud-matrix rocks. The blueschist blocks may well record a range of ages, reflecting metamorphism and cooling over several millions of years, which may be unresolvable by dating methods.

Further isotopic-age studies need to be performed to constrain the time of blueschist-facies metamorphism of tectonic blocks in the SSG. Suitable samples of phengite-bearing lawsonite-glaucophane schist in the SSG should be dated using the $^{39}Ar/^{40}Ar$ technique on separates of phengite and sodic amphibole. The white mica could reveal the time of blueschist metamorphism. The sodic amphibole may provide a record of resetting due to later thermal metamorphic events. The poor retention of argon by sodic amphibole makes it unlikely that it would record the time of blueschist-facies metamorphism.

Constraints on the Age of the SSG and Timing of Uplift

The formation of the SSG melange is constrained by the age of metamorphism of blueschist facies blocks and greenschist facies matrix rocks, and timing of uplift of erosion of matrix rocks. The oldest known blocks in the melange are the tonalites which are Early Cambrian in age. The age of the youngest blocks in the melange is not known, thus the maximum age (upper limit) of melange formation is uncertain. Blueschist facies metamorphism occurred during Middle Ordovician to Early Silurian, based on the present information from isotopic dates. Uplift and erosion of the melange occurred by the Late Silurian, based on the presence of metamorphic and plutonic clasts in conglomerates in Horseshoe Gulch.

The existence of hornblende-biotite tonalite to trondjhemitic clasts and siliceous metamorphic clasts in Late Silurian or younger conglomerate units in Horseshoe Gulch units has been noted by Potter and others (1977) and Potter (1982).

In thin section, schistose metamorphic clasts strongly resemble graphitic schist and quartz-albite schist of the SSG. These metamorphic clasts contain trace amounts of brown and olive-green tourmaline that is a distinctive characteristic of the siliceous schists of the SSG matrix. Tonalitic clasts bearing altered hornblende and biotite are also fairly common in the conglomerate and may range from 1 mm to boulder size.

Clasts bearing blue amphibole or lawsonite have not been found; greenschist facies, mafic-volcanic clasts have also not been observed.

The presence of schistose metamorphic and tonalitic detritus is significant because it shows that the matrix lithologies and tonalitic blocks had been uplifted and were being eroded by the Late Silurian. That observation, in view of the Late Ordovician to Early Silurian Rb-Sr phengite whole-rock age of 447 ± 9 for a quartz-albite schist (Cotkin and Armstrong, 1987) provides evidence that uplift soon followed metamorphism. The apparent absence of blueschist clasts in conglomerate is disappointing, yet may well be due to incomplete sampling. Even in the Franciscan terrane, however, only minor amounts of blueschist detritus are found, reworked into Franciscan sediment and conglomerate (Cloos, 1986).

STRUCTURE

Introduction

The schist of Skookum Gulch is interpreted to be a tectonic melange. Blueschist blocks within the schistose matrix are complexly deformed. The blueschist blocks reveal four major folding events and at least two definable ductile and brittle shear deformations. One period of metamorphism under blueschist facies conditions is recorded in the blueschist blocks. The blocks show little evidence of recrystallization or evidence of prograde greenschist-facies overprinting. Similar conclusions regarding lack of polymetamorphism of blueschist blocks were reached by Cotkin (1987). Schistose rocks of the matrix are less deformed than the blueschist blocks. Matrix schists show at least two phases of folding. The predominant foliation is the result of transposition and shear folding. Locally-developed, penetrative, asymmetric kink folds of this foliation represent the second phase of folding.

The problems addressed in the following sections are multiple and include: (1) structural style of deformation of blocks and matrix in the melange; (2) relationship between blueschist and greenschist facies metamorphism and deformation; and (3) timing of emplacement of high P/T and other blocks into the melange.

Terminology and Nomenclature

Descriptive structural terminology and nomenclature used in the following sections includes the definitions of Hobbs, Means and Williams (1976), and Turner and Weiss (1963) for folds, foliations, and lineations; Gray (1977) for crenulation cleavages and the method, employed by Bell and Duncan (1978), of listing lineations and fold axes. S-surfaces or schistosity surfaces are differentiated between matrix rocks and blocks. Matrix foliations and foliations common in blocks and matrix rocks are denoted with alphabetical subscripts, for example, S_B and S_K. Foliations of blocks are denoted with numerical subscripts, for example, S_1-S_4. An example of the nomenclature for lineations is the following: L_4^2, which indicates an intersection lineation of S_4 and S_2. F_2^2, translates as the second fold event that folds S_2, where the subscript refers to the fold event and the superscript refers to the surface folded not the fold generation or the axial plane.

Deformation History of Blocks

A summary of structural elements found in blueschist blocks as well as other blocks and matrix components appears in Table 8. Depictions of fold styles and plan maps of polydeformed blocks appear in Figures 21-25 and Plates 6, 7, and 8. The deformation of the blueschist blocks consists of the following stages.

(1) D1: Transposition, (F_1), of an early foliation defined by blue sodic amphibole, with the formation of the pervasive foliation S_2, and the development of a mineral lineation L_2^1 oriented parallel to S_2.

(2) D2: Tight to isoclinal outcrop and smaller scale folding (F_2) of the S_2 foliation with development of the S_3 axial plane and L_3^2 fold hinge.

(3) D3: Refolding of S_3 and S_2 into outcrop and smaller scale tight folds, (F_3), with the formation of the S_4 crenulation cleavage in the axial plane of F_3 folds and an intersection lineation, L_4^2.

(4) D4: Conspicuous, locally-developed, penetrative, asymmetric kink folds of S_2, (F_4) with formation of a hinge lineation L_K and axial surface, S_K.

(5) D5: Narrow ductile shear zones on S_2, associated with mineralization along the shear plane.

(6) D6: Brittle en-echelon extension fractures on S_2 associated with shear zones. Some extension fractures are mineralized, others are open.

Deformations, Fold Styles, and Microscopic Structures of Blocks

First Deformation

D1 records transposition of an early mineralogical layering and

Table 8: Observed structural elements of blueschist blocks, chert, marble, and plutonic blocks, and greenschist-facies matrix rocks of the Schist of Skookum Gulch

BLUESCHIST BLOCKS

D1

S_1: relict hinges and curved inclusion trails of blue amphibole, sphene ± lawsonite in albite and quartz

F_1: transposition of S_1 with the formation of S_2

S_2: predominant foliation in blocks

L_2^1: intersection mineral lineation, oriented parallel to the fold axes of transposed folds

D2

F_2: isoclinal to tight folds of S_2, (F_2)

S_3: axial plane to F_2

L_3^{2h}: hinge lineation of F_2

D3

F_3: isoclinal to tight refolds of S_2 and S_3, (F_3^2)

S_4: crenulation cleavage, axial plane to F_3

L_4^{3h}: hinge of F_3; intersection lineations L_4^2 and L_4^3

D4

F_4: asymmetrical kink folds of S_2, (F_4^2)

S_K: axial surface of the kink folds

L_K: hinge lineation; intersection lineation L_K^2

D5: ductile shear zones

D6: brittle shear zones and en-echelon extension shear fractures

CHERT, MARBLE, PLUTONIC, AND OTHER BLOCKS

D1

S_0: bedding in chert

S_1: solution cleavage (dark colored laminae) in marble; phyllitic cleavage in marble

F_1: folds of S_1 in marble; folds of S_B in greenschist blocks

D2

S_2: incipient crenulation cleavage in micaceous domains in marble

ROCKS OF THE MATRIX

D1

S_0: relict bedding in quartzose phyllite

F_1: isoclinal folds of bedding F_1^0 in quartzose phyllite; transposition of S_A in matrix schists with the formation of S_B, the predominant foliation

S_A: axial-plane cleavage of F_1^0 folds in quartzose phyllite; phyllitic cleavage domains in marble interlayered with matrix schists

S_B: dominant foliation in schistose rocks of the matrix

L_B^A: mineral lineation, oriented parallel to the fold axes of transposed folds

D2

F_2: kink folds of S_B

S_K: axial surface of kink folds

L_K: hinge line of kink folds

D3: ductile shear zones

D4: brittle deformation (fractures)

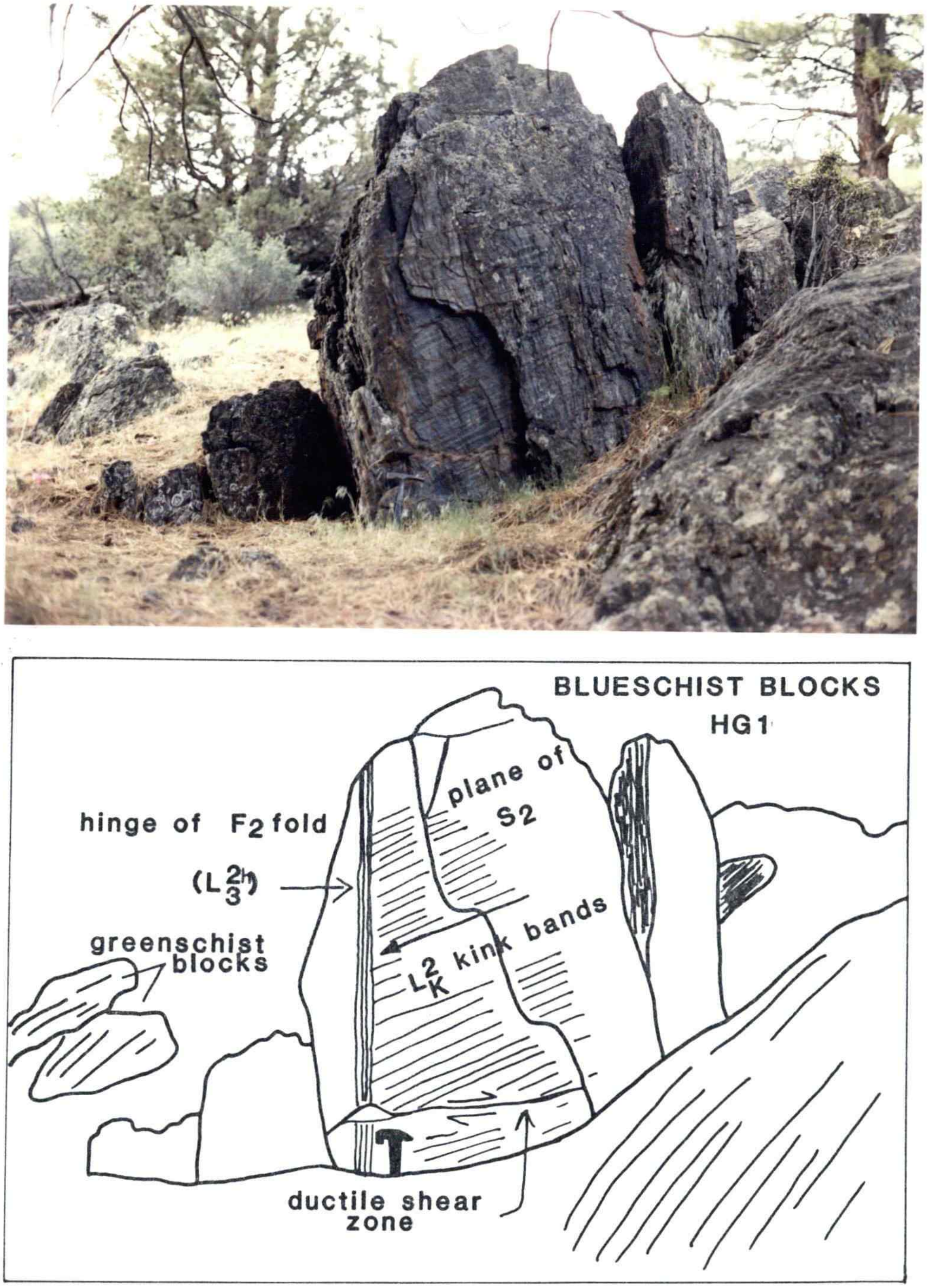

Figure 21. Deformational features exhibited by a blueschist block. Features include: predominant schistosity surface, S_2; hinge line, L_3^{2h}, of a nearly vertical, steeply plunging fold of S_2, (F_2 event); kink bands, L_K^2, (F_4, kink-folding event); and ductile shear zone (D_5). Lawsonite-Na-amphibole schist, outcrop HG1. See Plate 6 for a map view of the HG1 outcrop area.

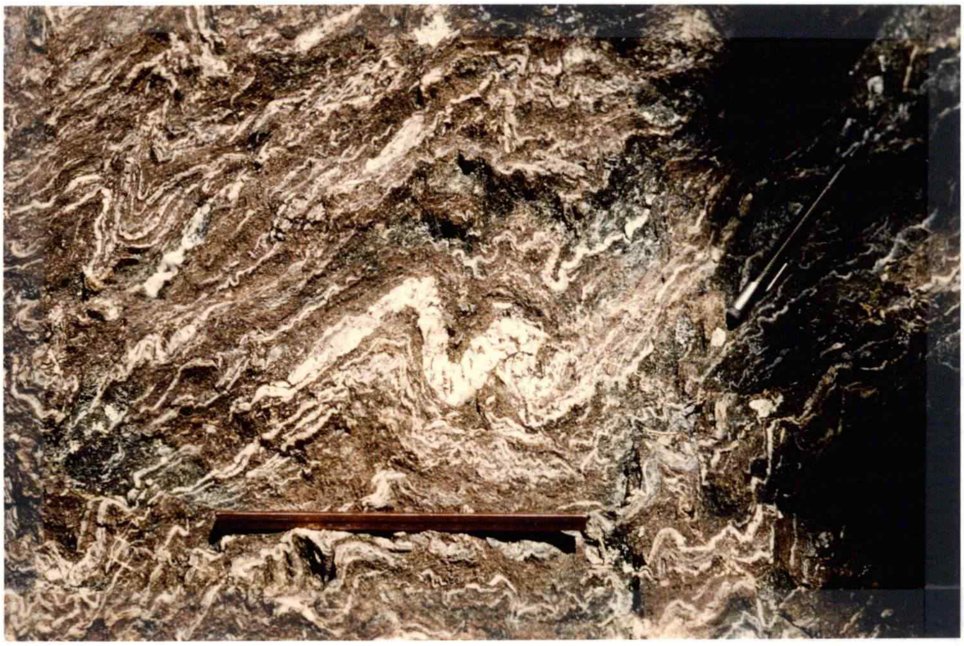

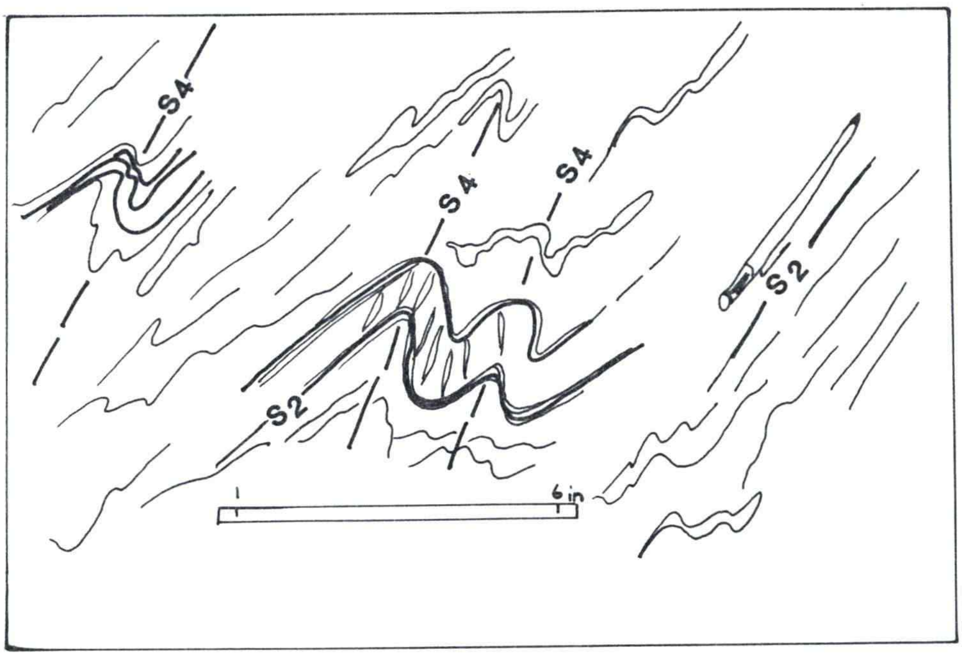

Figure 22. Tight to close folds of quartz veins in lawsonite-Na-amphibole schist, sample HG3. Small scale F_3 folds of S_2 are shown, with axial plane cleavage development, S_4. See Plate 7 for a map view of outcrop HG3.

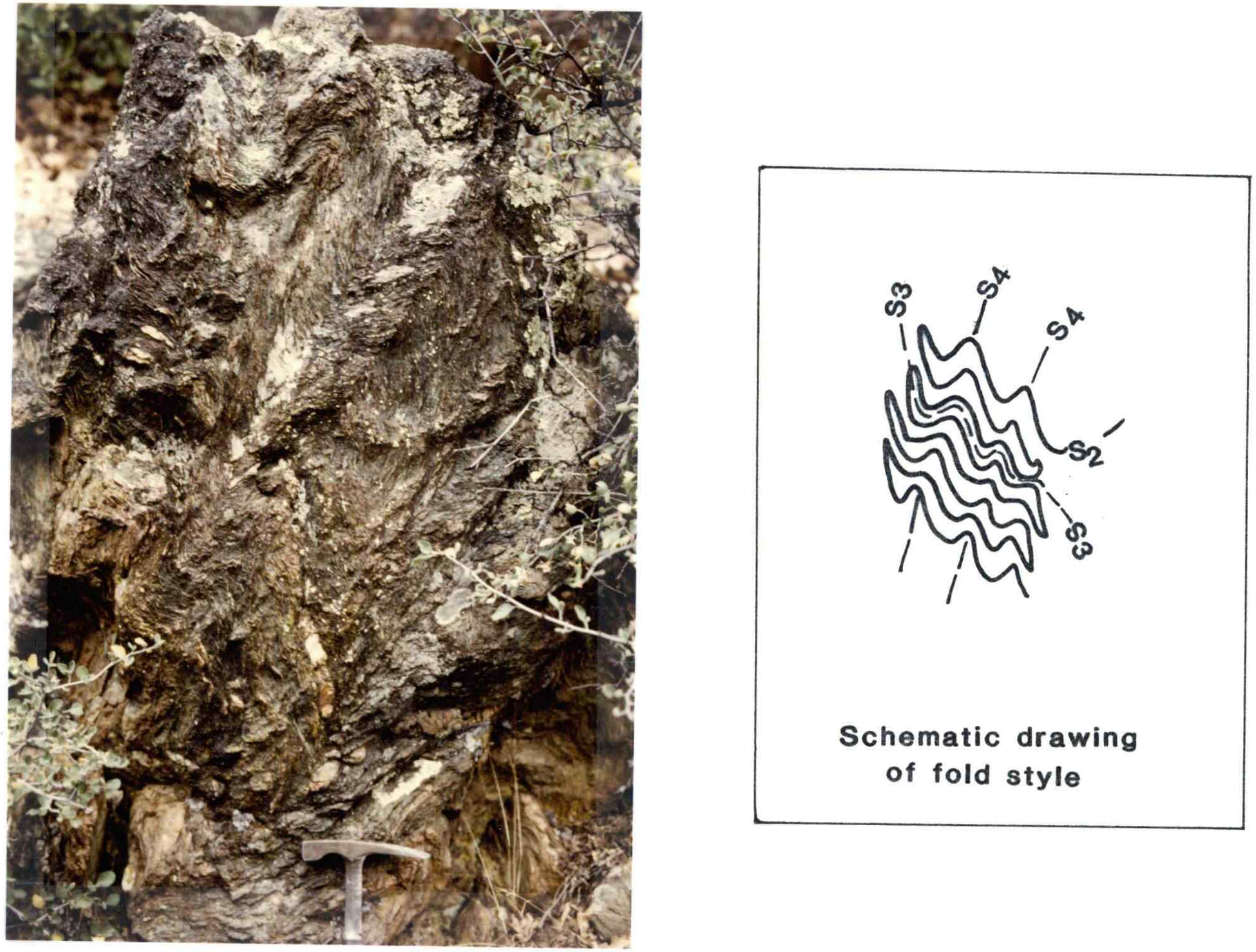

Figure 23. Refold pattern in epidote-Na-amphibole-bearing quartz-mica schist, outcrop UMG 59. Harmonic, "Z" shaped F_3 folds, refold S_2 and S_3. The axial surface of the F_3 folds is S_4.

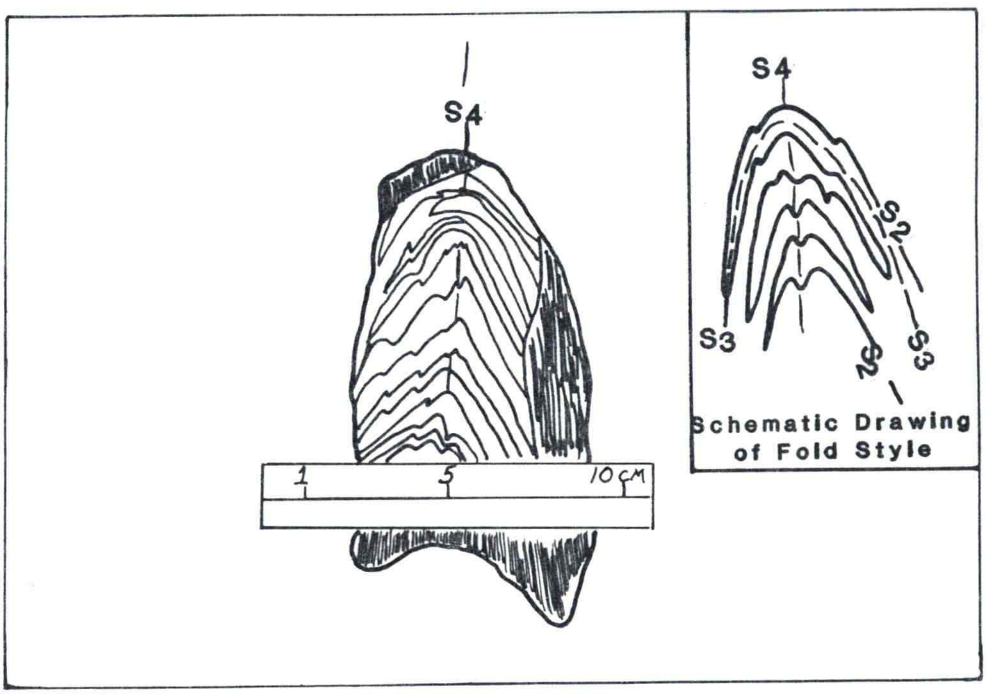

Figure 24. Close up view of fold style of outcrop UMG 59. Superposed fold pattern showing F_3 folds with incipient development of associated S_4 axial surface. Rock type is a high P/T transitional facies metasedimentary rock, containing epidote and blue amphibole.

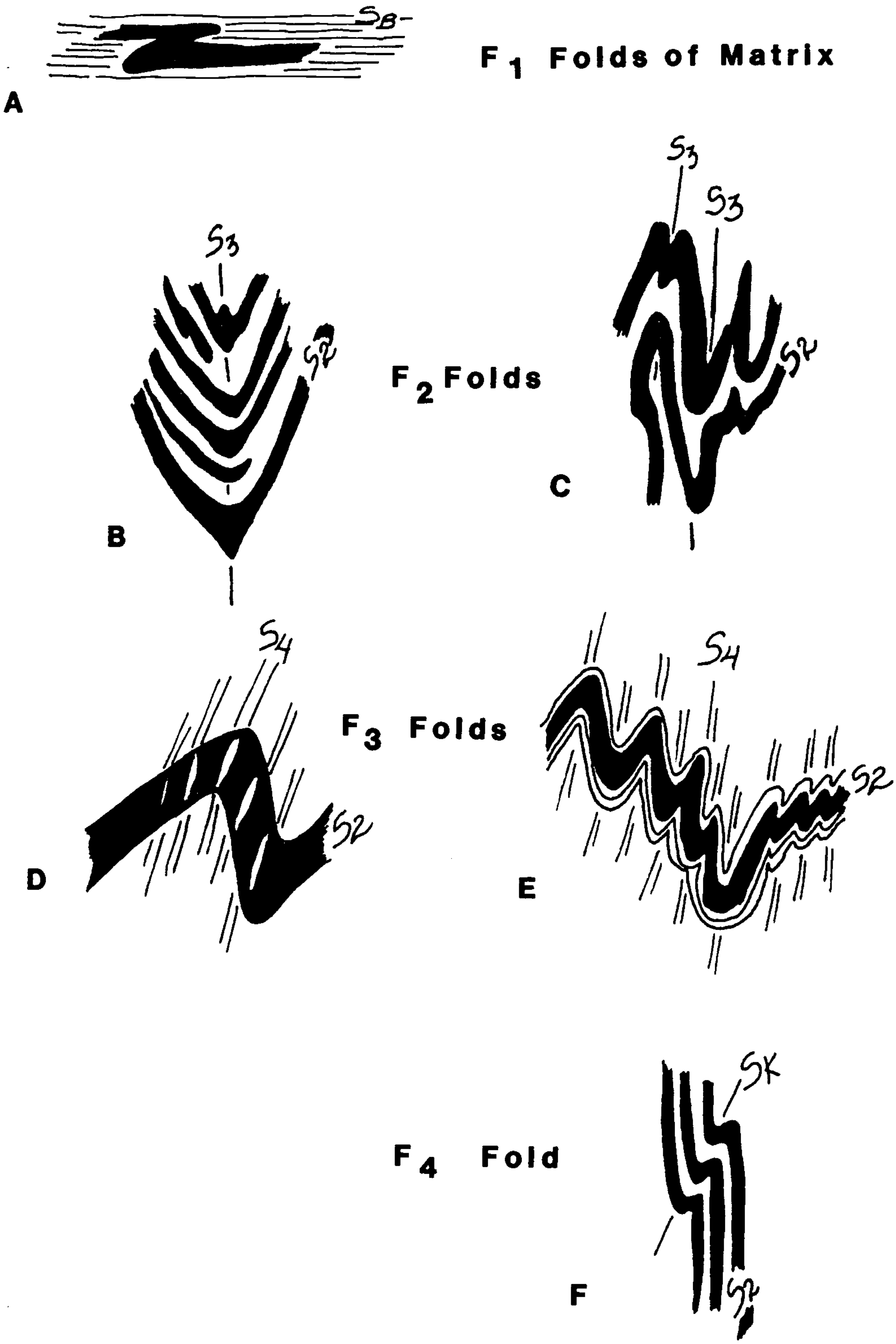

Figure 25. A. Intrafolial folds with predominant foliation, S_B, parallel to axial surface of fold. B and C. F_2 folds. Tight to isoclinal folds of S_2 (predominant foliation) with S_3 axial planes. D. and E. F_3 folds of quartz vein, and associated axial planar cleavage development, S_4. F. F_4 folds: asymmetric kink folds of S_2.

foliation defined by blue amphibole. Evidence of D1 is commonly obliterated, and only the pervasive foliation, S_2, is evident. Careful examination of thin sections reveals traces of compositional bands and intrafolial fold hinges of quartz + albite as evidence of mineral layering. Relicts of S_1 are preserved as helicitic inclusions of blue amphibole + sphene $\pm$ epidote $\pm$ lawsonite in albite porphyroblasts and in quartz + albite domains. Two rock samples show particularly well-preserved evidence of transposition (Figure 26). A mineral lineation L_2^1 of blue amphibole is associated with D1 and is an intersection lineation of S_2 and S_1. Few samples show coarse enough blue amphibole to define the trace of the mineral lineation on the S_2 schistosity surface. In the samples where the mineral lineation can be defined, it parallels the axes of the transposed folds. The transposed foliation S_2 is the dominant foliation of the blueschist and is the foliation measured in mapping. Sodic amphibole + lawsonite or sodic amphibole + chlorite domains define the S_2 foliation.

--Microscopic Textures of D1

D1 can be divided into two stages, early and late. Blueschist facies minerals, for example, lawsonite, sodic amphibole, epidote and associated minerals, chlorite, sphene, actinolite, and others, crystallized during early D1 and continued to crystallize during late D1. In early D1, plagioclase is replaced by lawsonite and glaucophane. Other igneous minerals such as pyroxene are entirely replaced by chlorite, epidote, sodic amphibole, lawsonite, and actinolite. Lawsonite and albite contain helicitic inclusions of S_1 minerals, blue amphibole + sphene, and thus grew syntectonically with S_1. Lawsonite forms static intergrowths in hinges of S_1 microfolds and continued to grow as porphyroblasts along with blue amphibole during formation of S_2. Curved inclusion trails of the S_2 foliation in epidote and lawsonite indicate that these minerals grew and were rotated syntectonically with development of S_2. Clear rims on lawsonite tablets indicate static growth after development of S_2. Figure 27 is a photomicrograph of a rather coarse-grained blueschist showing the dominant foliation, S_2.

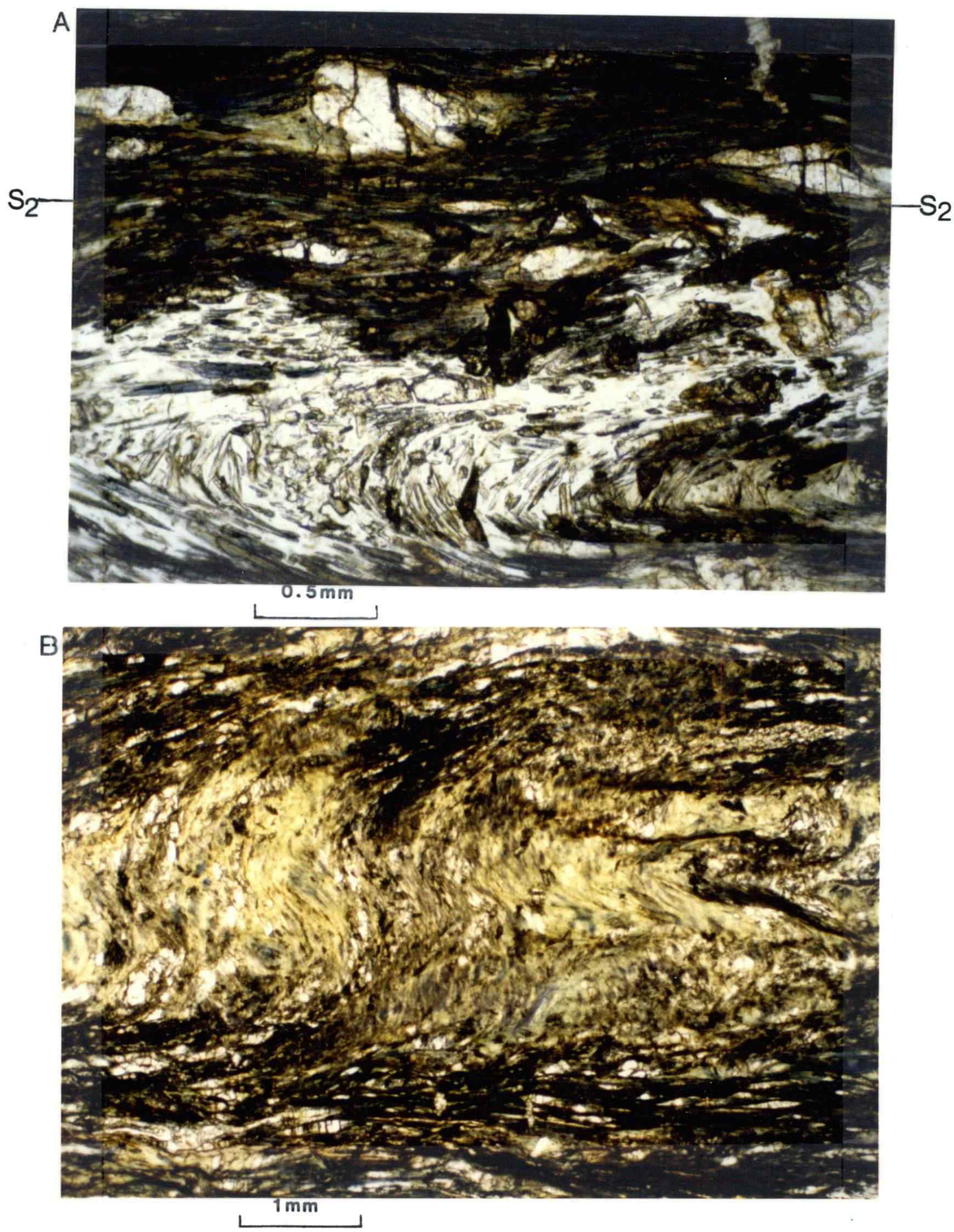

Figure 26. A. Curved trails of blue amphibole, sphene, and lawsonite, showing relict S_1 foliation. Colorless matrix is albite. Transposition of S_1 results in formation of S_2, the pervasive foliation; note aligned blue amphibole + chlorite in upper part of photo. Lawsonite-Na-amphibole schist, HG16b. 40X, PL, FOV = 3.3 mm B. Transposition of S_1 to form S_2. Blue amphibole lineation parallel to S_2 foliation. Lawsonite-Na-amphibole schist, HG16B. 20X, PL, FOV = 6.7 mm.

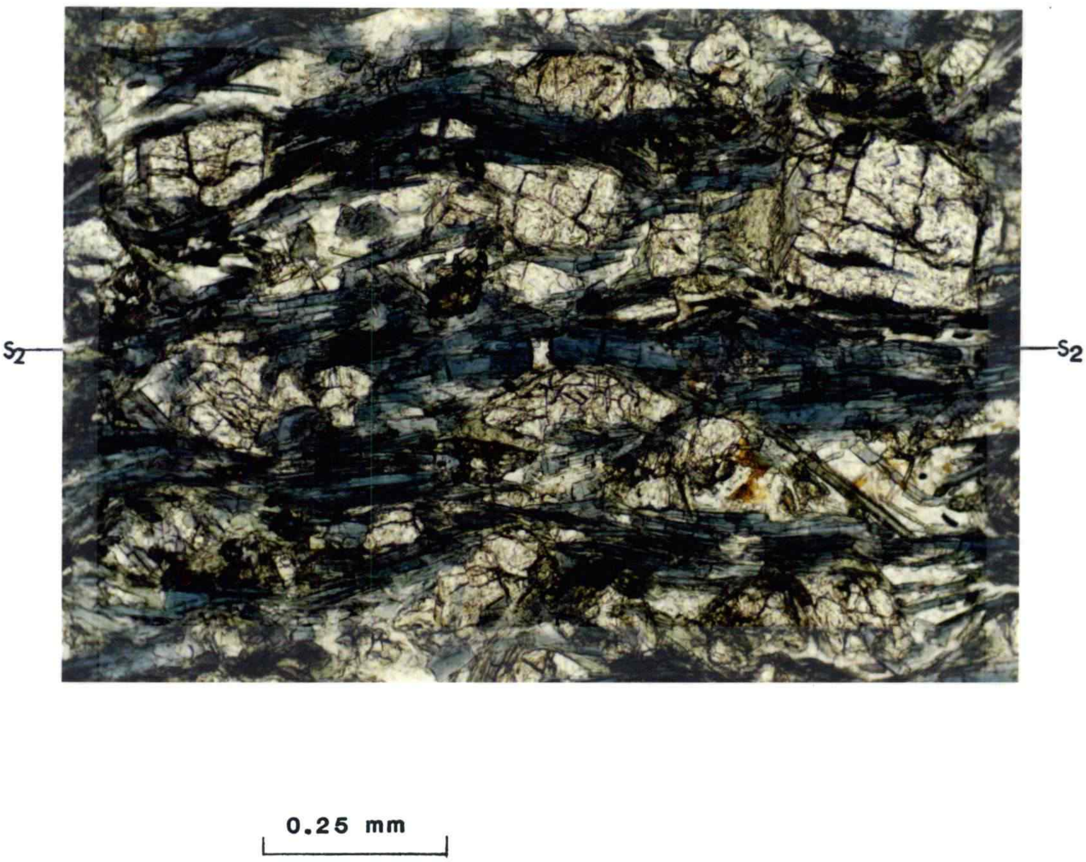

Figure 27. Lawsonite-Na-amphibole schist displaying predominant foliation, S_2, that anastomoses around colorless lawsonite porphyroblasts. Lineation parallel to S_2. Note fractured blue amphibole in center of photo with quartz growing in fracture. Lawsonite porphyroblasts show pressure shadows filled by chlorite and quartz. Dark crystals of high relief are sphene. Sample NNG31A. 100X, PL, FOV = 1.31 mm

Second Deformation

D2 is characterized by outcrop-scale and smaller tight F_2 folds of the S_2 foliation (Figures 21, 25b,c and Plates 6, 7 and 8). Outcrop-scale folds are rare but two good examples are known and occur at the Horseshoe Gulch locality, HG1 and HG3 (Plates 6 and 7). The two large F_2 folds in HG1 and HG3 are nearly vertical with steeply plunging fold axes. The axial plane of the F_2 folds is S_3. A well-developed axial plane cleavage is not associated with S_3; small minor folds with axes parallel to S_3 are noted at the hinge regions of the F_2 folds. Thin-section-scale tight F_2 folds occur, with fold limbs parallel to the dominant foliation, S_2. The lineation associated with F_2 is the hinge lineation, L_3^{2h} formed by the intersection of S_2 foliation and the S_3, axial plane (Figure 21).

--Microscopic Textures of D2

A small degree of blueschist-facies mineral growth is associated with the D_2 deformation. Static growths of small tablets of lawsonite are noted in the hinge regions of microfolds. Blue sodic amphibole forms polygonal arcs in hinges of F_2 microfolds. Lawsonite tablets in S_2 are polygonized in the hinge regions of microfolds; clear rims also occur on lawsonite tablets in the foliation.

Third Deformation

D1 is commonly observed as tight to close small-scale folds of S_2 and refolded isoclinal F_2 folds (Figures 22, 23, 24, and Plates 6 and 7). Refolds of S_2 and S_3 into tight to close asymmetrical folds include varieties of Class III superposed patterns of Ramsay and Huber (1987, p. 492), (Figures 23, 24). An incipiently developed axial-plane cleavage, S_4, is developed in the F_3 refolds (Figures 23, and 24). In most of the blueschist-facies blocks, the F_3 folds are expressed by a zonal crenulation cleavage to a weakly developed strain-slip cleavage, with the S_4 cleavage parallel to the F_3 axial plane. In blocks which do not show F_3 folds, the crenulation cleavage is commonly observed and cuts the S_2 cleavage at a low angle. These crenulation cleavages are a distinctive deformational feature of the blueschist. The lineation L_4^2 is defined by the intersection of S_2 and S_4 and by the hinges of F_3 folds. On S_2 schistosity surfaces, the crenulation lineation (trace of the hinge line on schistosity surfaces) is a conspicuous feature and is distinct from the more widely spaced F_4 kink bands. The hinge lines of the crenulations give a crinkled appearance to schistosity surfaces.

—Microscopic Textures of D3

Microscopic features of the F_3 folds and crenulation cleavages are shown in Figure 28. Features include bent and broken blue amphibole in the hinge zones. Blue amphibole, stretched lawsonite, and phengite form limbs of the microfolds. Pressure shadows of phengite or quartz form adjacent to lawsonite tablets in the limb regions. Even in thin sections where the crenulation cleavage is only weakly developed, lawsonite porphyroblasts as well as blue amphibole prisms have undergone microboudinage with quartz or phengite crystallizing adjacent to strained mineral grains.

Fourth Deformation

The fourth deformation is observed as asymmetric kink folds of the dominant foliation S_2. These F_4 folds are considered to be a locally developed, penetrative deformation and are observable in some but not all blueschist blocks (Figure 21, 25e). An axial surface S_K is associated with folds and is a discrete cleavage. A prominent lineation L_K^2 is defined by the hinges of the kink folds. Typically the distance between hinges of successive F_4 kinks is on the order of 0.5–10 cm. Folds are generally open with a long limb and short limb.

—Microscopic Textures of D4

In thin section, F_4 kink folds show growth of calcite in the hinge regions of the folds (Figure 29). Axial surfaces of the folds

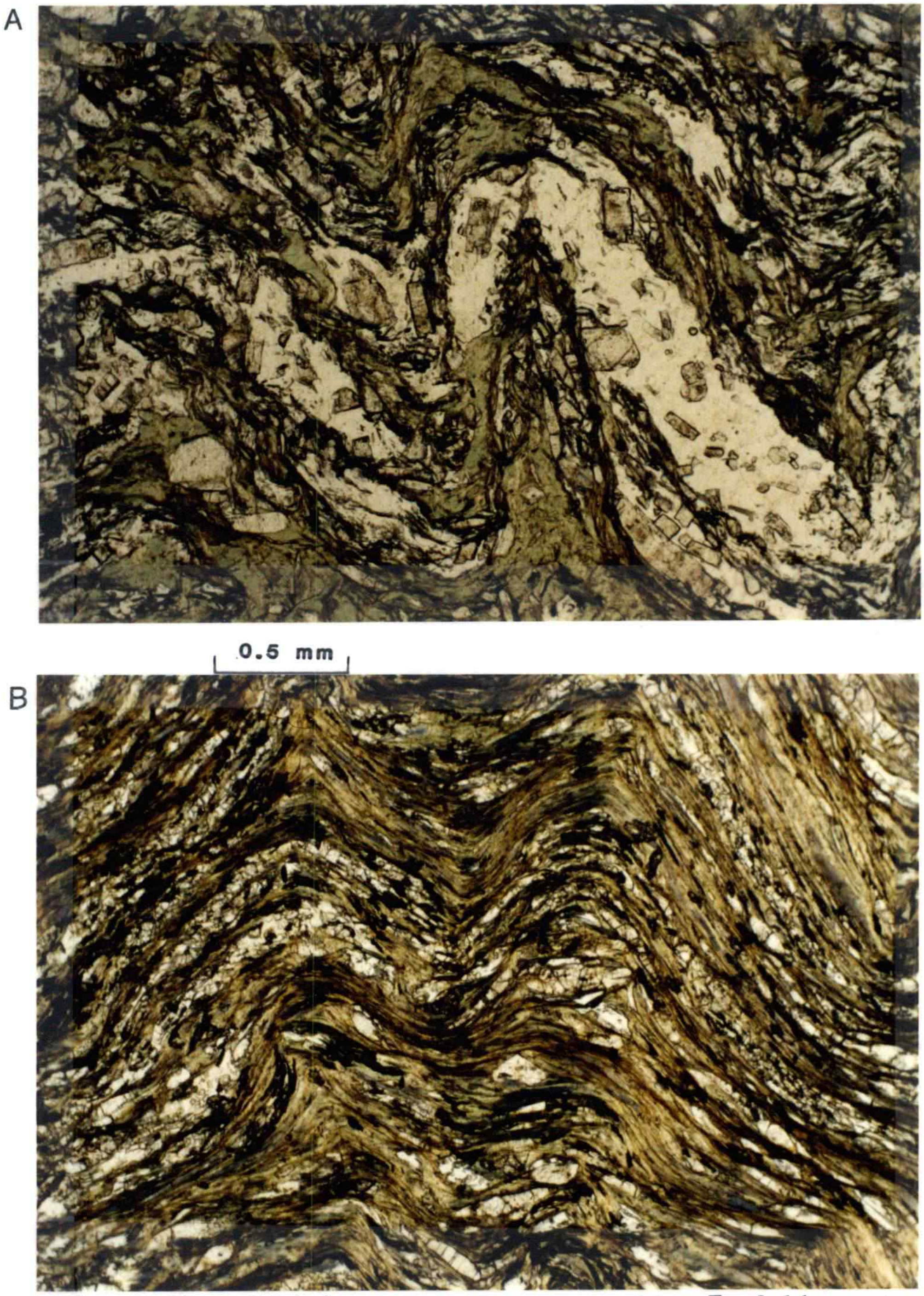

Figure 28. A. Microfolded quartz vein representing F_3 fold event. Incipient zonal crenulation cleavage, S_4, developed in axial planes of the F_3 folds. Sample HG3, lawsonite-Na-amphibole schist. 40X, PL, FOV = 3.3 mm. B. Well-developed zonal crenulation cleavage, axial planar to F_3 folds. Recrystallization of phengite on limbs of microfolds and stretched, boudined lawsonite tablets in limbs. Bent and broken blue amphibole in hinges. Lawsonite + quartz are concentrated at hinge regions. Cleavage zones have a higher proportion of blue amphibole and chlorite. Sample HG16B. 40X, PL, FOV = 3.3 mm

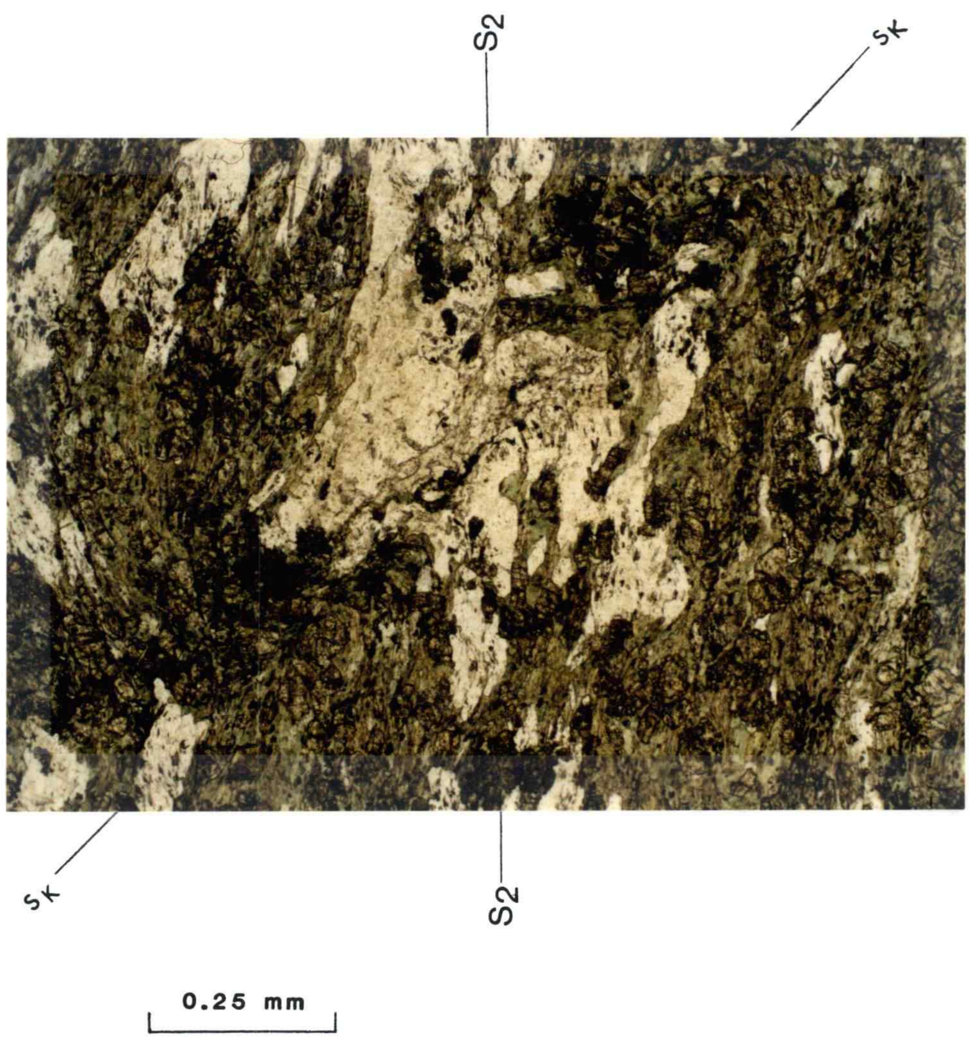

Figure 29. Microscopic view of F_4 kink fold in epidote-Na-amphibole schist, UMG 73. Note discrete cleavage defining the S_K axial surface of the fold. Calcite growth at the hinge zone associated with lawsonite tablets provides evidence of pressure solution associated with the cleavage. Grains of epidote are broken and brecciated along the cleavage. 100X, PL, FOV = 1.31 mm

appear as discrete, narrow, undulatory cleavage surfaces. Mineral grains such as epidote, blue amphibole, quartz, and lawsonite are finely brecciated along the cleavage. Small patches of chlorite are also associated with the cleavage. Lawsonite and sodic amphibole are fractured around the hinges of the kink bands.

Ductile and Brittle Shear Events, D5 and D6

At least two shear events are recorded in the blueschist blocks, evidenced by ductile shear zones, (D5), and en-echelon shear fractures associated with brittle shear zones, (D6). Both shear deformations are best observed on S_2 schistosity surfaces. These two shear deformations can be seen at outcrop HG1 (see Figure 21 for location of D_5). A detailed systematic study of the shear zones, their orientations, and sense of vergence was not carried out in this study. Mineralization occurs along the shear plane. Common minerals developed include albite, quartz, and calcite. The extension fractures associated with the brittle shear zones are usually open. In some cases, minerals have infilled the fractures and include calcite and minor quartz. Blocks are commonly cut by numerous veins filled with various minerasl such as calcite, albite, and less commonly, stilpnomelane and actinolite. These veins are associated with brittle deformation.

Deformation of Chert, Marble, Plutonic, and Other Blocks

Chert, marble, plutonic, and other blocks show a broad range in degree of apparent deformation. The feebly recrystallized chert block (MC97) in the Moffett Creek area shows bedding, S_0, which has been recrystallized. Ductile deformation, for example, folding is not evident, and brittle deformation is minimal.

Plutonic blocks of hornblende tonalite show evidence of brittle deformation. The rocks have undergone cataclasis and locally, show brecciated zones ranging in scale from a few millimeters to meters. Foliation is not developed in these rocks. Vein minerals commonly include prehnite and calcite.

Laminated marble blocks which have undergone very low-grade greenschist-facies metamorphism show some evidence of folding and brittle deformation. Marble blocks at the Horseshoe Gulch locality are gently folded or are not folded at all. A first cleavage S_1 is developed and forms a solution cleavage (Figure 11 and 12a). Other low-grade greenschist-facies marble blocks show a S_1 foliation defined by thin phyllitic domains that are pressure solution seams where micas have crystallized (Figure 12b).

Marble blocks that have undergone high P/T blueschist-facies metamorphism (NNG 34, NNG 45) show polyclinal folds with a foliation defined by mica + epidote + blue amphibole. An incipient zonal-crenulation cleavage has developed in these cleavage domains. At least two fold events have deformed these marbles, but the deformational sequence of the rocks is not as well known as for the schistose blueschist blocks.

Other block types include large bodies of greenschist and actinolite schist commonly enclosed in a predominantly greenschist matrix. Structural elements observed in these blocks include the predominant foliation, tight folds of the foliation (rare), mineral lineation and kink bands.

Deformational History of the Matrix Rocks

Matrix rock types include quartz-albite schist, graphitic schist, greenschist, quartzose phyllite, and marble. The most common rock type is schist of sedimentary origin, that is, quartz-albite schist and graphitic schist. Thin marble lenses are commonly interlayered with the quartzo-feldspathic schist (Figure 4). Greenschist of volcanic or volcaniclastic origin and quartzose phyllite of sedimentary origin are less common in the matrix. The matrix schist records a period of ductile deformation and metamorphism which resulted in metamorphic segregation, and isoclinal folding and transposition of layering to form the prominent foliation in all lithologies. These rocks record a later period of ductile deformation producing nonpenetrative kink folds and still later, brittle deformation. Matrix schist has been metamorphosed under low-grade, greenschist-facies conditions.

A summary of structural elements observed in schist of the matrix is detailed in Table 8. Fold styles are depicted in Figures 25a, 30 and 31. Stages of deformation are summarized below.

(1) D1: Matrix Schist
Isoclinal folding and transposition (F_1) of an early mineralogical layering, S_A, resulting in the formation of the dominant foliation, S_B. Development of a weakly defined mineral lineation of quartz, albite, and mica, $L_{\hat{B}}$.

Marble Interlayered with Schist
Development of a predominant lithological layering and foliation, S_A, defined by thin micaceous layers along pressure-solution seams in recrystallized carbonate rocks.

Quartzose Phyllite and Phyllite
Isoclinal folds of relict sedimentary bedding, S_O, with formation of an axial plane cleavage, S_A, in quartz-rich and feldspar-rich layers and a pervasive foliation in phyllitic layers.

(2) D2: Locally developed, penetrative, asymmetric kink folds of the predominant foliation of matrix schist and phyllite with formation of the S_K axial surface.

(3) D3: Ductile shear zones.

(4) D4: Brittle deformation.

Deformation Style and Microscopic Structures of Matrix Schist

First Deformation

S_B is the predominant foliation in matrix schists. This foliation is the result of tranposition of an early compositional banding or layering in schistose metavolcanic and metasedimentary rocks of the matrix (Figure 30). Whether this lithological layering reflects bedding or is the result of metamorphic differentiation and mineral segregation is not known. In contrast to the quartzose phyllite which preserves evidence of relict bedding, (Figure 31) the matrix schist is much more thoroughly recrystallized (Figures 9 and 10a). More likely, an early metamorphic layering was tranposed. The predominant foliation in thin lenses of marble interlayered with matrix schist is S_A, which appears not to have been folded or transposed. The S_A foliation in quartzose phyllite and phyllite is the result of

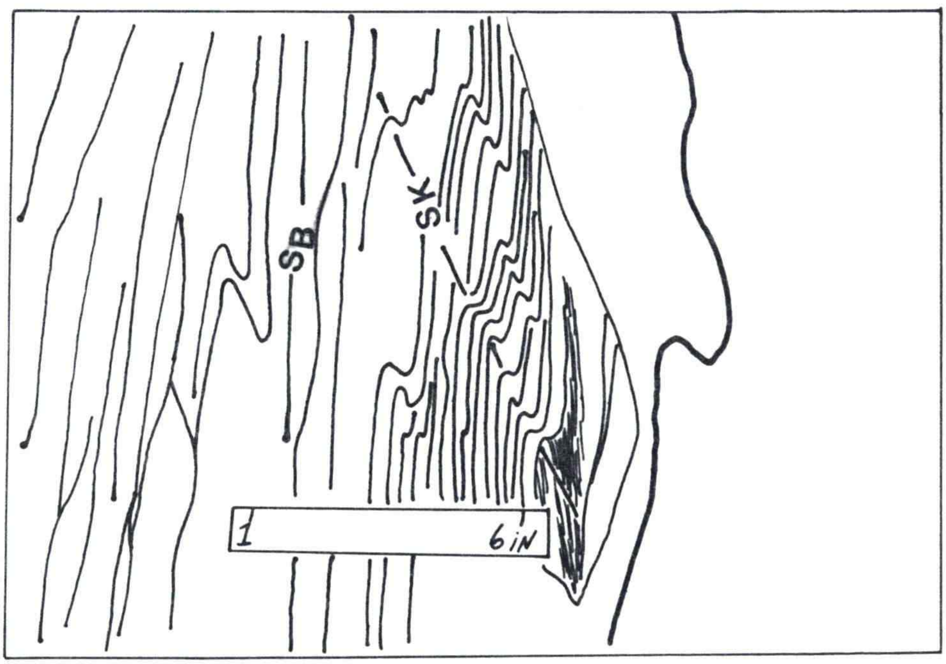

Figure 30. Greenschist matrix rocks showing a predominant foliation, S_B, and asymmetric kink folds of the foliation, F_4, with axial surface, S_K. Outcrop UMG 71.

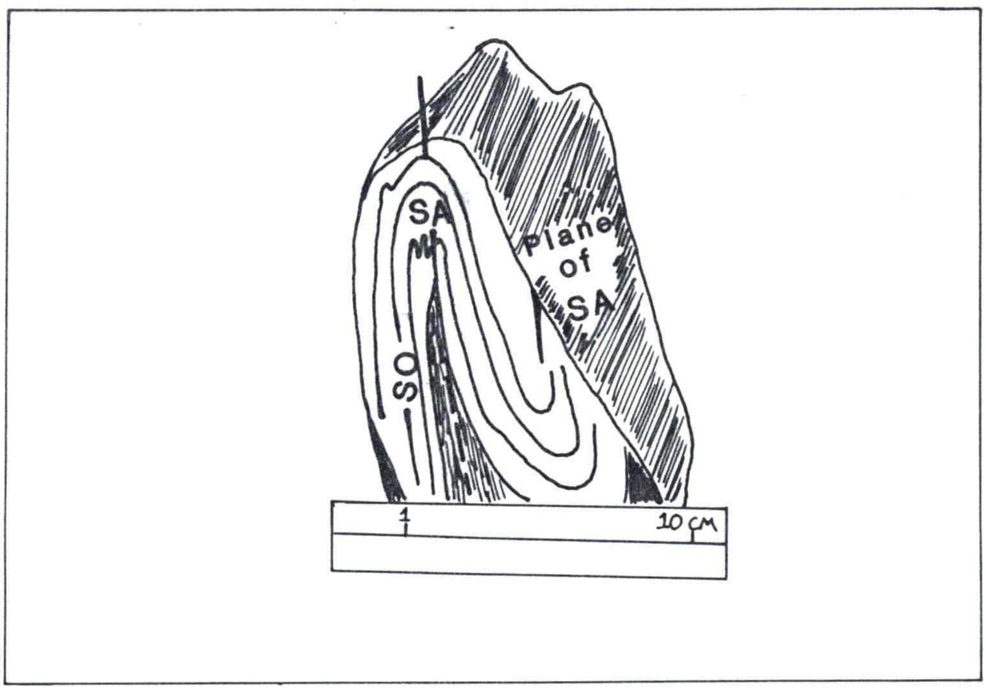

Figure 31. Isoclinal fold in quartzose phyllite, (matrix rock type), outcrop MC 96. Bedding, S_0, light gray in color, is transposed and micas, dark greenish-gray, define an axial plane schistosity, S_A, which is the dominant foliation.

tranposition of relict bedding and is denoted by S_A.

A lineation defined by the orientation of white mica and chlorite and stretched quartz and albite is apparent in the matrix schist and is considered to be an intersection lineation, L_B^A, of S_A and S_B. In rocks where the lineation is well defined, it parallels the axes of tranposed folds.

--Microscopic Textures of D1

In thin section as well as in outcrop, schistose metasediments display a marked mineralogically differentiated layering. Graphitic schist and quartz-albite schist have a continuous planer cleavage in mica domains. The cleavage is less continuous in quartz-albite microlithons (Figure 9). Intrafolial folds of quartz + albite are evidence of layer transposition and are aligned parallel to the dominant foliation. Individual albite porphyroblasts in micaceous domains grew synchronously to after development of the foliation. Albite porphyroblasts are flattened and have pressure shadows of quartz and chlorite. Greenschist-facies minerals, for example, albite, white mica, chlorite, graphite, $\pm$ epidote, sphene, crystallized during D1.

Greenschist is somewhat variable in texture. Some is compositionally layered, with chlorite-rich cleavages alternating with quartz-rich or albite- and quartz-rich microlithons (Figure 30, UMG 71, 77). Stretched and elongated intrafolial folds of quartz are common and are evidence for an early layer transposition to form the present foliation. The compositionally layered greenschist has a dominantly planar fabric.

Other greenschist has a domainal schistosity where chlorite anastomoses around albite porphyroblasts and aggregates of quartz (UMG 55, 66). In these rocks, flattened albite porphyroblasts have pressure shadows composed of quartz and chlorite. Chlorite formed a pressure fringe first and was detached from the albite grain by growth of a pressure shadow of polygonal quartz.

In the greenschists, the metamorphic assemblage of chlorite + albite + quartz + epidote + sphene grew during late D1. Helicitic inclusions of blue amphibole, sphene, and epidote in albite poikiloblasts in some greenschist attest to an earlier foliation that formed during early D1. The inclusion trails have an internal fabric, S_i, discordant to the fabric of the chloritic matrix foliation. Blue sodic amphibole does not occur elsewhere in the rock. The presence of sodic amphibole only within the albite poikiloblasts indicates that high-pressure metamorphic conditions occurred early in the rock's history. The internal fabric of the poikiloblasts is interpreted as traces of the earliest foliation, which was transposed to form the present foliation, S_B. After crystallization of sodic amphibole and chlorite and subsequent transposition, the rocks were no longer at a high enough pressure for continued formation of sodic amphibole. The formation of the albite poikiloblasts occurred during or after the formation and folding of the early matrix foliation S_A.

Second Deformation

The second deformation recognized in the schistose and phyllitic matrix rocks is recorded by locally developed asymmetric kink folds and kink bands of the predominant foliation, S_B (or S_A in the quartzose phyllite). The axial surface of the folds is S_K. The folds vary in aspect from conspicuous folds in greenschist (Figure 30) to small amplitude, widely spaced kink bands in quartz-albite schist and to more closely spaced, small amplitude crenulations and kink bands in quartzose phyllite. The hinge of the kink folds forms a lineation L_K on S_B schistosity surfaces.

Very few thin sections show this deformation, unfortunately. Mica grains are bent around hinges of the kink folds and show sweeping extinction. Around some hinges, micas are broken and the S_K cleavage is a discrete one. No major recrystallization appears to have occurred during the fold event.

Ductile and Brittle Shear Deformations, D3 and D4

Similarly to the blocks, matrix schist shows ductile shear zones on the predominant shear surfaces. Some mineralization is associated along the shear plane. Schists show brittle deformation as well in the form of small-scale faults cutting the foliation at a high angle, and small thin-section scale microfractures infilled by calcite.

Structure Diagrams

Stereonets, displaying orientation data of structural elements, S-surfaces, and lineations from the three localities mapped are shown in Appendix 4. Figure 32a,b shows compiled data from measured S-surfaces from all three localities.

Planer Elements

D1: S_1 of Blocks

The S_1 foliation of laminated marble blocks in matrix is shown. For the most part, the blocks show a preferred planer orientation with S_1 striking NE and steeply dipping to the NW and SE.

D1: S_B of Matrix

The prominent foliation of the matrix, S_B, demonstrates the pervasive structural fabric of the melange. The S_B foliation strikes NE and dips, mostly steeply, to the NW and SE.

D1: S_2 of Blocks

The predominant foliation of the blueschist blocks shows some variation, but two concentrations are apparent paralleling the structural fabric of the enclosing matrix. Most of the blocks are aligned with the matrix foliation. Exceptions, however, are common (see Plate 7, outcrop HG3 and plot of S_2 of No Name Gulch, Figure A3, Appendix 4).

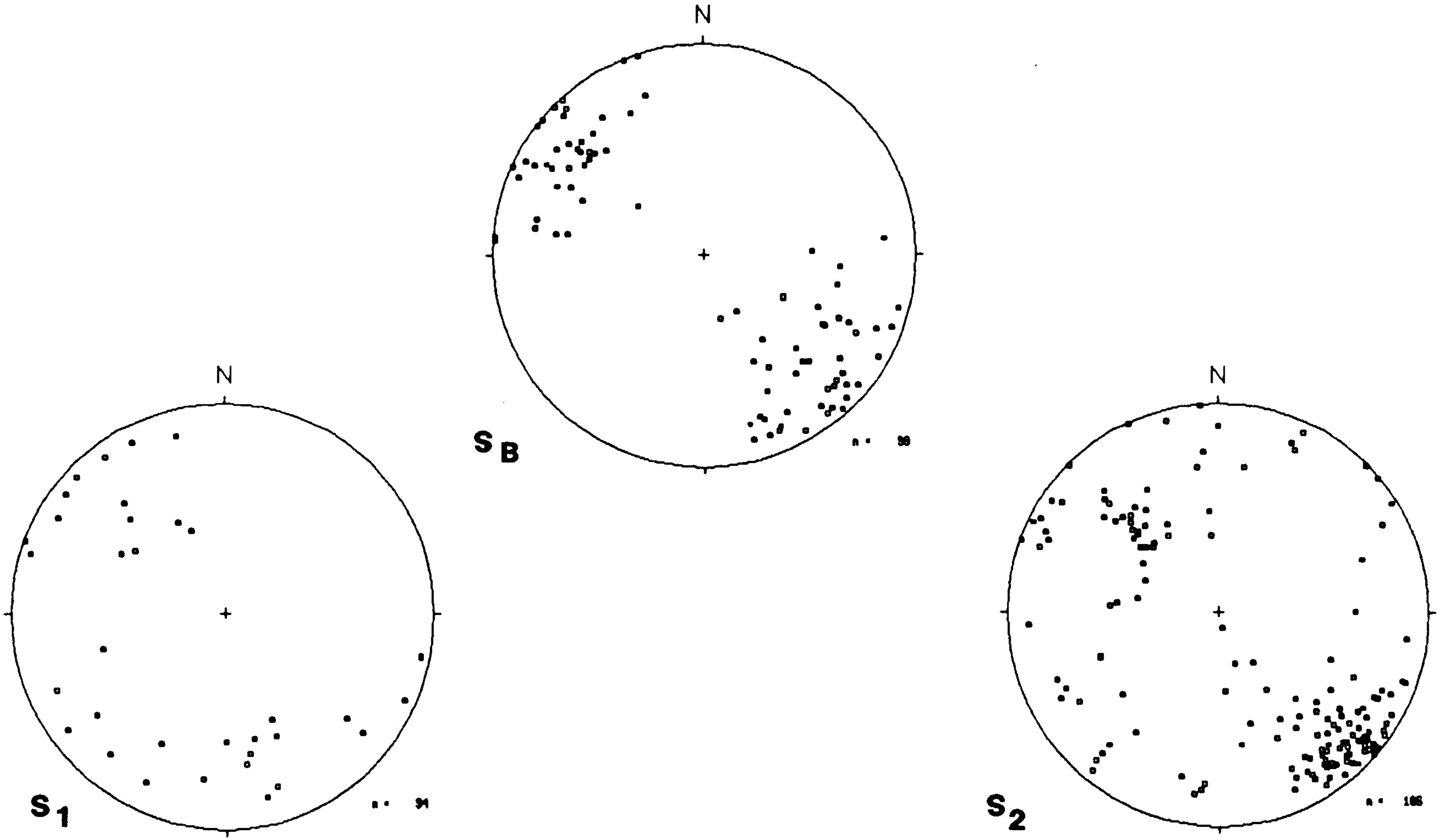

Figure 32A. Stereonet plots showing poles to foliation. Data is combined from all three localities. S_1 = foliation of marble blocks in matrix. S_B = matrix foliation. S_2 = predominant foliation of blocks in the matrix.

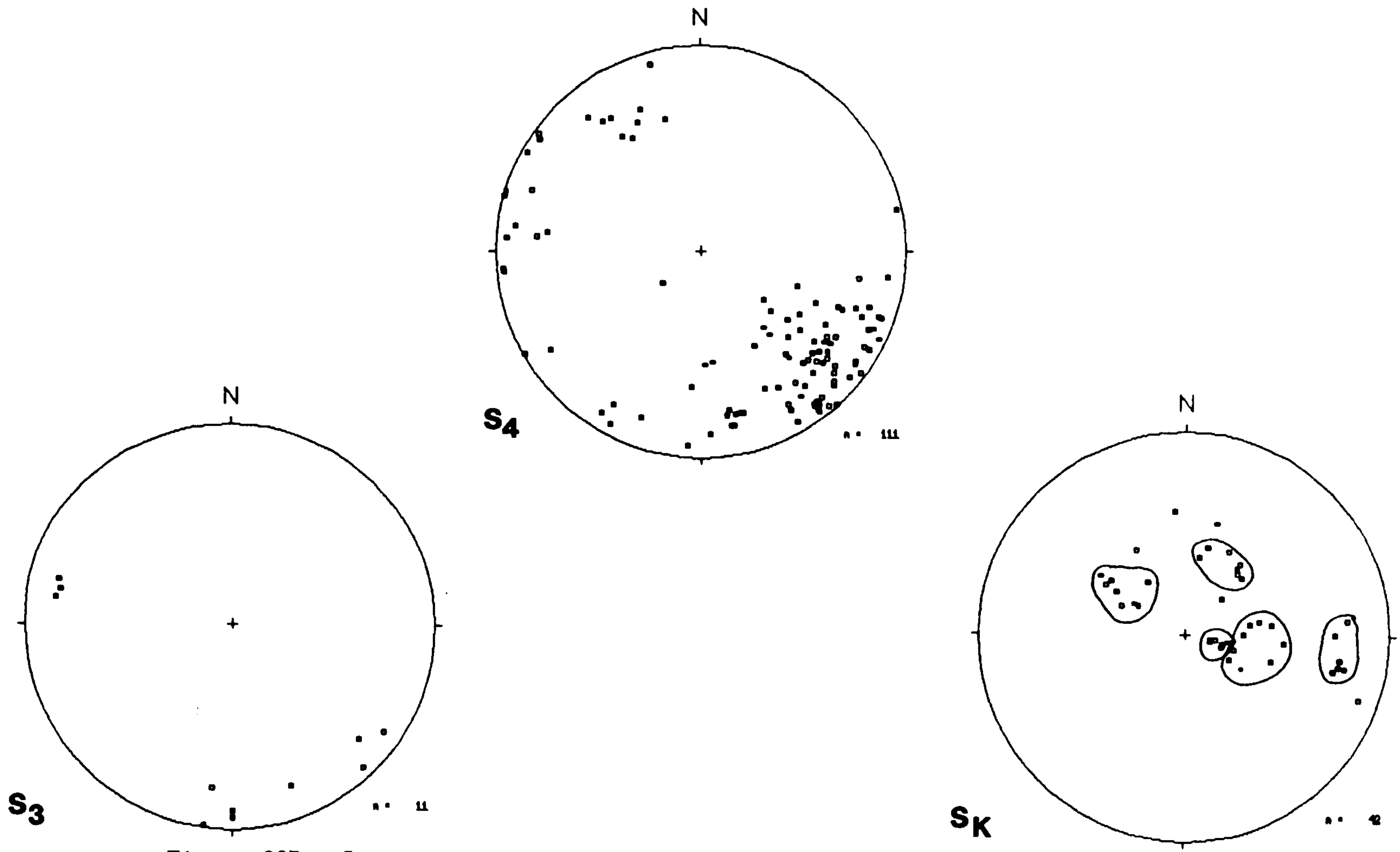

Figure 32B. Stereonet plots showing poles to foliation. Data is combined from all three localities. S_3 = axial plane of F_2 folds. S_4 = axial plane and associated crenulation cleavage of F_3 folds. S_K = axial surface of kink folds in blocks and matrix. Circles enclose poles obtained from single outcrops.

D2: S_3 of Blocks

Data for this S-surface are sparse. S_3 axial planes of F_2 folds are essentially parallel to the predominant S_2 foliation of blocks (Plates 6 and 7)) and reflect tight to isoclinal folding of S_2 around steeply plunging fold axes.

D3: S_4 of Blocks

Data for this S-surface shows a concentration of poles striking NE and dipping NW. The structural orientation of this foliation is markedly parallel to that of the dominant structural grain of the matrix and the preferred orientation the S_2 schistosity of blocks in the matrix.

D4: Kink Folds of Blocks and Matrix

A combined plot from all three localities of axial surfaces to kink folds of the predominant foliation of blocks and matrix, appears at first glance (imagine the circles are not there) to be a fairly broad concentration of poles to foliation. The circles around groups of points reflect orientations of axial surfaces from single outcrops. One interpretation of the different concentrations of S_K surfaces is that several kink episodes are represented. Another interpretation is that the kink folds represent the same deformational event and blocks were rotated subsequent to deformation. The kink folds may also reflect a single deformational episode that occurred in blocks oriented at different attitudes. The later interpretation seems most likely, although some rotation after the folding cannot be ruled out.

Linear Elements

Data on linear elements are compiled from the three localities mapped and are shown in Figure 33.

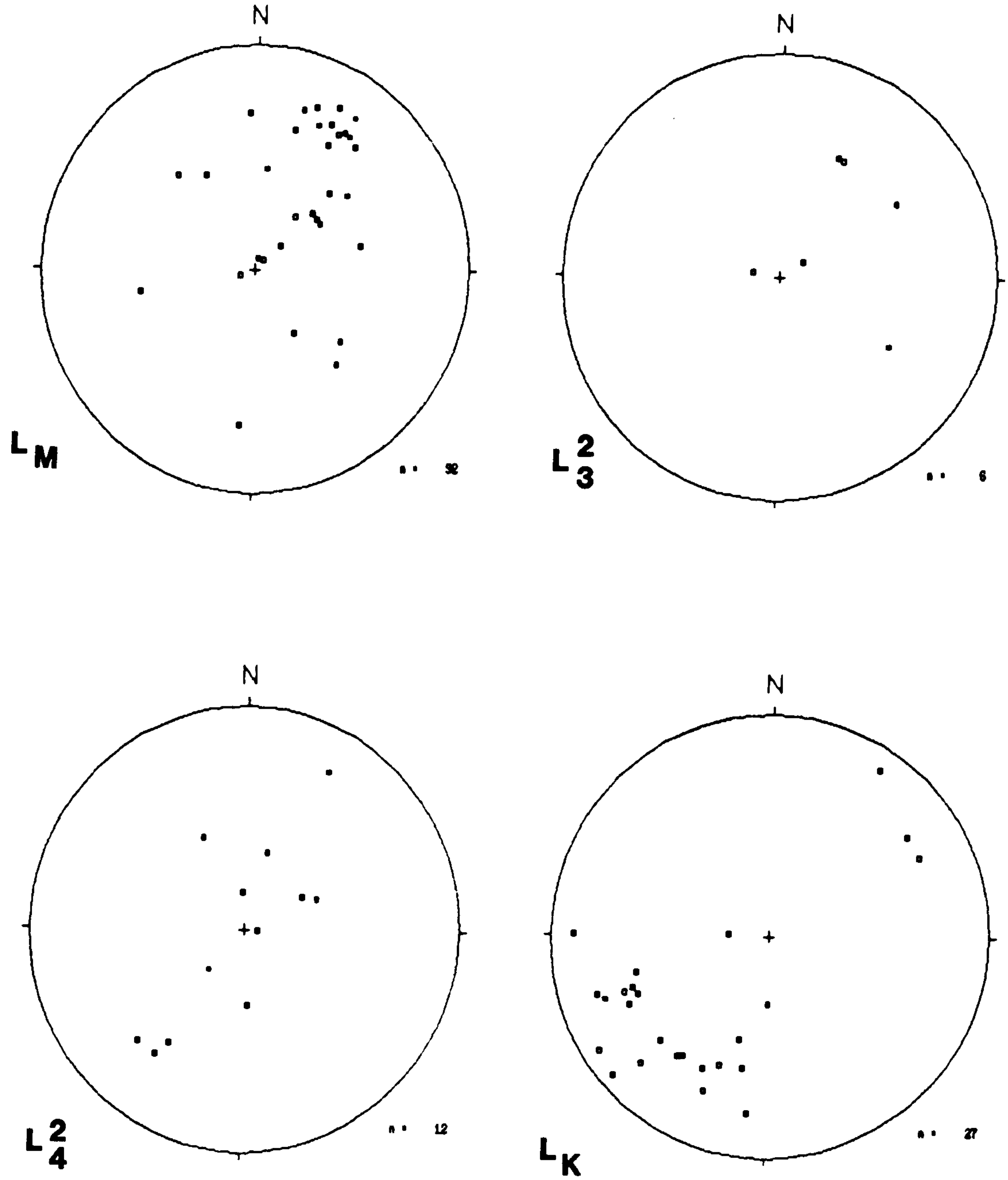

Figure 33. Stereonet plots showing trend and plunge of linear elements. Data is combined from all three localities. L_M = mineral lineation (intersection lineations L_2 of blocks and L_B of matrix. L_2 = intersection of S_2 and S_3 of blocks. L_4 = intersection lineation of S_4 and S_2 of blocks. L_K = hinge line of kink folds of S_2 and S_B.

D1: L_M of Blocks and Matrix

Mineral lineations L_2^1 of blocks and L_B^A of matrix rocks are denoted by L_M. Mineral lineations generally trend NE and have variable plunges; a concentration of points shows shallow plunges.

D2: L_3^2 of Blocks

Data is sparse for this linear element. Most of the data indicates that the intersection lineation L_3 trends NE-SW and plunges shallowly.

D3: L_4^2 of Blocks

Intersections of the S_4 cleavage on S_2 show a more pronounced preferred orientation trending NE and SW with moderate to steep dips.

D4: L_K of Blocks and Matrix

The hinge lines of kink band folds on the predominant schistosity surface trend SE and plunge moderately steeply.

Macroscopic Faults and Folds

Dominant macroscopic structures present in the Callahan-Yreka area are faults and to a lesser extent, folds.

The fault bounding the SSG on the west is a low-angle, west-dipping fault that separates the schist from the Duzel Phyllite and the Sissel Gulch Graywacke. This fault is known locally as the Mallethead Thrust. The SSG is exposed as a window beneath this thrust and is locally, the basement unit of the area. Little is known about the contact relations along the thrust fault due to poor exposure. The Sissel Gulch Graywacke structurally underlies the Duzel Phyllite. Interfingering between the two units and conformable dips in bedding suggest that the Duzel Phyllite was deposited on the graywacke, but, recent isotopic dating studies of zircons from the two units have shown that the Duzel is older than the Sissel Gulch. The age of the Mallethead Thrust is interpreted to be Early Devonian or younger as it overrides the Early Silurian to Middle Devonian Gazelle Formation in the Lime Gulch area of the Yreka Quadrangle.

On the east, the SSG is in fault contact with the Sedimentary and Volcanic Rocks of Horseshoe Gulch. Map relations indicate that the fault dips to the east but little is known about the nature of this fault contact.

Macroscopic folds were not discernable within the SSG. The SSG shows a dominant structural grain trending NE. The possibility exists that macroscopic isoclinal folds of the SSG exist, with limbs trending to the NE, but no fold hinges have been detected. More detailed mapping outside of the localities studied may permit identification of macroscopic folds in the SSG.

Broad open folds as described by Hotz (1977; 1978), involving entire thrust plates in the Callahan-Yreka area are indicative of the latest regional folding episode. This folding post-dates small-amplitude kink folds recognized in the Duzel Phyllite and is believed to postdate all fold events in the SSG. Anticlinal folds expose the SSG in the Moffett Creek area. The sedimentary rocks in the vicinity of Callahan to the south and east of the study area, are part of a large syncline that plunges slightly to the south.

Structural Interpretation

Structural analysis of the SSG leads to the following observations and conclusions regarding the structural style and deformational history of the melange.

(1) The dominant structural grain in the SSG trends NE as is evidenced from the matrix foliation and preferred orientation of blocks in the matrix. Although many blocks are diversely oriented with respect to this structural grain, many of the blocks are preferentially aligned so that their predominant foliation is oriented parallel to that of the enclosing matrix. This implies that during emplacement, the blocks were preferentially oriented.

(2) Large fault blocks of foliated blueschist and tonalite occur in the melange that are oriented differently than the pervasive fabric. They may have been faulted into the melange rather late in its development. Or, such large blocks may have behaved as static blocks unable to be rotated into alignment within the matrix.

(3) Matrix schist anastomoses around blocks or ends abruptly against blocks and eventually becomes reoriented to the dominant structural orientation at some distance away from the blocks. Analogous to this is the manner in which a foliation wraps around and encloses a porphyroblast in metamorphic rocks on the scale of a thin-section.

(4) The many varieties of blocks incorporated into the melange show a varied deformational history. The blueschist blocks, however, show a more extensive deformational history than the chert, marble, greenschist, and tonalite blocks.

(5) The fact that metamorphic grade and degree of deformation attained by the greenschist rocks of the matrix is far different than that of the matrix rocks indicates that these rocks did not experience the same early history. This interpretation is contrary to that of Cotkin (1987, p. 192) who states that:

> "a variety of schists are intimately interlayered and complexly folded with dolomite marble. Structural and petrographic studies indicate that these lithologies have shared a common metamorphic and deformational history".

The interpretation offered here is that the blueschist blocks underwent blueschist-facies metamorphism synkinematically with D1 and D2 and then were uplifted to shallower levels and emplaced into the melange matrix during D_3. The minor folding of blueschist-facies blocks and the development of a crenulation cleavage, S_4, occurred during or after emplacement of the blocks into the melange and concurrently with transposition in the matrix schist (D1 of matrix). Evidence for this includes the following: (a) the deformational event represented by small-scale F_3 folds and associated crenulation cleavages in blueschist blocks was not accompanied by metamorphism; (b) similarities between the structural orientation of S_4 axial planes with the foliation of the enclosing matrix (S_B) implies coeval development; (c) similar later deformation was experienced by the blocks and matrix lithologies, that is, kink folding (D4 of blocks, D2 of matrix) and ductile and brittle deformation.

DISCUSSION

Deformation and Metamorphism

Blueschist facies metamorphism of blocks in the schist of Skookum Gulch reached its maximum during D1 and phased out by the end of D2 (Figure 34). High P/T blueschist-facies minerals sodic amphibole and lawsonite developed during D1 and early D2. Temperatures and pressures of metamorphism were in the range of 275 $\pm$ 50 and 7 $\pm$ 1.5 kbar (Cotkin, 1987). No new mineral phases are seen in D3 folds and associated crenulation cleavages. Both D2 and D3 deformations show bent and broken minerals for example, lawsonite, sodic amphibole, and actinolite. White mica, quartz, and chlorite, which are present in D1, grow in pressure shadows of flattened and broken lawsonite and blue amphibole. Evidence of retrograde metamorphism overprinting D1 and D2 minerals is not observed. By D3, blueschist blocks were undergoing folding and deformation related to uplift and emplacement in the melange. D4 kink folds seem to be a less ductile folding event and are associated with brecciation of existing minerals. Little recrystallization occurs other than calcite locally.

Matrix schists record one period of greenschist-facies metamorphism associated with the D1 deformation which produced a transposed foliation (Figure 9). Evidence in greenschists indicates that at intial stages of D1 metamorphism, at least some of the rocks were at high pressures favorable for the formation of sodic amphibole. During late D1, pressures were reduced and chlorite-grade greenschist facies mineral assemblages developed. Late stage kink folding is not associated with new mineral crystallization. D1 mineral phases are bent and broken in the hinge regions of the kink folds.

Vein-mineral assemblages in both blocks and matrix rocks can provide evidence of P/T uplift paths and conditions, perhaps during emplacement of various blocks into the melange (Figure 17b). Vein minerals common in blueschist blocks include calcite, albite, and minor quartz, chlorite, actinolite, and stilpnomelane. These minerals are indicative of greenschist-facies metamorphic conditions. The fairly high temperature of formation of blueschist mineral assemblages in the

Figure 34. Mineral occurrence in blueschist and transitional schist and relation to deformation stage.

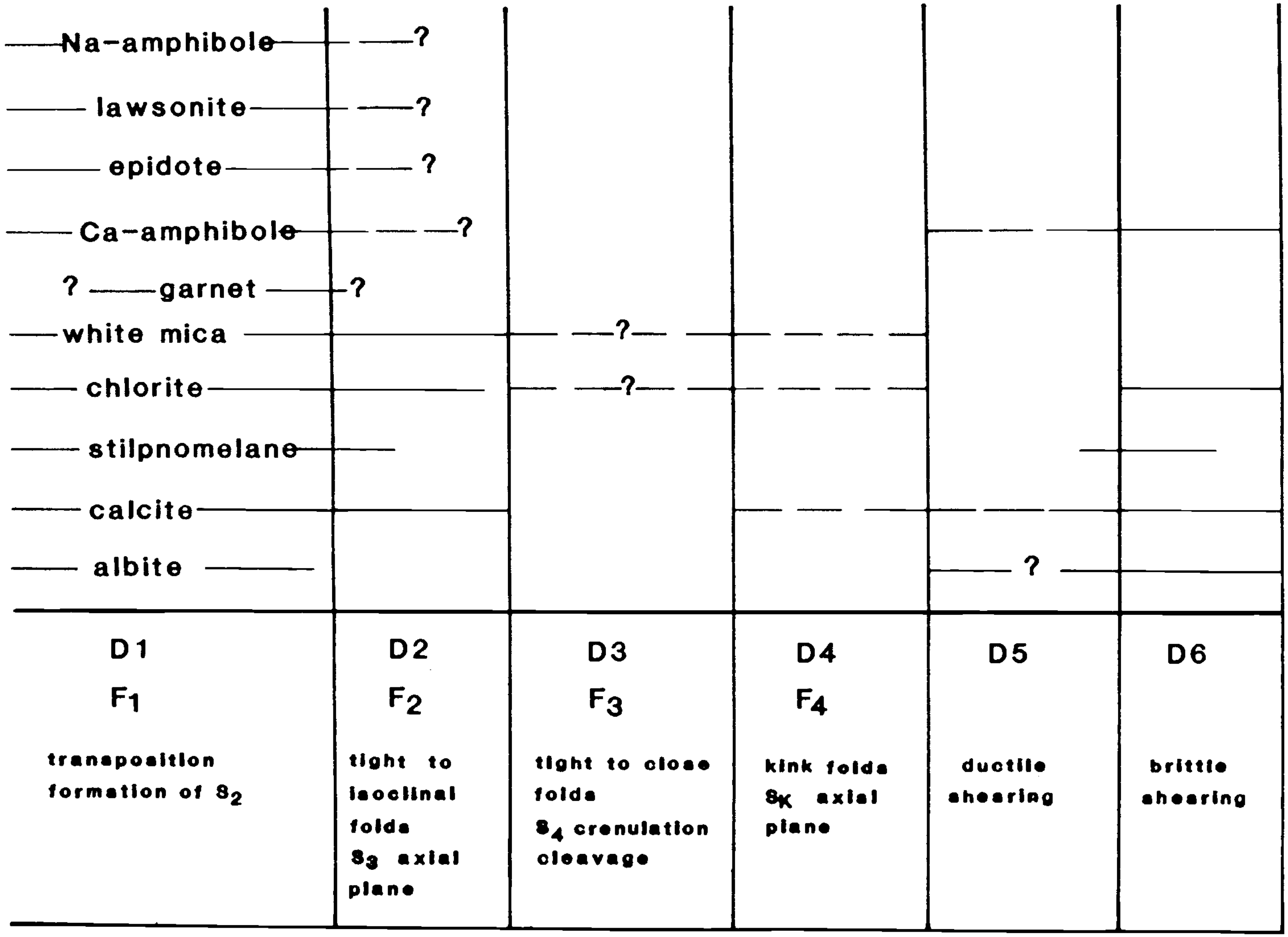

SSG, up to 325°C, indicates that though pressure decreased during uplift, temperature was high enough to favor growth of such minerals as actinolite and stilpnomelane in veins. Tonalite blocks in the SSG contain the vein minerals prehnite, albite, calcite, and quartz. Lower temperature and pressure conditions of the prehnite-pumpellyite facies accompanied emplacement of tonalite blocks into the melange. Vein mineral assemblages common in matrix rocks include calcite and quartz, also characteristic of low-grade metamorphism or hydrothermal alteration.

Emplacement of Blocks into the Matrix

Structural analysis has been effective in helping to establish constraints on timing of emplacement of blocks into the melange. Figure 35 shows the timing relationships between protolith formation, deformation and incorporation of blocks into the matrix. Emplacement of blocks into the melange is interpreted to be associated with the D3 deformation event. Development of a crenulation cleavage in blueschist blocks (D3 of blocks) occurred during layer transposition of schist of the matrix (D1 of matrix). Both blocks and matrix shared a common deformational history after emplacement of the blocks. Shared deformations include the D3 event, kink folding associated with D4, and ductile-shear deformation and brittle deformation. The shared deformational history provides evidence that both blueschist and less common greenschist blocks were incorporated into the melange before the D3 event. Timing of incorporation of less deformed blocks for example, laminated marble, chert, and tonalite is more problematic. The less deformed blocks show both ductile and brittle deformational features, such as pressure-solution induced stylolitization, cataclasis, and faulting. These blocks are probably late entrants into the melange when it was at a shallow crustal level. Slide blocks of marble and chert could have become incorporated into the melange by olistostromes or debris slides or may have been tectonically inserted by faulting. Tonalite blocks appear to have been incorporated into the melange along faults at a late stage, during D6.

Several important facts constrain the time of melange formation.

Figure 35. Flow chart recording the deformational history of the schist of Skookum Gulch.

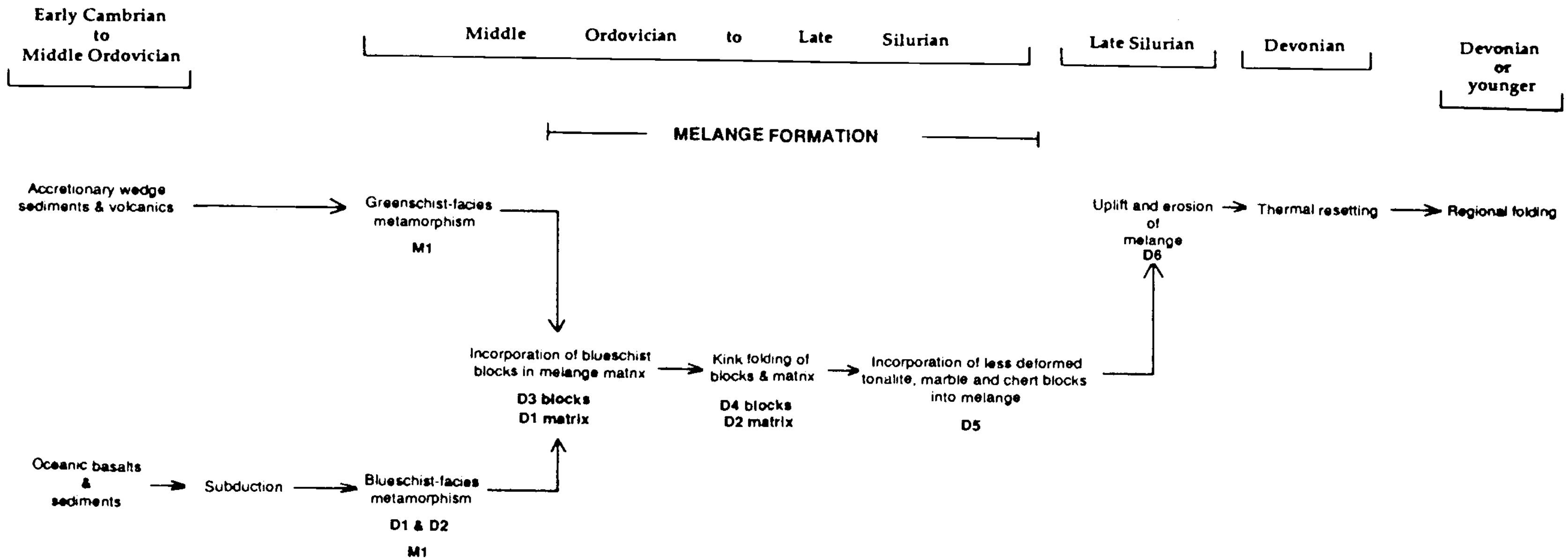

The melange developed as an entity in Ordovician to Silurian time based on metamorphic age and uplift age. Blueschist and greenschist facies metamorphism of blocks and matrix components, respectively, occurred during the Middle Ordovician to Early Silurian. Uplift occurred fairly rapidly after blueschist facies metamorphism as clasts of foliated matrix lithologies (quartz-albite schist and graphitic schist) occur in Late Silurian conglomerates in Horseshoe Gulch. Though evidence is not conclusive, the major deformational events of folding and brittle deformation are interpreted to have occurred during the Middle Ordovician to Early Silurian. Although the blueschist appears to be thermally reset in the Devonian (Rb-Sr data of Cotkin, 1987), a related deformational event cannot be assigned to the SSG with any certainty.

Regional Geologic Implications

Two aspects of the metamorphic history of the schist of Skookum Gulch make it important to the study of blueschist-facies metamorphism. First, the schist contains blocks with typical high-pressure low-temperature parageneses of lawsonite + sodic amphibole as well as higher temperature transitional facies parageneses of epidote + sodic amphibole $\pm$ actinolite. The SSG also contains rocks with the parageneses lawsonite + actinolite + sodic amphibole that may be considered as "transitional" between blueschist and epidote-blueschist.

Second, the initial or prograde blueschist-facies assemblages are very well preserved with little evidence of greenschist-facies, (higher temperature, lower pressure) overprinting. Colorless rims on some sodic amphibole grains may be signs of slight greenschist-facies overprinting but the timing of this possible overprinting is uncertain; Rb-Sr mineral ages appear to be reset in the Devonian, although K-Ar ages do not show signs of resetting due to argon loss.

Structural evidence and evidence from local stratigraphy, combined with the well-preserved blueschist facies assemblages, indicates that the SSG was uplifted soon after the blueschist blocks were incorporated into the matrix. Preservation of high-pressure low-temperature mineral assemblages typical of blueschists is accomplished by uplift rapid enough to prevent reequilibration at higher temperature and lower pressure (Draper and Bone, 1981), or long term refrigeration at shallow crustal levels (<10 km) during steady state subduction (Cloos, 1986).

Semi-ductile to brittle deformation occurred during emplacement of the blocks into the matrix. Margins of some blueschist blocks show signs of reaction with the surrounding matrix during emplacement. Chlorite rinds and growth of white mica on some outer schistosity surfaces of blueschist blocks are noted. Interiors of the blocks, however, show no evidence of reactions. Veins in blueschist-facies blocks truncate fabrics produced during prograde metamorphism. The vein minerals albite, calcite, and minor stilpnomelane and actinolite indicate reduced pressures during crystallization of these minerals.

Albite and calcite veins also occur in the matrix schists.

Other evidence for rapid uplift of the melange is found in sedimentary rocks adjacent to the melange belt. Clasts of quartz-albite schist graphitic schist, and tonalite in Late Silurian conglomerate in Horseshoe Gulch indicate uplift and erosion had occurred by the Late Silurian (Potter, 1982). Erosion by the Late Silurian also effectively constrains the deformation of the SSG to occurring before the Late Silurian.

The SSG is significant to the tectonic history of the Klamath Mountains in that it records evidence of Late Ordovician to Early Silurian subduction. Hypothesized back-arc spreading resulting in the formation of the Trinity ultramafic complex (Quick, 1981), disrupted sediments and carbonates of a possible forearc-accretionary wedge, and extrusion of volcanic rocks are suggestive of subduction-related events occurring the Middle Ordovician to Early Silurian. The SSG melange represents part of a subduction complex. The location and source of protoliths of the SSG are poorly known, but some of the matrix rocks of sedimentary origin resemble volcanogenic graywacke, and perhaps micaceous silty sandstone such as the Moffett Creek Formation and the Duzel Phyllite. Maximum ages of depostion of these sedimentary units, based on detrital zircon ages, are roughly coeval with the metamorphic age of the SSG, that is, Early Ordovician to Early Silurian. These sediments may have been deposited just before (or after) metamorphism of the SSG.

The structural characteristics of the SSG are compared with that of the Duzel Phyllite and amphibolite of the Central Metamorphic Belt to gain some insight into tectonic evolution of the Callahan-Yreka area.

The pervasive structural grain of the SSG trends NE with foliations generally dipping steeply mostly to the NW and to lesser extent, the SE. Axial planes to F_3 folds and crenulation cleavages associated with emplacement of blocks in the melange also trend NE and dip steeply to the NW. Structural trends of the amphibolite of the Central Metamorphic Belt and the Duzel Phyllite in the Callahan-Yreka area differ from the SSG. Cashman (1980) notes that the penetrative S_1 foliation of the phyllite and amphibolite are parallel to one another and strike NE to NNE and dip steeply to the SE. Hornblende mineral lineations in amphibolite and B_1 isoclinal fold axes associated with transposition in phyllite both trend SE and plunge at shallow to moderate angles. Deformational events and structural elements found in the SSG cannot be tied to those found in the Duzel Phyllite or amphibolite of the Central Metamorphic Belt. This is further evidence that metamorphism and subsequent deformational events recorded both in blocks and matrix of the SSG occurred prior to the Late Silurian.

The intriguing question that arises is why the SSG dips to the NW and whether that has anything to do with the subduction direction. Cotkin (written communication) interpreted subduction associated with formation of the SSG to be westward-directed. Not enough is known about the structure of other disrupted and unmetamorphosed units (for example, the Sedimentary and Volcanic Rocks of Horseshoe Gulch), that may have been part of the subduction zone and accretionary complex, to definitively answer the question of subduction direction. However, it seems likely that subduction was east-directed based on the following lines of evidence: (1) the Sedimentary and Volcanic Rocks of Horseshoe Gulch may be remants of disrupted trench-slope deposits or accretionary melange and (2) igneous rocks, roughly coeval in age with the time of blueschist-facies metamorphism, occur in the Lovers Leap and Gregg Ranch area to the east.

Structural trends of the SSG are consistent with NW to SE compression with respect to the present position of the Eastern Klamath terrane. Some geologists (Irwin, 1981, 1985; Hamilton, 1969) interpret the Klamath terranes as being successively accreted from east to west along east-dipping subduction zones. More recent structural studies and paleomagnetic evidence suggest that the present configuration of the Klamath Mountains is due to Late Mesozoic and Early Tertiary deformation. Paleomagnetic evidence from studies of sedimentary rocks overlying the Trinity complex indicates that the Klamaths have undergone from 90-110 degrees of clockwise rotation, relative to stable North America since the Late Triassic (Mankinen and others, 1982; Achache and others, 1982; Fagin and Gose, 1983). Studies of the kinematics of thrusting of the Central Metamorphic Belt amphibolites beneath the Trinity complex indicate west-directed thrusting and a N90E to N120E convergence direction. With the effect of clockwise rotation removed, transport of the Trinity complex over the Central Metamorphic Belt would be along a N to N20E transport direction (Canat and Boudier (1985). The similarities between the NE-trending structural grain in the SSG and the Central Metamorphic Belt suggest that with clockwise rotation taken into account, N to NNE-SSW convergence began in the Middle Ordovician and continued through the Devonian. Perhaps the dominant westward dip of foliation of the SSG indicates west-directed subduction or, when corrected for rotation, SSW-directed subduction. On the other hand, the NW-dipping fabric of the SSG melange could be an artifact of faulting and rotation associated with uplift and may not at all reflect the dip of the subduction zone. But, igneous rocks approximately coeval with the time of metamorphism of the SSG occur to the SE near Lovers Leap and Gregg Ranch, for example, a 440 Ma tonalite clast in conglomerate at Lovers Leap and 435 $\pm$ 21 Ma microgabbro dike intruding the Trinity Complex. These rocks may represent arc magmatism contemporaneous with blueschist metamorphism. If so, the areal distribution of blueschist and igneous rocks suggests subduction in a present-day SE-dipping direction.

REFERENCES

Achache, J., Cox, A., O'Hare, S., 1982, Paleo-magnetism of the Devonian Kennett Limestone and the rotation of the eastern Klamath Mountains, California: Earth and Planetary Science Letters, v. 61, p. 365-380.

Alabaster, T., Pearce, J. A., and Malpas, J. 1982, The volcanic stratigraphy and petrogenesis of the Oman Ophiolite Complex: Contributions to Mineralogy and Petrology, v. 81, p. 168-183.

Aldiss, D. T., 1978, Granitic rocks of ophiolites, [Ph.D. thesis]: Open University.

-----, 1981, Plagiogranites from the ocean crust and ophiolites: Nature, v. 289, p. 577-578.

Armstrong, R. L., Harakal, J. E., Forbes, R. B., Evans, B. W., and Thurston, S. P., 1986, Rb-Sr and K-Ar study of metamorphic rocks of the Seward Peninsula and Southern Brooks Range, Alaska: Geological Society of America Memoir 164, p. 185-203.

Arth, J. G. and Barker, 1976, Rare-earth partitioning between hornblende and dacitic liquid and implications for the genesis of trondhjemitic-tonalitic magmas: Geology, v. 4, p. 534-536.

Barker, F., 1979, Trondhjemite: definition, environment and hypothesis of origin, in Barker, F. ed., Trondhjemites and related rocks: Elsevier, Amsterdam, p. 1-12.

Barker, R., Millard, H. T., Jr., and Knight, R. J., 1979, Reconnaissance geochemistry of Devonian island-arc volcanic and intrusive rocks, West Shasta District, California, in Barker, F., ed., Trondhjemites and related rocks: Elsevier, Amsterdam, p.531-545.

Bell, T. H., and Duncan, A. C., 1978, A rationalized shorthand terminology for lineations and fold axes in tectonites: Tectonophysics, T1-T5.

Berthe, D., Choukroune, P. and Jegouzo, P., 1979, Orthogneiss, mylonite, and non coaxial deformation of granites: the example of the South Amorican shear-zone: Journal of Structural Geology, v. 1, p. 31-42.

Black, P. M., 1973, Mineralogy of New Caledonian metamorphic rocks, I. Garnets from the Ouegoa District: Contributions to Mineralogy and Petrology, v. 38, p. 221-235.

-----, 1973, Mineralogy of New Caledonian metamorphic rocks, II. Amphiboles from the Ouegoa District: Contributions to Mineralogy and Petrology, v. 39, p. 55-64.

Bond, G. C. and Kominz, M.A., 1984, Construction of tectonic subsidence curves for the early Paleozoic miogeocline, southern Canadian Rocky Mountains: implications for subsidence mechanisms, age of breakup, and crustal thinning: Geological Society of America Bulletin, v. 95, p. 155-173.

Bond, G. C., Nickeson, P. A., and Kominz, M. A., 1984, Breakup of a supercontinent between 625 Ma and 555 Ma: new evidence and implications for continental histories: Earth and Planetary Science Letters, v. 70, p. 325-345.

Brothers, R. N. and Blake, M. C., Jr., 1987, Comment and reply on Blueschists and Eclogites: Geology, v. 15, p. 773-775.

Brothers, R. N., and Yokoyama, K., 1982, Comparison of the high-pressure schist belts of New Caledonia and Sanbagawa, Japan: Contributions to Mineralogy and Petrology, v. 79, p. 219-229.

Brouxel, M., Lapierre, H., Michard, A., Albarede, F., 1987, The deep layers of a Paleozoic arc: geochemistry of the Copley-Balaklala Series, northern California: Earth and Planetary Science Letters, v. 85, p. 386-400.

Brown, E. H., 1974, Comparison of the mineralogy and phase relations of blueschists from the North Cascades, Washington and greenschists from Otago, New Zealand: Bulletin of the Geological Society of America, v. 85, p. 333-344.

-----,1977, Phase equilibria among pumpellyite, lawsonite, epidote and associated minerals in low-grade metamorphic rocks: Contributions to Mineralogy and Petrology, v. 64, p. 123-136.

Brown, E. H. and Ghent, E. D., 1983, Mineralogy and phase relations in the blueschist facies of the Black Butte and Ball Rock areas, northern California Coast Ranges: Am. Mineralogist, v. 68, p. 365-372.

Canat, M. and Boudier, F., 1985, Structural study of intra-oceanic thrusting in the Klamath Mountains, Northern California: implications on accretion geometry: Tectonics, v. 4, p. 435-452.

Carlson, W. D. and Rosenfield, 1981, Optical determination of topotactic aragonite-calcite growth kinetics: metamorphic implication: Journal of Geology, v. 89, p. 615-638.

Cashman, S. M., 1977, Structure and petrology of part of the Duzel Formation and related rocks in the Klamath Mountains southwest of Yreka, California, [Ph.D. thesis]: University of Washington, Seattle, WA, 93 p.

-----, 1980, Devonian metamorphic event in the northeastern Klamath Mountains, California: Geological Society of America Bulletin, v. 91, p. 453-459.

Churkin, M., Jr., and Eberlein, G. D., 1977, Ancient borderland terranes of the North American Cordillera: correlation and microplate tectonics: Geological Society of America Bulletin, v. 88, p. 769-786.

Churkin, M., Jr., and Langenheim, R. L., Jr., 1960, Silurian strata of the Klamath Mountains, California: American Journal of Science, v. 258, p. 258-273.

Cloos, M. 1983, Comparitive study of melange matrix and metashales from the Franciscan subduction complex with the basal Great Valley sequence, California: Journal of Geology, v. 91, p. 291-306.

-----, 1985, Thermal evolution of convergent plate margins: thermal modeling and reevaluation of isotopic Ar-ages for blueschists in the Franciscan Complex of California: Tectonics, v. 4, p. 421-433.

-----, 1986, Blueschists in the Franciscan Complex of California: petrotectonic constraints on uplift mechanisms: Geological Society of America Memoir 164, p. 77-93.

Coleman, R. G., and Lanphere, M. A., 1971, Distribution and age of high-grade blueschists, associated eclogites, and amphibolites from Oregon and California: Geological Society of America Bulletin, v. 82, p. 2387-2412.

Coleman, R. G. and Papike, J. J., 1968, Alkali amphiboles of Cazadero, California: Journal of Petrology, v. 9, p. 105-122.

Coleman, R. G., and Peterman, Z. E., 1975, Oceanic plagiogranite: Journal of Geophysical Research, v. 80, p.1099-1108.

Coombs, D. S., 1960, Lower grade mineral facies in New Zealand: Internat. Geol. Ang. XXI, Pt. XIII, p. 339-351.

Cotkin, M. L. and Cotkin, S. J., 1985, Structural style, metamorphism and tectonic implications of Early Paleozoic blueschist, eastern Klamath Mountains, California: Geological Society of America, Abstracts with Programs v. 17, p. 349.

Cotkin, S. J., 1986, Mineralogy and petrology of blueschist from the schist of Skookum Gulch, eastern Klamath Mountains, California: Geological Society of America, Abstracts with Programs v. 18, p. 96.

Cotkin, S. J., 1987, Conditions of metamorphism in an Early Paleozoic blueschist, Schist of Skookum Gulch, northern California: Contributions to Mineralogy and Petrology, v. 96, p. 192-200.

Cotkin, S. J., and Armstrong, R. L., 1987, Rb/Sr age, geochemistry and tectonic significance of blueschist from the schist of Skookum Gulch, eastern Klamath Mountains, California: Geological Society of America, Abstracts with Programs, v. 19, no. 6, p. 367-368.

Cowan, D. S., 1974, Deformation and metamorphism of the Franciscan subduction zone complex northwest of Pacheco Pass, California: Geological Society of America Bulletin, v. 85, p. 1623-1634.

Cullers, R. L. and Graf, J. L., 1984, Rare-earth elements in igneous rocks of the continental crust: intermediate and silicic rocks -- ore petrogenesis, in Henderson, P. ed., Rare earth element geochemistry: Elsevier, Amsterdam, p. 276-316.

Defant, M. J., Drummond., M. S., Arthur, J. D., and Ragland, P. C., 1988, An example of trondhjemite petrogenesis: the Blakes Ferry pluton, Alabama, U.S.A.: Lithos, v. 21, p. 161-181.

Dixon, S. and Rutherford, M., 1979, Plagiogranites as late-stage immiscible liquids in ophiolite and mid-ocean ridge suites: an experimental study: Earth and Planetary Science Letters, v. 45, p. 45-60.

Dressel, C. F. K., Brothers, R. N., and Black, P. M., 1978, Coalification and graphitization in high-pressure schists in New Caledonia: Contributions to Mineralogy and Petrology, v. 68, p. 63-78.

Dungan, M. A., Vance, J. A. and Blanchard, D. P., 1983, Geochemistry of the Shuksan greenschists and blueschists, North Cascades, Washington: variably fractionated and altered metabasalts of oceanic affinity: Contributions to Mineralogy and Petrology, v. 82, p. 131-146.

Ernst, W. G., 1963, Petrogenesis of glaucophane schists: Journal of Petrology, v. 4, p. 693-711.

-----, 1972, Occurrence and mineralogic evolution of blueschist belts with time: American Journal of Science, v. 272, p. 657-668.

-----, 1979, Coexisting sodic and calcic amphiboles from high-pressure matamorphic belts and the stability of barroisitic amphibole: Mineralogical Magazine, v. 43, p. 269-278.

Ernst, W. G., Seki, Y., Onuki, H., and Gilbert, M. C., 1979, Comparative study of low-grade metamorphism in the California Coast Ranges and the outer metamorphic belt of Japan: Geological Society of America Memoir, 124, 276 p.

Evans, B. W. and Brown, E. H., 1987, Comment and reply on Blueschists and Eclogites: Geology, v. 15, p. 773-775.

Fagin, S. W., and Gose, W. A., 1983, Paleomagnetic data from the Redding Section of the eastern Klamth belt, northern California: Geology, v. 11, p. 505-508.

Frey, M., 1978, Progressive low-grade metamorphism of a black shale formation, central Swiss Alps, with special reference to pyrophyllite and margarite-bearing assemblages: Journal of Petrology, v. 19, p. 93-135.

Frey, F. A., Bryan, W. B. and Thompsen, G., 1974, Atlantic Ocean floor geochemistry and petrology of basalts from Legs 2 and 3 of the Deep Sea Drilling Project: Journal of Geophysical Research, v. 79, p. 5507-5527.

Gerlach, D. C., Ave' Lallemant, H. G., Leeman, W. P., 1981, An island arc origin for the Canyon Mountain ophiolite complex, eastern Oregon, U.S.A.,: Earth and Planatary Science Letters, v. 53, p. 255-265.

Gray, D. R., 1977, Morphologic classification of crenulation cleavage: Journal of Geology, v. 85, p. 229-235.

Gregg, J. M. and Sibley, D. F., 1984, Epigenetic dolomitization and the origin of xenotopic dolomite texture: Journal of Sedimentary Petrology, v. 54, p. 908-931.

Gromet, L. P. and Silver, 1987, REE variations across the Peninsular Ranges batholith: implications for batholithic petrogenesis and crustal growth in magmatic arcs: Journal of Petrology, v. 28, p. 75-125.

Haessig, Polly A., Potter, A. W., Wallin, E. T., and Mattinson, J. M., 1987, Early Cambrian tonalite-plagiogranite from the Yreka-Callahan-Gazelle area, eastern Klamath mountains, northern California: Geological Society of America Abstracts with Programs, v.19, p. 689.

Hamilton, W., 1978, Mesozoic tectonics of the Western United States, in Howell, D. G. and McDougall, K. A. eds., Mesozoic paleogeography of the Western United States: Pacific Section Society of Economic Paleontologists and Mineralogists, p. 33-70.

Hobbs, B. E., Means, W. D. and Williams, P. F., 1976, An outline of structural geology: New York, John Wiley & Sons, 571 p.

Holland, T. J. B., 1980, The reaction albite=jadeite + quartz determined experimentally in the range 600-1200°C: American Mineralogist, v. 65, p. 129-134.

Hotz, P. E., 1974, Preliminary geologic map of the Yreka Quadrangle, California: U.S. Geological Survey Miscellaneous Field Studies Map, MF-568, scale 1:62,500.

-----, 1977, Geology of the Yreka Quadrangle, Siskiyou County, California: U.S. Geological Survey Bulletin 1436, p. 1-72.

-----, 1978, Geologic map of the Yreka Quadrangle and parts of the Fort Jones, Etna, and China Mountain Quadrangles, California: U.S. Geological Survey Open File Report 78-12, scale 1:62,500.

Humphris, S. E., and Thompson, G., 1978, Hydrothermal alteration of oceanic basalts by seawater: Geochemica et Cosmochimica Acta, v. 42, p. 107-125.

Irwin, W. P., 1969, Geologic reconnaissance of the northern Coast Ranges and Klamath Mountains, California, with a summary of the mineral resources: California Division of Mines Bulletin, 179, 80 p.

-----, 1981, Tectonic accretion of the Klamath Mountains, _in_ Ernst, W. G., ed., The geotectonic Development of California: Prentice Hall, Inc., Englewood Cliffs, NJ, p. 30-49.

-----, 1985, Age and tectonics of plutonic belts in accreted terranes of the Klamath Mountains, California and Oregon, _in_, Howell, D. G., ed., Tectonostratigraphic terranes of the Circum-Pacific Region, Earth Science Series, vol. 1,: Circum-Pacific Council for Energy and Mineral Resources, Houston, TX, p. 187-199.

Jahn, B. M., 1986, Mid-ocean ridge or marginal basin origin of the East Taiwan Ophiolite: chemical and isotopic evidence: Contributions to Mineralogy and Petrology, v. 92, p. 194-206.

Johannes, W., and Puhan, D., 1971, The calcite-aragonite transition, reinvestigated: Contributions to Mineralogy and Petrology, v. 31, p. 28-38.

Johnston, A. D., 1986, Anhydrous P-T phase relations of near-primary high-alumina basalt from the South Sandwich Islands: Contributions to Mineralogy and Petrology, v. 92, p. 368-382.

Klein, C., 1968, Two amphibole assemblages in the system actinolite-hornblende-glaucophane: American Mineralogist, v. 54, p. 212-237.

Landis, C. A., 1971, Graphitization of dispersed carbonaceous material in metamorphic rocks: Contributions to Mineralogy and Petrology, v. 30, p. 34-45.

Lapierre, H., Albarede, F., Albers, J., Cabanis, B., and Coulon, C., 1985, Early Devonian volcanism in the eastern Klamath Mountains, California: evidence for an immature island arc: Canadian Journal of Earth Science, v. 22, p. 214-227.

Lapierre, H., Cabanis, B., Coulon, C, Brouxel, and Albarede, F., 1985, The geodynamic setting of Early Devonian Kuroko-Type sulfide deposits in the Eastern Klamath Mountains (Northern California) inferred by the petrological and geochemical characteristics of the associated island-arc volcanic rocks: Economic Geology, v. 80, p. 2100-2113.

Lapierre, H., Brouxel, M., Albarede, Coulon, C., Lecuyer, C., Martin, P., Mascle, G., and Rouer, O., 1987, Paleozoic and Lower Mesozoic magmas from the eastern Klamth Mountains (North California) and the geodynamic evolution of northwestern America: Tectonophysics, v. 140, p. 155-177.

Lee, D. E., Coleman, R. G., Baston, H., and Smith, V. C., 1966, A two-amphibole glaucophane schist in the Franciscan Formation, Cazadero area, Sonoma County California: U.S. Geological Survey Professional Paper, 550-C, p. 148-157.

Lindsley-Griffin, N., 1977, Paleogeographic implications of ophiolites: the Ordovician Trinity complex, Klamath Mountains, California, in Stewart, J. H., Stevens, C. H., and Fritsche, A. E., eds., Paleozoic paleogeography of the western United States: Pacific Section, Society of Economic Paleontologists and Mineralogists, Pacific Coast Paleozoic Paleogeography Symposium v. 1, p. 409-420.

-----, 1982, Structure, stratigraphy, petrology and regional relationships of the Trinity ophiolite, eastern Klamath Mountains, California, [Ph.D. thesis]: University of California, Davis, CA, 445 p.

Lindsley-Griffin, N, and Griffin, J. R., 1983, The Trinity terrane: an Early Paleozoic microplate assemblage: in Stevens, C. H., ed., Pre-Jurassic rocks in western North American suspect terranes: Pacific Section, Society of Economic Paleontologists and Mineralogists, p. 63-76.

Liou, J. G., 1971, P-T stabilities of laumontite, wairakite, lawsonite, and related minerals in the system $CaAl_2Si_2O_8$-SiO_2-H_2O: Journal of Petrology, v.12, p. 379-411.

Liou, J. G. and Maruyama, S., 1987, Parageneses and compositions of amphiboles from Franciscan jadeite-glaucophane type facies series metabasites at Cazadero, California: Journal of Metamorphic Geology, v. 5, 371-396.

Liou, J. G., Maruyama, S., and Cho, M., 1985, Phase equilibria and mineral parageneses of metabasites in low-grade metamorphism: Mineralogical Magazine v. 49, p. 321-333.

Lister, G. S., and Snoke, A. W., 1984, S-C mylonites: Journal of Structural Geology, v. 6, p. 617-638.

Malpas, J., 1979, Two contrasting tondhjemite associations from transported ophiolites in western Newfoundland: intial report, in, Barker, F., ed., Trondhjemites and related rocks: Elsevier, Amsterdam, p. 465-487.

Mankinen, E. A. and Irwin, W. P., 1982, Paleomagnetic study of some Cretaceous and Tertiary sedimentary rocks of the Klamath Mountains Province, California: Geology, v. 10, p. 82-87.

Mankinen, E. A., Irwin, W. P., Gromme, C. S., 1982, Tectonic Rotation of the Eastern Klamath Mountains terrane, California: EOS, American Geophysical Union Transactions, v. 63, p. 914.

Maresch, 1977, Experimental studies on glaucophane: an analysis of present knowledge: Tectonophysics, v. 43, p. 109-125.

Maruyama, S., Cho, M., and Liou, J. G., 1986, Experimental investigations of blueschist-greenschist transition equilibria: pressure dependence of Al_2O_3 contents in sodic amphiboles; Geological Society of America Memoir, 164, p. 1-16.

Maruyama, S. and Liou, J. G., 1985, The stability of Ca-Na pyroxene in low-grade metabasites of high-pressure intermediate facies series: American Mineralogist, v. 70, p. 16-29.

Maruyama, S., and Liou, J. G., 1987, Clinopyroxene -- a mineral telescoped through the process of blueschist facies metamorphism: Journal of Metamorphic Geology, v. 5, p. 529-554.

Maruyama, S., and Liou, J. G., 1988, Petrology of Franciscan metabasites along the jadeite-glaucophane type facies series, Cazadero, California: Journal of Petrology, v. 29, p. 1-37.

Miyashiro, A., and Banno, S., 1958, Nature of glauconphanitic metamorphism: American Journal of Science, v. 256, p. 97-110.

Nakajima, T., Banno, S., and Suzuki, T., 1977, Reactions leading to the disappearance of pumpellyite in low-grade metamorphic rocks of the Sanbagawa metamorphic belt in Central Shikoku, Japan: Journal of Petrology, v. 18, p. 263-284.

Newton, R. C., and Smith, J. V., 1967, Investigations concerning the breakdown of albite at depth in the earth: Journal of Geology, v. 75, p. 268-286.

Passchier, C. W., and Simpson, C., 1986, Porphyroclast systems as kinematic indicators: Journal of Structural Geology, v. 8, p. 831-843.

Pearce, J. A., Harris, N. B. W., and Tindle, A. G., 1984a, Trace element discrimination diagrams for the Tectonic interpretation of granitic rocks: Journal of Petrology, v, 25, p. 856-983.

Pearce, J. A., Lippard, S. J., and Roberts, S., 1984b, Characteristics and tectonic significance of supra-subduction zone ophiolites, in Kokelaar, B. P., and Howells, M. F., eds. Marginal Basin Geology: Blackwell Scientific Publications, Oxford, England, P. 77-94.

Pedersen, R. B., and Malpas, J., 1984, The origin of oceanic plagiogranites from the Karmoy ophiolite: Contributions to Mineralogy and Petrology, v. 88, p.36-52.

Potter, A. W., Scheidegger, K. F., Corliss, J. B. and Dasch, E. J., 1975, Magma types present in Paleozoic keratophyres and spilites from the Gazelle area, eastern Klamath Mountains, northern California: Geological Society of America, Abstracts with Programs, v. 7, p. 1231-1232.

Potter, A. W., Scheidegger, K. F., and Corliss, J. B., 1976, Magma types of Early Paleozoic altered volcanic rocks of the eastern Klamath Mountains, northern California: further results: EOS, American Geophysical Union Transactions, v. 57: 1023.

Potter, A. W., Hotz, P. E., and Rohr, D. M., 1977, Stratigraphy and inferred tectonic framework of Lower Paleozoic rocks in the eastern Klamath Mountains, northern California: Pacific Section, Society of Economic Paleontologists and Mineralogists, Pacific Coast Paleogeography Symposium, v. 1, p. 421-440.

Potter, A. W., Hotz, P. E., and Lanphere, M., 1981, Evidence of Ordovician - Silurian subduction and Silurian or older igneous units of possible magmatic arc origin, eastern Klamath mountains, northern California: Geological Society of America Abstracts with Programs v. 13, no. 2, p. 101.

Potter, A. W., 1982, Klamath Mountains, in Ross, R. J., Jr. and 27 others, The Ordovician System in the United States: International Union of Geological Science, v. 12, p. 30-33.

-----, 1987, Stratigraphy and selected Ordovician brachiopods from the Horseshoe Gulch and Gregg Ranch areas, eastern Klamath Mountains, Northern California, [Ph.D. thesis]: Oregon State University, Corvallis, OR, 367 p.

Raymond, L. A., 1984, Classification of melanges, in: Raymond, L. A., ed., Melanges: Their nature, origin, and significance: Geological Society of America Special Papaer, 198, p. 7-20.

Ramsay, J. G. and Huber, M. I., 1987, The techniques of modern structural geology, Vol. 2, folds and fractures: Academic Press, London, p. 309-700.

Rohr, D. M., 1977, Stratigraphy, structure and Paleozoic Gastropoda of the Callahan area, Klamath Mountains, California, [Ph.D. thesis]: Oregon State University, Corvallis, OR, 315 p.

Saunders, A. D. and Tarney, J. 1984, Geochemical characteristics of basaltic volcanism within back-arc basins, in Kokelaar, B. P., and Howells, M. F., eds., Marginal Basin Geology: Blackwell Scientific Publications, Oxford, England, p. 59-76.

Saunders, A. D., Tarney, J., Stern, C. R., and Dalziel, I. W. D., 1979, Geochemistry of Mesozoic marginal basin floor igneous rocks from southern Chile: Bulletin of the Geological Society of America, v. 90, p. 237-258.

Schilling, J. G., 1975, Rare earth variations across normal segments of the Reykjanes Ridge, 60-53°N, Mid-Atlantic Ridge, 29°S, and East Pacific Rise, 2-19°S, and evidence of the composition of the underlying low velocity layer: Journal of Geophysical Research, v. 80, p. 1459-1473.

Silberling, N. J., Jones, D. L., Blake, M. C., Jr., and Howell, D. G., 1987, Lithotectonic terranes of the western conterminous United States: U.S. Geological Survey, Miscellaneous Field Studies Map, MF-1874-C.

Silver, E. H. and Beutner, E. C., 1980, Melanges: Geology, v. 8, p. 32-34.

Simpson, C., and Schmid, S. M., 1983, An evaluation of criteria to deduce the sense of movement in sheared rocks: Bulletin of the Geological Society of America, v. 94, p. 1281-1288.

Sorensen, S. S., 1986, Petrologic and geochemical comparison of the blueschist and greenschist units of the Catalina Schist terrane, southern California: Geological Society of America Memoir, 164, p. 59-75.

Spilber, S. D. and Rutherford, M. J., 1983, The origin of rhyolite and plagiogranite in oceanic crust: an experimental study: Journal of Petrology, v. 24, p. 1-25.

Stern, C. R., 1979, Open and closed system igneous fractionation within two Chilean ophiolites and the tectonic implication: Contributions to Mineralogy and Petrology, v. 68, p. 243-258.

Streckeisen, A., 1976, To each plutonic rock its proper name: Earth Science Reviews, v. 12, p. 1-33.

-----, 1979, Classification and nomenclature of volcanic rocks, lamprophyres, carbonatites, and melilitic rocks: recommendations and suggestions of the IUGS subcommission on the systematics of igneous rocks: Geology, v. 7, pl 331-335.

Suppe, J. and Armstrong, R. L, 1972, Potassium-argon dating of Franciscan metamorphic rocks: American Journal of Science, v. 272, p. 217-233.

Toriumi, M., 1974, Actinolite-alkali amphibole miscibility gap in an amphibole composite-grain in glaucophane schist facies, Kanto Mountains, Japan: Journal of the Geological Society of Japan, v. 80, p. 75-80.

Turner, F. J. and Weiss, L. E., 1963, Structural analysis of metamorphic tectonites: New York, McGraw-Hill Book Co, Inc., 545 p.

Turner, F. J., 1981, Metamorphic petrology, (second edition): McGraw-Hill, New York, 524 p.

Vance, J. A., 1957, The Geology of the Sauk River area in the Northen Cascades of Washington [Ph.D. thesis]: University of Washington, Seattle, WA., 313 p.

Wallin, E. T., Mattinson, J. M., and Potter, A. W., 1988, Early Paleozoic magmatic events in the eastern Klamath Mountains, northern California: Geology, v. 16, p. 144-148.

Wallin, E. T., 1986, Eocambrian - Early Cambrian plutonic rock in the Eastern Klamath Province, northern California: Geological Society of America Abstracts with Programs, v. 18, no. 2, p. 195.

Wanless, H. R., 1979, Limestone response to stress: pressure solution and dolomitization: Journal of Sedimentary Petrology, v. 49, p. 437-462.

Wells, F. G., Walker, G. W. and Merriam, C. W., 1959, Upper Ordovician(?) and upper Silurian formations of the northern Klamath Mountains, California: Geological Society of America Bulletin, v. 70, p. 645-650.

Whetten, J. T., 1975, The geology of the southeastern San Juan Islands, in Russell, R. H., ed., Geology and water resources of the San Juan Islands: Washington Department of Ecology Water Supply Bulletin 46, p. 341-357.

Wildberg, H. G. H., 1987, High level and low level plagiogranites from the Nicoya ophiolite complex, Costa Rica, Central America: Geologische Rundshau, v. 76, p. 285-301.

Winkler, H. G. F., 1979, Petrogenesis of Metamorphic Rocks, fifth edition: Springer Verlag, New York, 348 p.

Yokoyama, K., Brothers, R. N., and Black, P. M., 1986, Regional eclogite facies in the high-pressure metamorphic belt of New Caledonia: Geological Society of America Memoir 164 p. 407-423.

Zdanowicz, T. A., 1971, Stratigraphy and structure of the Horseshoe Gulch area, Etna and China Mountain Quadrangles, California: [M.S. thesis]: Oregon State University, Corvallis, OR., 88 p.

APPENDIX 1

Mineralogy Tables

Table A1. List of abbreviations used in Tables A2-A4

Qtz	=	Quartz
Ab	=	Albite
Chl	=	Chlorite
Wm	=	White Mica
Law	=	Lawsonite
Epi	=	Epidote
Clz	=	Clinozoisite
Pu	=	Pumpellyite
Ca-am	=	Calcic Amphibole
Na-am	=	Sodic Amphibole
Sph	=	Sphene
Stlp	=	Stilpnomelane
Gar	=	Garnet
Cpx	=	Clinopyroxene
Gph	=	Graphite
Hem	=	Hematite
Apt	=	Apatite
Zir	=	Zircon
Tour	=	Tourmaline
Cc	=	Calcite
Dol	=	Dolomite
Pyr	=	Pyrite
Opq	=	Opaque
mat	=	melange matrix
blk	=	tectonic block in melange
ils	=	interlayered sequence within a coherent fault block in the melange
X	=	mineral present
m	=	mineral present in minor amounts, 5% or less
tr	=	mineral present in trace amounts, 1% or less
ia	=	inclusions in albite
rlc	=	relict mineral
sv	=	secondary mineral present in veins
ap	=	after pyrite
plag	=	plagioclase feldspar

Table A2. Mineral Assemblages of the Horseshoe Gulch Locality

	Qtz	Ab	Chl	Wm	Law	Epi-Clz	Pu	Ca-am	Na-am	Sph	Stlp	Gar	Cpx	Gph	Hem	Apt	Zir	Tour	Cc	Dol	Pyr	Opq
GREENSCHIST FACIES																						
Metasediments																						
HG 2C mat	X	X	X	X		m				m				X	m	tr	tr		X,sv			
HG 10C mat	X	X	X	X								tr		X		m	m		X			tr
HG 7B mat	X	X	X	X						m				m	m	m	tr	tr	X			
HG 14 mat	X	X	X	X											m	m	tr	tr	X			tr
HG 15A mat	X	X	X	X										m	m	m	tr	tr	X		tr	
HG 20 mat	X	X	X	X											m	m	tr	tr	X,sv			tr
Metacarbonates																						
HG 7D mat	X,sv																		sv	X		
HG 22 blk	sv																		sv	X		
HG 23 blk	sv																		sv	X		
HG 24 blk	m,sv																		sv	X		
HG 27 blk	sv		m																sv	X		
Metavolcanics																						
HG 2D mat	X	X	X	m		X				X					m	m	tr		X,sv			tr
HG 8C mat	X	X	X	X		X				X					m	m	tr		X			tr
HG 25A mat	X	X	X	X		X			ia	X					m	tr	tr		X			tr
BLUESCHIST FACIES																						
Metavolcanics																						
HG 1 blk	X	X	X		X	m			X	X					m		tr		X,sv			
HG 4C blk	X	X,sv	X		X				X	X		X			m				X,sv			tr
HG 8A blk	X	X	X	X	X	m			X	X					m		tr		X,sv			
HG 12 blk	X	X,sv	X	X	X	m			X	X					m				X,sv			
HG 25B blk	X	X	X	X	X	m			X	X					m				X			

(Table A2 continued)

	Qtz	Ab	Chl	Wm	Law	Epi-Clz	Pu	Ca-am	Na-am	Sph	Stlp	Gar	Cpx	Gph	Hem	Apt	Zir	Tour	Cc	Dol	Pyr	Opq
BLUESCHIST FACIES																						
Metavolcanics																						
HG 3B blk	X	X	X	m	X	m			X	X					m				X,sv			
HG 3D blk	X	X	X	m	X	X			X	X					m		tr		X,sv			
HG 4B blk	X	X	X		X	X			X	X					m		tr					
HG 4D blk	X	X	X		X	X			X	X					m				X,sv			tr
Hg 6B blk	X	X	X		X	m			X	X					m				X			tr
HG 9A blk	X	X,sv	X		X	X			X	X				m	m		tr		X,sv			
HG 26 blk	X	X	X		X	X			X	X					m		tr		X,sv			tr
HG 2A blk	X	X	X	m	X	m		X	X	X	X				m				X			tr
HG 2B blk	X	X	X	m	X	X		X	X	X	X				m				X,sv			tr
HG 5 blk	X	X	X	m	X	X		X	X	X					m				X,sv			
HG 9B blk	X	X	X		X			X	X	X					m		tr		X,sv			tr
HG 11 blk	X	X	X	m	X	X		X	X	X					m				X,sv			
HG 13A blk	X	X,sv	X		X	X		X	X	X					m	m			X			
HG 16A blk	X	X,sv	X		X	X		X	X	X					m		tr					tr
HG 19 blk	X	X	X		X	X		X	X	X					m				X			tr
HG 21 blk	X	X	X	m	X	X		X	m	X					m				X,sv			
Metasediments																						
HG 9C blk	X	X,sv	X		X	X		X		m				m								

Table A3. Mineral Assemblages of the No Name Gulch Locality

	Qtz	Ab	Chl	Wm	Law	Epi-Clz	Pu	Ca-am	Na-am	Sph	Stlp	Gar	Cpx	Gph	Hem	Apt	Zir	Tour	Cc	Dol	Pyr	Opq
GREENSCHIST FACIES																						
Metasediments																						
NNG 51 mat	X	X	X	X						X				X	m,ap	tr	tr					tr
NNG 33E mat	X	X	X	X		X				X				X	m	tr	tr		X,sv			
NNG 47 mat	X	X	X	X											m,ap	tr	tr	tr	X,sv		tr	
NNG 43 mat	X	X	X	X						m					m	tr	tr	tr				
NNG 41E mat	X	X	X	X		m				m					m	tr	tr	tr				
Metavolcanic																						
NNG 33C mat	X	X	X	X		m				X					m,ap	tr	tr		X,sv		tr	
Metachert																						
NNG 48 blk	X		X	X											m	tr	tr	tr				tr
BLUESCHIST FACIES																						
Metavolcanic																						
NNG 45 blk	X	X	X			X			X	X									X			
NNG 41C blk	X	X	X	m					X	X					m				X			
NNG 49C blk	X	X	X	m					X	X					m				X			
NNG 49D blk	X	X	X	X					X	X					m				X			
NNG 30A blk	X	X	X	X	X	m			X	X					m		tr		X			
NNG 31A blk	X	X	X	m	X				X	X					m		tr		X,sv			
NNG 33A blk	X	X	m	m	X	m			X	X					m				X			
NNG 33B blk	X	X	X	X	X	m			X	X					m	tr			X,sv			
NNG 33D blk	X	X	X	m	X	m			X	X					m	tr			X,sv			
NNG 41A blk	X	X	X		X	X			X	X						tr	tr		X,sv			
NNG 42 blk	X	X	X	X	X				X	X									X,sv			tr
NNG 46 blk	X	m	X	m	X	X			X	X									X,sv			tr
NNG 35 ils	X	X	X	X	X	m		X	m	X					m	tr	tr		X			
NNG 39 ils	X	X	X	m	X	m		X	m	X					m				X,sv			
NNG 31B blk	X	X	X	m	X			X	X	X					m	tr			X,sv			
NNG 36 ils	X	X	X	m	X	m		X	X	X					m				X,sv			
NNG 37 ils	X	X	X	X	X	m		X	X	X					m	tr			X,sv			
NNG 38 ils	X	X,sv	X		X	m		X	X	X					m	tr			X,sv			
NNG 40 ils	X	X	m	X	X	m		X	X	X		X			m	tr			X,sv			tr
NNG 44 ils	X	X,sv	X	X	X	m		X	X	X		X			m	tr			X,sv			tr
Metacarbonate																						
NNG 34 ils	X	X	X	X	X	tr			m	X					m	tr			X			

Table A4. Mineral Assemblages of the Upper McConaughy Gulch Locality

	Qtz	Ab	Chl	Wm	Law	Epi-Clz	Pu	Ca-am	Na-am	Sph	Stlp	Gar	Cpx	Gph	Hem	Apt	Zir	Tour	Cal	Dol	Pyr	Opq
GREENSCHIST FACIES																						
Metasediments																						
UMG 64 mat	X	X	X	X										X	m		tr		X,sv			
UMG 69 blk	X	X	X	X							m				m		tr	tr				
Metachert																						
UMG 56 blk	X	tr	X	X			sv					X			m			tr				
Marble																						
UMG 61 mat	X	plg	X	X											m				X,sv			
UMG 65 mat			X																sv	X		
Metavolcanic																						
UMG 66 mat	X	X	X	X		X			ia	X					m		tr					tr
UMG 55 blk	X	X	X	m		X			ia	X					m		tr	tr				tr
UMG 60a mat	X	X	X	X		X			ia	X					m	X	tr	tr				
UMG 60b mat	X	X	X	X		X			ia	X					m	X	tr	tr				X
UMG 70 blk	m	X,sv	X	m		X		X	m	X			rlc		m				X,sv			
UMG 74 mat	X	X	X	X		X			ia	X					m	X	tr					
UMG 71 mat	X	X	X	X		X			ia	X					m	X	tr	tr	X		tr	
BLUESCHIST FACIES																						
Metasedimentary																						
UMG 59 blk	X	X	X	X		X			X	X					m	X	tr	tr			tr	
Metachert																						
UMG 72 blk	X	X	m	X		X			X	X					m		tr		m			
Metavolcanic																						
UMG 67 blk	X	X	X	X		X			X	X					m	X	tr	tr				X
UMG 77 blk	X	X	X	X		X			X	X					m	X	tr	tr	sv		tr	
UMG 70 blk	m	X	X	m		X		X	m	X			rlc		m				X,sv			
UMG 57 blk	X	X	X	m		X		X	X	X			rlc		m	X			X			
UMG 73 blk	X	X	X	X		X		X	X	X					m				X,sv		tr	
UMG 62 blk	X	X,sv	X		X	X		X	X	X	sv				m				X,sv			
UMG 63 blk	X	X,sv	X		X	X		X	X	X	m				m				X,sv			

APPENDIX 2

Chemical Analyses: Sample Preparation, Methods, and Standards Used

Sample Preparation

After removing weathered surfaces from samples, rocks were crushed in a porcelain-lined jaw crusher and pulverizer. Reduction to a fine fraction of 200 mesh was accomplished using a 95% alumina-pure shatterbox.

Chemical Analysis and Standards Used

Concentrations of selected trace and rare-earth elements were determined by me using techniques of Instrumental Neutron Activation Analysis (INAA) following the method outlined by Laul (1979). Analyses were run and data was reduced during winter and spring term of 1986 while the author was taking courses related to INAA procedures.

Approximately 200 milligram samples along with U.S. Geological Survey and U.S. Bureau of Standards rock standards were irradiated twice in the TRIGA research reactor at Oregon State University. A rabbit-run (short irradiation) and two short counts were completed. Samples were irradiated again for 4 megawatt hours. Sequential long counts one week and four weeks following long irradiation were completed. Gamma-ray spectra were reduced to concentration values using the Cyber main-frame computer or a hand calculator. Parts-per-million (ppm) trace-element contents of the samples analyzed are shown in Tables 6 and 7. Errors reported in the results were estimated by combining counting errors with uncertanties in the reproducibility of rock standards.

Standards used in long counts included: GSP-1, BCR-2, SRM-1633, PCC-1 and REE2.

APPENDIX 3

Chemical Data and REE Signature of Quartz Keratophyre of Horseshoe Gulch

Quartz Keratophyres of Horseshoe Gulch

Sample #	HG10-12	HG34-18	HGZ-21
(oxides in weight percent, recalculated on a water-free basis)			
SiO_2	75.61	76.63	77.84
TiO_2	0.45	0.43	0.20
Al_2O_3	11.38	11.36	11.34
FeO*	5.33	4.59	4.50
MgO	1.36	1.16	1.46
CaO	0.15	0.81	0.12
Na_2O	4.55	4.63	4.23
K_2O	0.99	0.41	0.26
(trace elements in ppm)			
Zr	50	50	50
Cr	35	73	—
La	3.4	3.7	3.5
Ce	6.5	6.3	6.0
Sm	2.1	2.2	2.3
Eu	0.69	0.76	0.56
Tb	0.42	0.51	0.48
Yb	1.7	2.7	2.2
Lu	0.28	0.43	0.39
Sum REE	28	24	21
La/Lu_{cn}	0.93	0.89	0.82

Notes: Samples collected by A. W. Potter. Major elements by atomic absorbtion. Analyst: K. F. Scheidegger at Oregon State University.
Zr, Rb, Sr, Nb, Y by XRF. Analyst: A. W. Potter, at Universtity of Oregon. REE by INAA. Analyst: John Corliss, at Oregon State University.

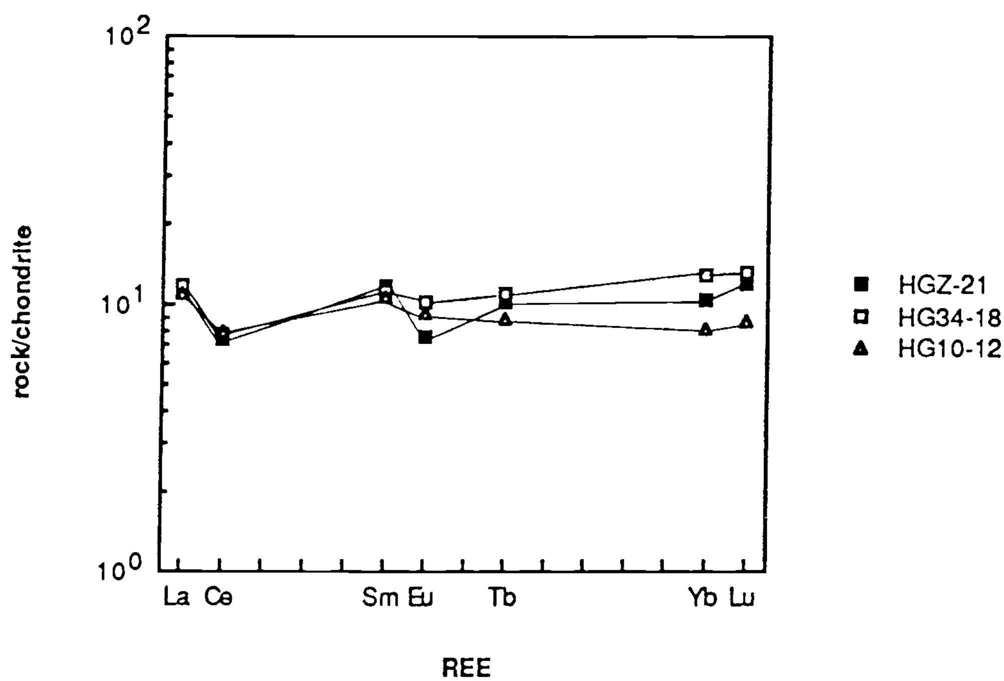

Figure A1. A. Chemical analyses of quartz keratophyre samples from Horseshoe Gulch. Analytical data provided by A. W. Potter. B. Chondrite normalized REE pattern of samples of quartz keratophyre of Horseshoe Gulch.

APPENDIX 4

Stereonet Plots

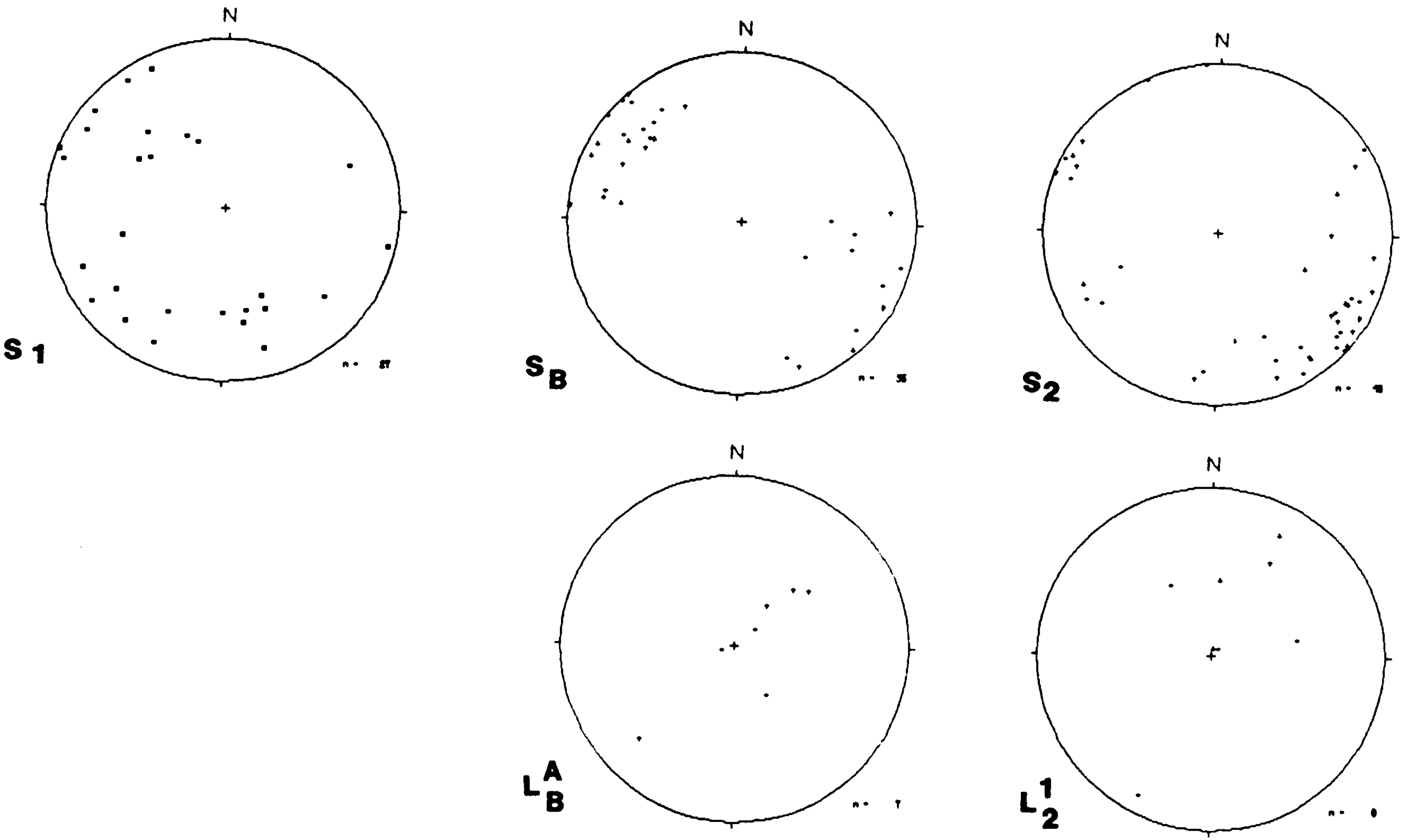

Figure A2. Structural data for the Horseshoe Gulch Locality

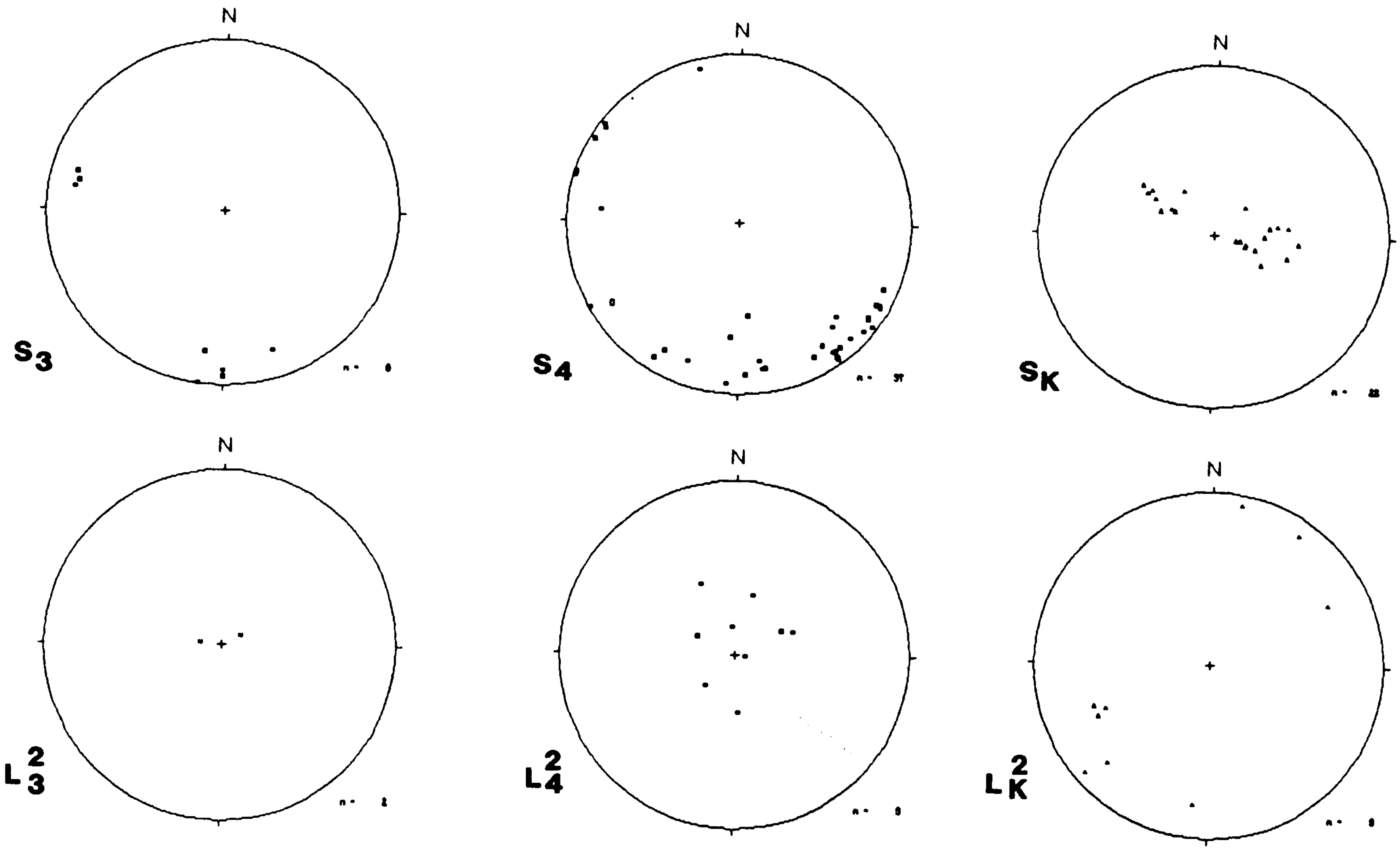

(Figure A2 continued)

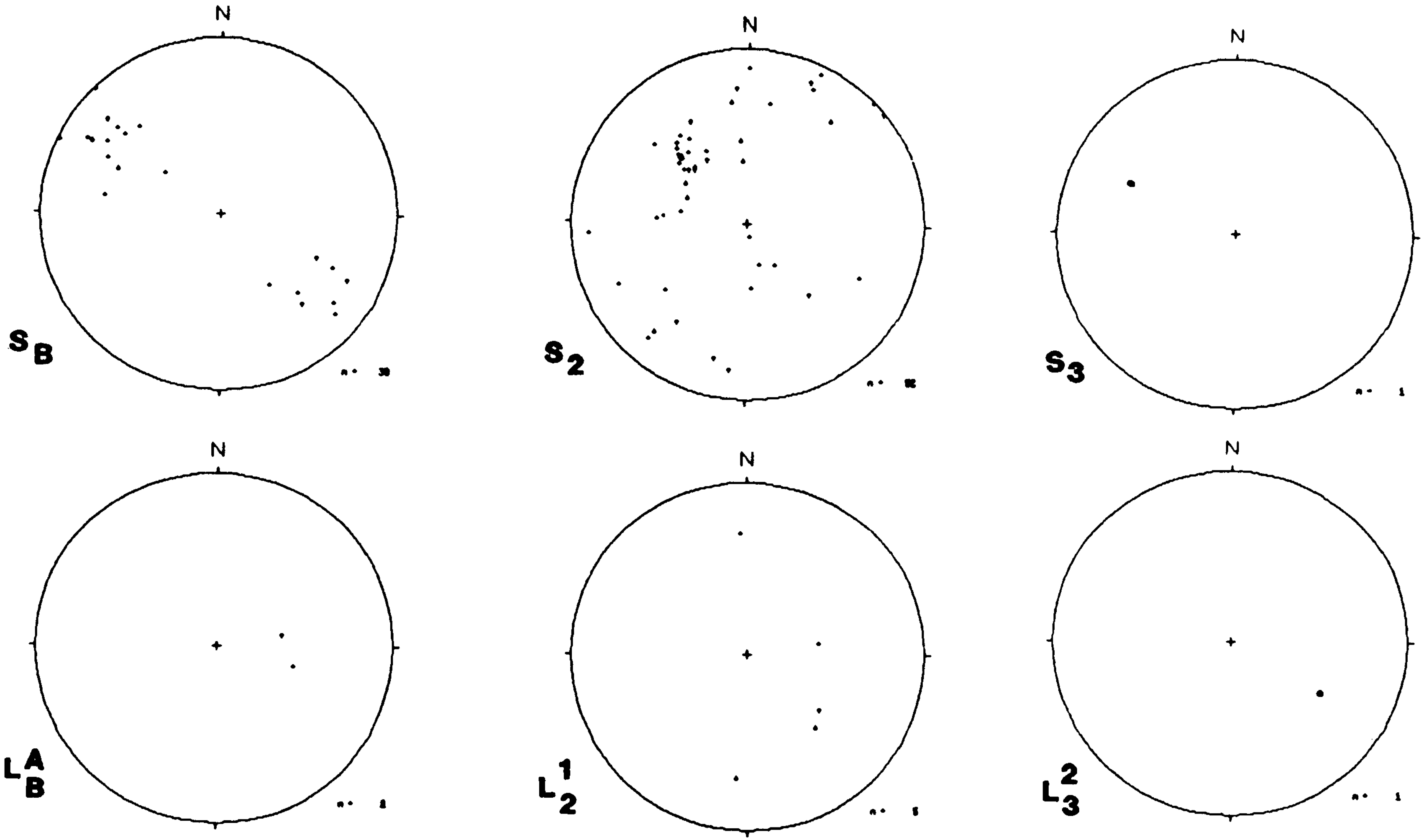

Figure A3. Structural data for the No Name Gulch Locality

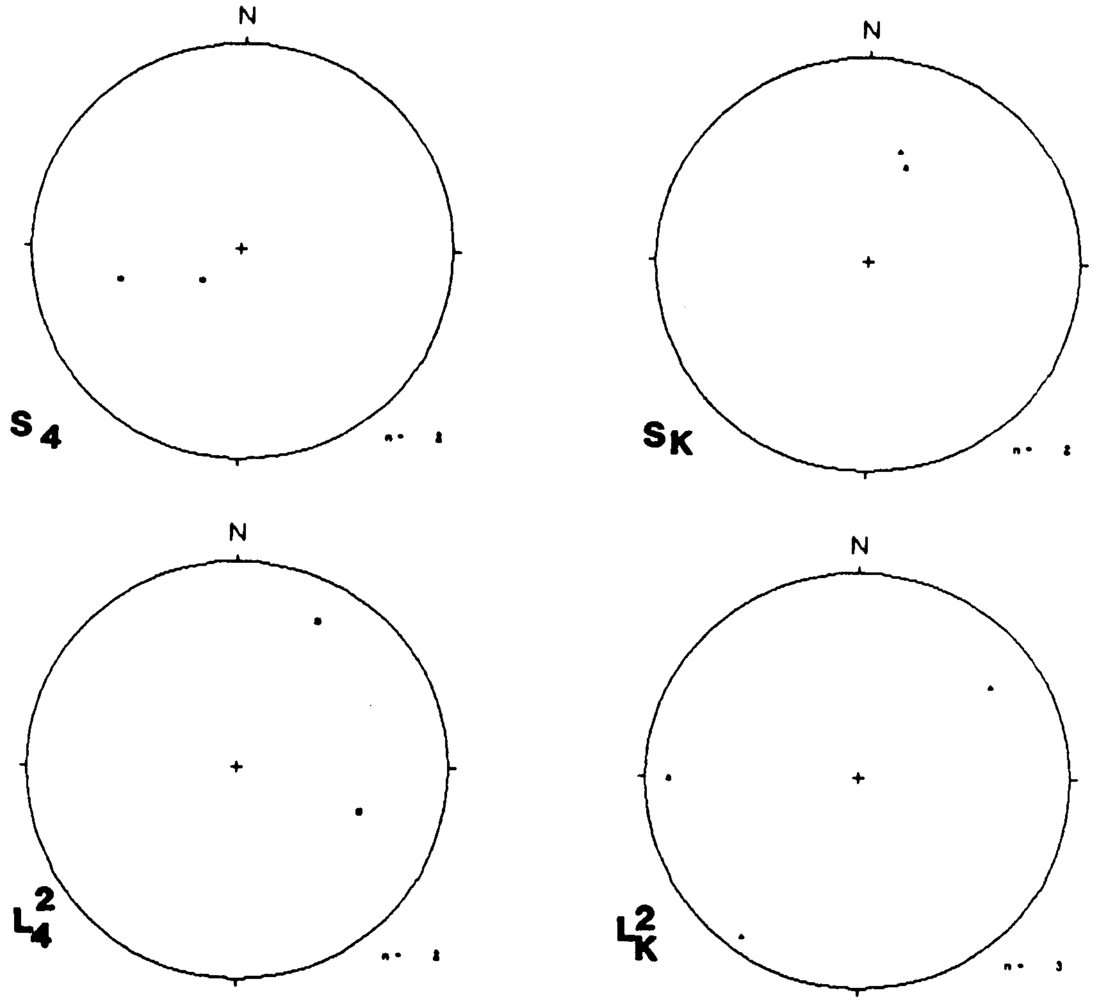

(Figure A3 continued)

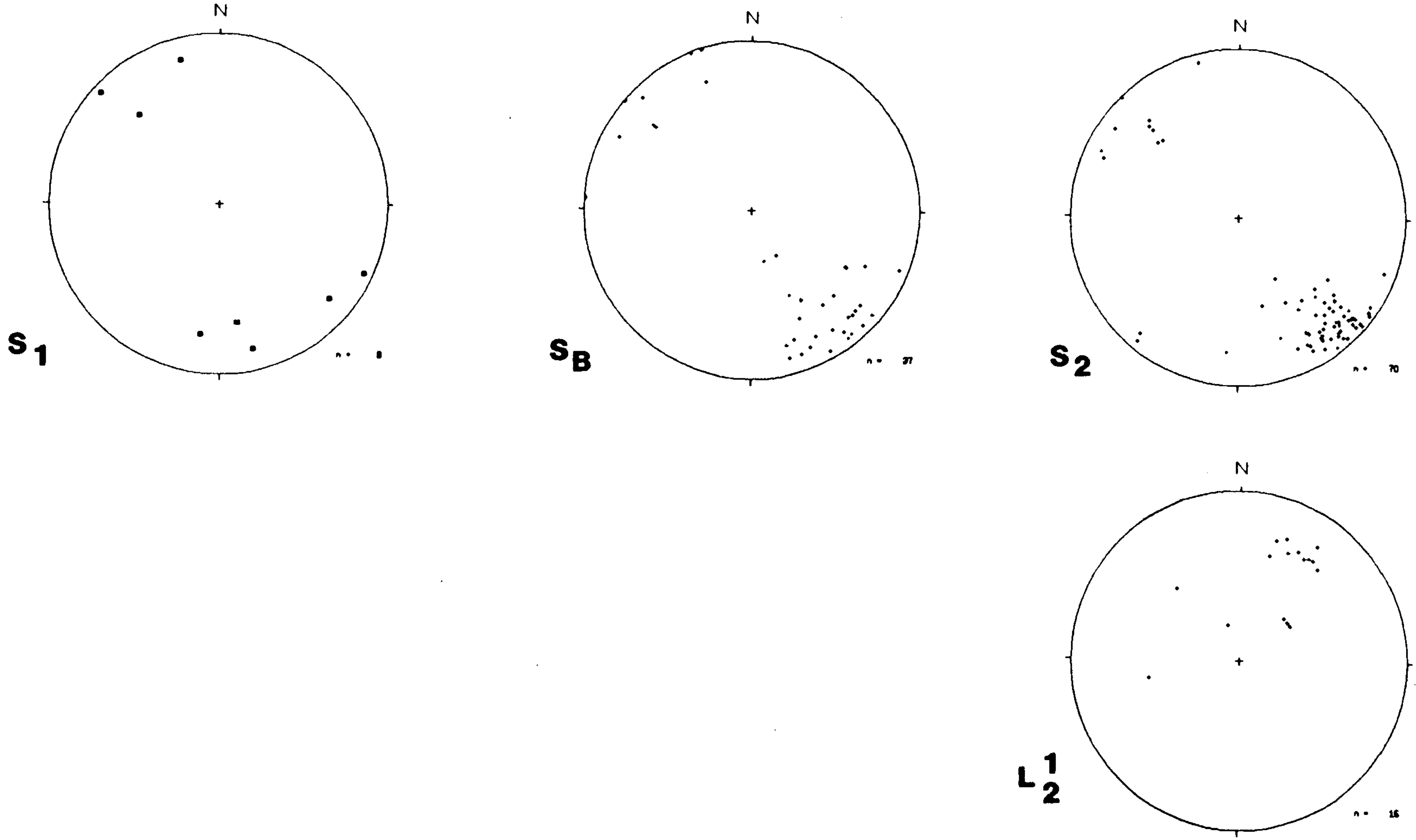

Figure A4. Structural data for the Upper McConaughy Gulch Locality

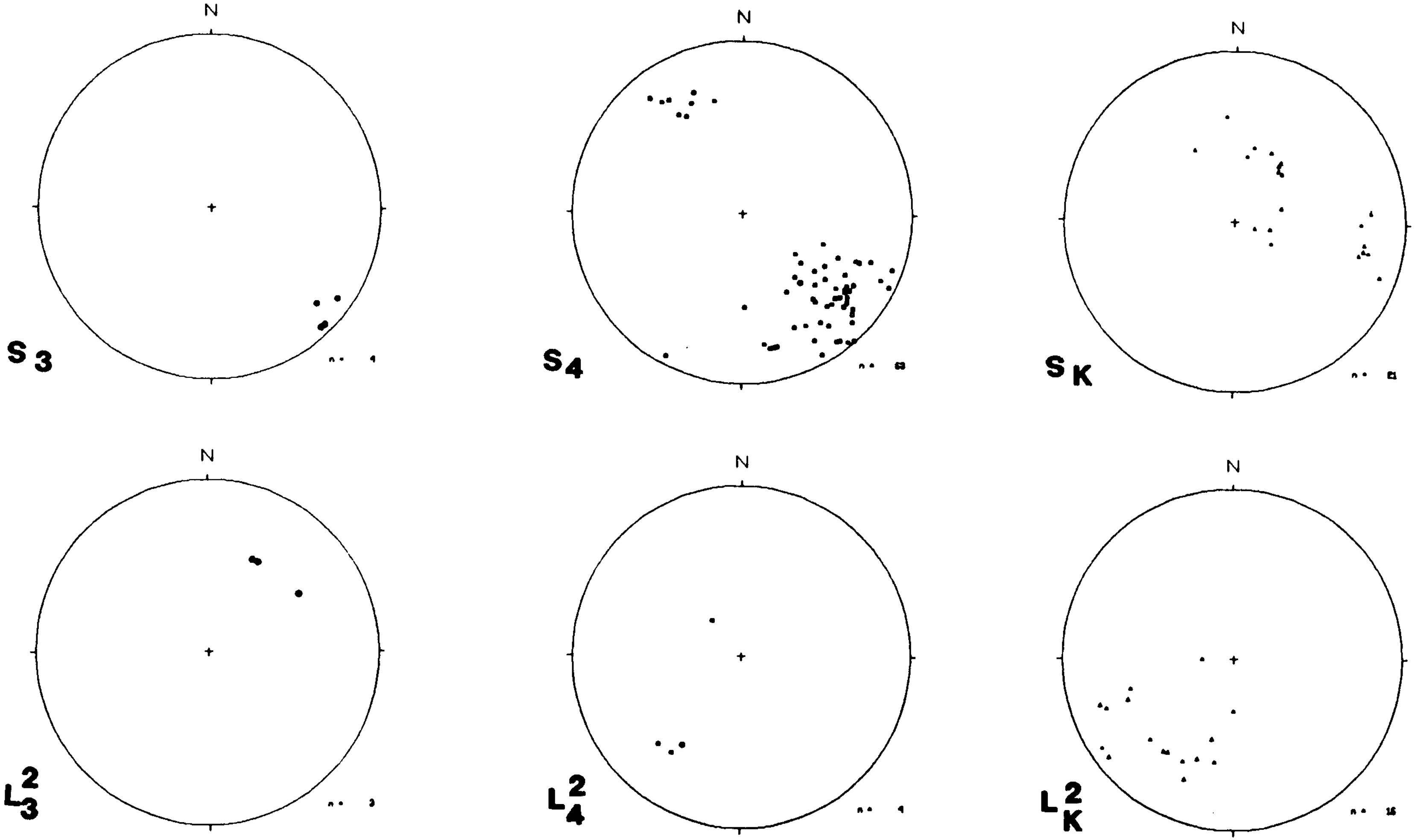

(Figure A4 continued)